

Rational Design of Triplet Sensitizers for the Transfer of Excited State Photochemistry from UV to Visible

Luke D. Elliott,^{*[a]} Surajit Kayal,^[b] Michael W. George^[b,c] and Kevin Booker-Milburn^{*[a]}

[a] School of Chemistry, University of Bristol, Cantock's Close, Bristol, BS8 1TS; [b] School of Chemistry, University of Nottingham, University Park, Nottingham, UK, NG7 2RD; [c] Department of Chemical and Environmental Engineering, The University of Nottingham Ningbo China, Ningbo 315100, China orcid.org/0000-0002-7844-1696

ABSTRACT: Time Dependent Density Functional Theory (TD-DFT) has been used to assist the design and synthesis of a series of thioxanthone triplet sensitizers. Calculated energies of the triplet excited state (E_T) informed both the type and position of auxochromes placed on the thioxanthone core, enabling fine-tuning of the UV-Vis absorptions and associated triplet energies. The calculated results were highly consistent with experimental observation in both the order of the λ_{max} and E_T values. The synthesised compounds were then evaluated for their efficacies as triplet sensitizers in a variety of UV and visible light preparative photochemical reactions. The results of this study exceeded expectations; in particular [2+2] cycloaddition chemistry that had previously been sensitized in the UV was found to undergo cycloaddition at 455 nm (blue) with a 2 to 9-fold increase in productivity (g/h) relative to input power. This study demonstrates the ability of powerful modern computational methods to aid the design of successful and productive triplet sensitized photochemical reactions.

INTRODUCTION

Excited state photochemistry¹ involves the formation of bonds by the reaction of molecules in an electronically excited state. Its purest embodiment occurs without catalysts or reagents by irradiation with UV light, most commonly in the region of 250-400 nm. This 'reagentless' approach to synthesis is highly desirable in an ever more economic and green focused society. Reactions typically occur from either the lowest energy excited singlet (S_1) or triplet (T_1) states, the latter accessed via intersystem crossing (ISC) from the singlet. These 'electronic isomers' of the ground state species can react in exotic ways to give rapid access to complex or highly strained species with favorable properties for drug discovery² or further reactivity.³ Unfortunately the overall efficiency, and hence synthetic utility, of a photochemical reaction is often dependent on the lifetime of these states relative to the rate of chemical reaction, which in turn is determined by the physical properties of the compound. Therefore, many interesting photochemical reactions may remain of academic curiosity due to poor yields and low-productivities. Whilst the short-lived S_1 state is inherently difficult to control, the much longer lifetime of the T_1 state can be exploited to significantly enhance the overall quantum efficiency of a reaction.

Since the early 1960s⁴ it has been understood that photosensitizers can enable population of the T_1 excited state of a substrate by energy transfer even though the substrate does not absorb at the sensitizer absorbing wavelength (Figure 1A). As a result a number of photochemical reactions have been enabled by sensitization when direct irradiation has been ineffective.⁵ The ideal triplet sensitizer has a strong extinction coefficient to allow for efficient light absorption at low concentrations, a relatively small S_1 - T_1 energy difference for irradiation at the longest wavelength, ISC close to unity for maximum quantum efficiency and a long lived T_1 state for efficient energy transfer to a ground state species. All these features can circumvent the most common

causes for a low productivity in a photochemical reaction. Furthermore, where the singlet and triplet manifolds have different reaction outcomes it is possible to switch between S_1 and T_1 chemistry by addition of a sensitizer.⁶

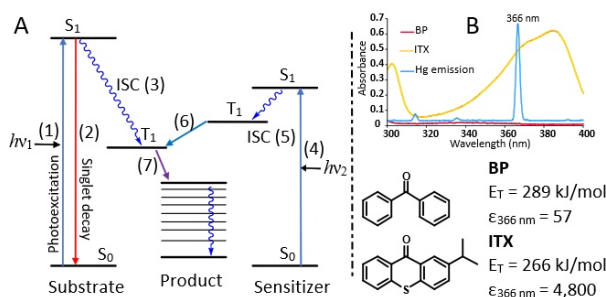


Figure 1. (A) Simplified Jablonski diagram of a triplet mediated photochemical reaction: (1) Direct excitation of substrate to S_1 ; (2) Singlet decay by radiative and non-radiative processes; (3) ISC to reactive T_1 ; (4) Photoexcitation of sensitizer; (5) Rapid ISC to T_1 ; (6) Triplet energy transfer to substrate; (7) Chemical reaction and relaxation to ground state. (B) UV absorption of BP and ITX at 1×10^{-4} M, overlaid with UVA emission from medium pressure Hg lamp.

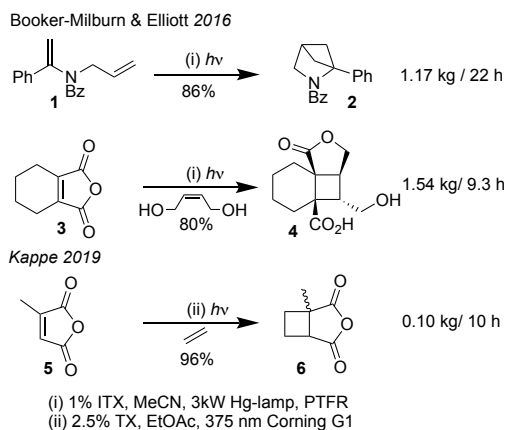
In addition to an energy transfer pathway, sensitizers have also allowed for efficient scale-up of photo-initiated processes by alternative methods.⁷ For example, in recent years there has been explosive growth in the development of photoredox catalysis,⁸ i.e. organic or organometallic catalysts that upon photoexcitation act as powerful one-electron oxidants or reductants in a variety of bond forming processes. Modification of a ligand on a

transition metal complex⁹ or substituents on an organic dye¹⁰ allows the redox potential to be fine-tuned to match that of a substrate. Within this recent work it has been found that some of the organometallic photoredox catalysts can alternatively function as classic triplet sensitizers in, for example [2+2] photocycloadditions.¹¹ However, the possibility that transition metal photocatalysts can react via either electron or energy transfer can make determination of the mode of activation difficult as highlighted in a recent study on eniminium [2+2] cycloaddition using laser flash photolysis.¹²

Herein we report the rational design of a family of *triplet sensitizers* for chemical synthesis¹³ that share a common chromophore, but individually cover a range of triplet energies. From our experience of photochemical synthesis in the UV, we were inspired to design a range of organic sensitizers that would span the 350–450 nm region.

A key goal of the present study was to see if it was possible to move useful UV chemistry into the visible (≥ 400 nm) with similar or better productivities to match readily available high intensity LED light sources. It should be noted that use of sensitizers can result in practical issues, especially if energy transfer is inefficient or the sensitizer has a low extinction coefficient (ϵ). In these instances high sensitizer concentrations/equivalents are required (e.g. acetophenone & acetone), often resulting in degradation, purification and separation issues. With this in mind we considered the design of highly absorbing sensitizers that could be used in low molar equivalences and be stable to high UV/Vis powers (≥ 500 W). Traditionally, sensitizer screens involve a range of chromophores with different triplet energies, but very different absorption characteristics (cf. BP and ITX, Figure 1B). A sensitizer series based around single chromophore is therefore highly desirable for consistency and reliability.

Scheme 1. Scale-up of [2+2] photocycloadditions using thioxanthone sensitization.



In 2016 as part of a campaign to enable the scale-up of UV photochemistry using flow-reactors we designed a parallel tube

flow reactor (PTFR)¹⁴ which displayed productivities of between 1–8 kg/day for a range of photochemical reactions in the UV (Scheme 1). The large-scale examples in Scheme 1 required a triplet sensitizer to enable a productivity increase to multi-kg/day quantities. Of a number of sensitizers screened, isopropylthioxanthone (ITX) was demonstrably superior in terms of productivity at exceptionally low loadings (1%). The isopropyl derivative proved to be more soluble than the parent thioxanthone, making bulk purification by trituration easier. The high extinction coefficient of ITX (Figure 1B) is important for its excellent sensitization properties at the 1% loadings used, and remarkably we found no sensitizer degradation was observed despite the very powerful 3 kW Hg-UV lamp employed.

In 2019 Kappe¹⁵ reported a study of maleimide and maleic anhydride [2+2] cycloadditions (UVA) using a variety of known sensitizers chosen for their matching triplet energies. They also observed that thioxanthone proved to be a superior sensitizer where the substrate triplet energy was a suitable match. In the visible region, Bach¹⁶ has shown that thioxanthone can be used as a sensitizer by irradiation at the tail of the absorption using 420 nm light. Jockush and Sivaguru¹⁷ have shown that 2,2'-bromo thioxanthone induces a moderate (~ 15 nm) bathochromic shift enabling sensitized cycloadditions with near UV light (395–405nm). However, photolabile halo derivatives (Cl, Br, I) can be problematic due to the potential of photodehalogenation.¹⁸ A further advantage of thioxanthone over other common sensitizers, such as BP is the nature of the reactive triplet state. For TX this is (π, π^*) whilst for BP it is (n, π^*) making TX less likely to take part in competing H-atom abstractions which are well documented for BP and derivatives.¹⁹

RESULTS and DISCUSSION

DFT Informed Sensitizer Design. It was our aim to induce predictable shifts in absorbance by substituting thioxanthone with a range of auxochromes that electronically modify the UV/Vis absorption of a chromophore. Rather than embark on a time consuming hit-and-miss synthetic approach, we opted to use time-dependent density functional theory (TD-DFT) to calculate the triplet energies for a range of auxochrome substituted thioxanthone derivatives. This would enable the selection of potential sensitizer candidates to be made before synthesis. In terms of substituents we chose a balance between those that are known auxochromes and would likely be photochemically robust. Based on prior experience with substituted benzophenones and acetophenones we narrowed down the auxochrome choice to fluoro- and methoxy-substituents.

Initial TD-DFT calculations of thioxanthone derivatives bearing these two auxochromes were highly informative in predicting a sensitizer series spanning a broad range of triplet energies. Once a range of nine candidates were selected from these computational studies, they were then synthesized using an Ullman coupling/Friedel Crafts approach (see SI).

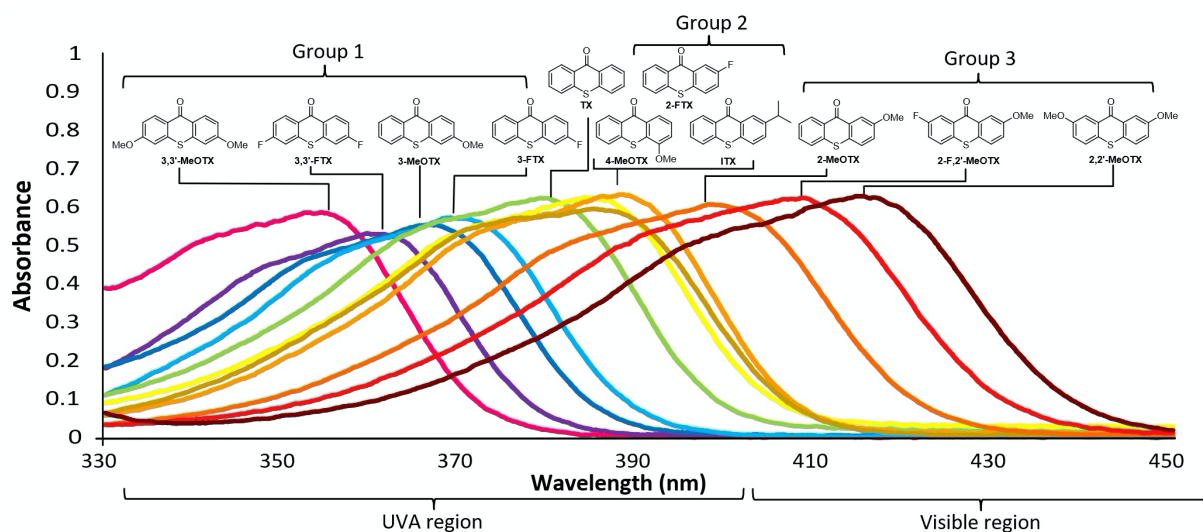


Figure 2. UV-Vis absorption spectra for the synthesized thioxanthone sensitizer series including the parent commercially available thioxanthone and 2-isopropyl thioxanthone. All were run at a concentration of 1×10^{-4} M in acetonitrile.

Photophysical Characterisation. The UV-Vis absorption of the nine synthesized thioxanthone derivatives (plus TX and ITX) are represented in Figure 2 as a composite spectrum for comparison. The placement of these auxochromes has the desired effect of shifting the UV-Vis absorption relative to the parent thioxanthone core. In the UV-Vis spectra, substituents in the 2-position induce a bathochromic shift whilst 3-substituents induce a hypsochromic shift compared to the parent thioxanthone, in excellent agreement with DFT. The effect is more pronounced for the MeO derivatives (compared to F) and the effect is additive. The sensitizer absorption energies can be split into three distinct groups. Absorbing at shorter wavelengths, and hence higher energies than the parent thioxanthone, are the series of 3-substituted thioxanthenes (Group 1). Within this group a clear energy order is apparent with $3,3'$ -MeOTX > $3,3'$ -FTX

> 3 -MeOTX > 3 -FTX. Absorbing at slightly longer wavelength, and hence lower energy than TX are the 2-FTX and 2-*i*PrTX derivatives along with 4-MeOTX (Group 2). These absorptions are clustered close together but an expansion of the weak tail end at longer wavelengths suggests $ITX > 2$ -FTX \geq 4-MeOTX. The absorbances of the Group 2 series, along with TX begin to overlap with the visible region of the spectrum above 400 nm. Absorbing at significantly longer wavelengths are the series of 2-MeO derivatives with a clear energy order 2 -MeOTX > 2 -F, $2'$ -MeOTX > $2,2'$ -MeOTX (Group 3). This moves the lowest energy absorption bands well into the visible region and is expected to enhance their efficiency as visible light active triplet sensitizers with readily available and powerful LED sources (e.g. 36 W at 455 nm).

Table 1. Calculated and measured photophysical parameters for substituted thioxanthone derivatives

Entry	TX	λ_{\max} (nm) ^a	E_T (Calc.) ^b (kJ/mol)	E_T (Calc.) ^c (kJ/mol)	E_T (Meas.) ^d (kJ/mol)	τ_S ^e	τ_T ^h	Φ_{ISC} ⁱ
1	$3,3'$ -MeOTX	354	292	289	298 ^e	10 ± 3 ps	862 ± 40 ns	0.93
2	$3,3'$ -FTX	362	290	285	289 ^e	10.5 ± 1.8 ps	456 ± 25 ns	0.92
3	3 -MeOTX	367	284	279	283 ^e	31 ± 4 ps	867 ± 50 ns	>0.9
4	3 -FTX	370	282	277	282 ^e	21 ± 3 ps	520 ± 25 ns	0.83
5	TX (R/R'=H)	380	274	268	274 ^e	70 ps ²⁰	760 ± 30 ns	0.76 ¹⁷
6	ITX (R'=H, R = 2- <i>i</i> Pr)	385	270	263	266 ^e	220 ± 8 ps	880 ± 50 ns	0.86
7	2-FTX	388	263	257	261 ^e	270 ± 10 ps	585 ± 20 ns	0.81
8	4-MeOTX	385	267	260	263 ^e	1.9 ± 0.4 ns	1.8 ± 0.3 μ s	0.70
9	2-MeOTX	399	252	245	242 ^f	3.3 ± 0.2 ns	1.7 ± 0.6 μ s	0.83
10	2-F, $2'$ -MeOTX	408	242	235	235 ^f	9.1 ± 0.7 ns	1.2 ± 0.2 μ s	0.62
11	$2,2'$ -MeOTX	415	235	227	231 ^f	6.2 ± 0.5 ns	863 ± 60 ns	0.66

^aLongest wavelength absorption maximum (MeCN); ^bCalculated E_T , no solvent model, B3LYP 6-31G (d,p); ^cCalculated E_T , no solvent model, B3LYP 6-31+G (d,p); ^dMeasured E_T (Phosphorescence, ^eMCH glass, 77 K; ^f2-MeTHF glass, 77 K); ^gSinglet lifetime measured with TRIR, CD₃CN; ^hTriplet lifetime measured with TRIR, CD₃CN; ⁱISC quantum yield calculated from bleach recovery kinetics

The TD-DFT calculated triplet energies for the thioxanthone derivatives are summarized in Table 1 along with the corresponding λ_{\max} and E_T as measured by phosphorescence emission spectroscopy. Gratifyingly the TD-DFT calculated triplet energies corresponded well with the order of the observed absorption λ_{\max} and measured E_T values. The three lowest energy (group 3) derivatives displayed overlapping fluorescence and phosphorescence in MCH at 77 K which hampered the estimation of the triplet energy. The analysis of the emission spectra of these compounds in 2-MeTHF at 77 K more readily allowed estimation of the triplet energy (Table 1, entries 9-11). The thioxanthone derivatives span a remarkably wide range of triplet energies from approximately 230 to 290 kJ/mol. As a point of reference, benzophenone has a triplet energy of 289 kJ/mol,²¹ thioxanthone 274 kJ/mol²² and $[\text{Ir}(\text{dF}(\text{CF}_3)\text{ppy})_2(\text{dtbpy})]\text{PF}_6$ is 255 kJ/mol.²³

Also shown in Table 1 are the singlet and triplet lifetimes, as measured using ps and ns time-resolved infrared spectroscopy (TRIR) as this structurally sensitive technique allows characterisation and dynamics of both the singlet and triplet species, together with an estimation of the triplet quantum yield in one convenient measurement at room temperature. These measurements showed a large variation in singlet state lifetime with the different thioxanthone derivatives. The higher energy derivatives with substituents in the 3-position have much shorter singlet state lifetimes before undergoing ISC to the triplet state. These singlet lifetimes are approximately $1000\times$ shorter lived than the lowest energy derivatives (entries 8-11).

Consistent with previous computational studies of thioxanthone,²⁴ DFT calculations predicted the lowest excited singlet state (S_1) was of $\pi\pi^*$ character and S_2 was $n\pi^*$ in polar solvents (MeCN). The T_1 states were calculated to be of $\pi\pi^*$ character, regardless of solvent polarity. There was a strong correlation between the measured singlet state lifetime and the $S_2(n\pi^*)-S_1(\pi\pi^*)$ energy difference (See SI). The smaller the energy difference, the faster the rate of ISC to the triplet state. This could possibly be due to increased involvement of the $n\pi^*$ state, when it is sufficiently close in energy, allowing faster ISC to the triplet states due to El-Sayed's rule.²⁵ This has previously been observed in the case of 1-azathioxanthones which were investigated as antenna chromophores in lanthanide (III) based dyes.²⁶ Triplet quantum yields (Φ_{ISC}) were estimated using bleach recovery kinetics. These were generally between 80 – 90%, but the two lowest energy derivatives, along with 4-MeOTX, were measured at just 60 - 70%.

Sensitizer Evaluation in Alkene Isomerisation. We first assessed the performance of these sensitizers in the simple isomerization of *trans*-alkenes to photostationary *cis/trans* mixtures (Figure 3). Using the pure *trans*-isomers of both β -Me styrene ($E_{T(E)} = 249 \text{ kJmol}^{-1}$, $E_{T(Z)} = 275 \text{ kJmol}^{-1}$)²¹ and methyl cinnamate ($E_T = 229 \text{ kJmol}^{-1}$)²¹ each of the 10 sensitizers were investigated in turn for their ability to effect a photostationary *cis/trans* isomer mixture. To allow rapid screening of the whole sensitizer series with minimal material usage, 0.5 ml samples (0.2 M, 5% sensitizer) in deuterated acetonitrile were irradiated in NMR tubes placed next to a 9 W PL-S low pressure UVA lamp. Multiple samples could be irradiated at once and the reaction was monitored by periodic $^1\text{H-NMR}$ analysis. Pleasingly, for all 10-sensitizers isomerization to a photostationary state was observed within a similar reaction time (30-45 mins), implying equally efficient overall energy transfer rates. These

results immediately demonstrated that the full range of thioxanthone sensitizers can all act as effective sensitizers if the triplet energy is sufficiently high.

Higher energy Group 1 sensitizers gave essentially 1:1 isomerized mixtures in both cases. Slight enrichment in the *cis*-isomer was observed for the medium energy Group 2. Significant enrichment in the *cis*-isomer was observed for the lower energy Group 3 which reached a maximum of 5:1 for β -Me styrene and 2:1 for methyl cinnamate when 2-F,2'-MeOTX was used. Although initially a surprise, this is a known trend observed by others and can be attributed to selective sensitization of the *trans*-isomer with lower energy sensitizers.²⁷ The subsequent drop in *cis/trans* ratio for the lowest energy sensitizer was also noted in the earliest studies and the unusual behaviour observed for low energy triplet sensitizers has been attributed to non-vertical triplet energy transfer.²⁸ Recently there has been renewed interest in the use of organic/organometallic sensitizers for enrichment of *cis*-styrenes by selective isomerization of *trans*.²⁹

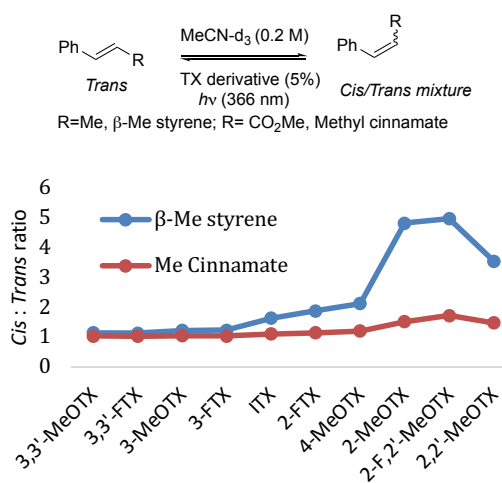


Figure 3. Photostationary *cis/trans* ratios of β -Me styrene and methyl cinnamate with the full range of substituted TX sensitizers at 366 nm (low-pressure UVA lamp).

Sensitizer Evaluation in Preparative Photochemistry.

To investigate the effectiveness of the sensitizer set on a preparative scale, reactions were screened for the intra- and intermolecular [2+2] cycloadditions shown in Figure 4 using a 125 W medium pressure Hg-lamp and a 150 ml immersion well batch reactor. Despite the large predicted triplet energy range, the intramolecular cross [2+2] (Reaction A) showed only moderate variation of productivity across the sensitizer range. This was maintained, even in the case of lowest energy derivative (2,2'-MeOTX). The final yields, as determined by quantitative NMR all exceeded 90% at full conversion.

The intermolecular [2+2] of THPA and propargyl alcohol (Reaction B)³⁰ also proceeded with a similar productivity of 22-26 mmol/h with the first six highest energy sensitizers. The productivity then drops off sharply to 8 mmol/h with 4-MeOTX. This is presumably when the triplet energy of the sensitizer falls below that of THPA. At full conversion the [2+2] yields all reached around 75%, which is typical for this reaction.

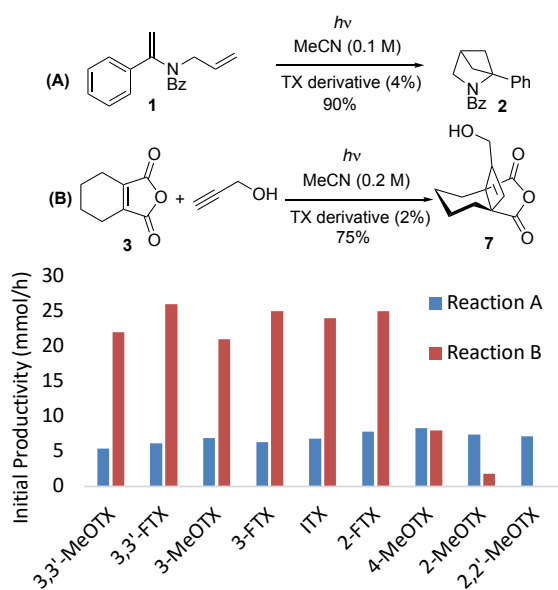


Figure 4. Initial productivities of intra- and intermolecular [2+2] cycloadditions (A) and (B) with a 150 ml immersion well batch reactor and 125 W Hg lamp

Reactions (A) and (B) are both well-studied and reliable triplet sensitized photochemical reactions. To further test the synthetic use of the sensitizer set, a reaction was investigated which is more sensitive to variations in reaction conditions (Figure 5). Reaction (C) is a novel cross [2+2] / retro-Mannich sequence giving γ -amino acid derivative **10**.³¹ In all cases the initial productivity was around 3 mmol/h but there was a large variation in yield across the sensitizer series, with the higher energy sensitizers giving the greatest yields. 3,3'-MeOTX stands out as giving the highest isolated yield of 66%. Conversely, the lowest energy sensitizer (2,2'-MeOTX) resulted in almost full degradation of the reaction mixture within a short period of time. It is possible that the lower energy sensitizers could be undergoing electron transfer from the electron rich enamine or amine intermediate.³²

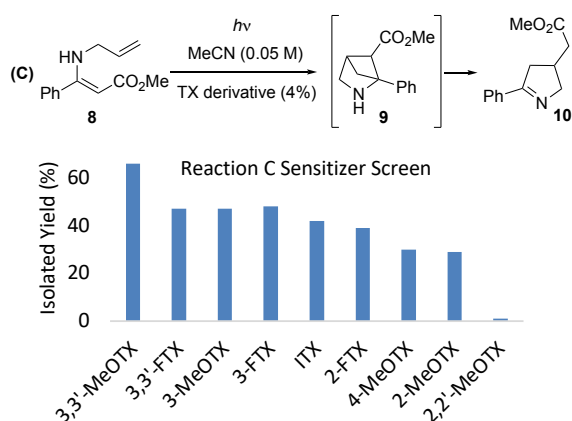


Figure 5. Isolated yields of [2+2] / retro-Mannich product **10**

The above examples were optimized on a preparative scale with a 150 ml batch reactor due to the ready availability

of the starting materials. In cases where the photochemical precursor synthesis is more difficult, it was prudent to screen irradiation conditions on a small scale to save material and prevent unnecessary wastage of the sensitizer. The NMR technique described above was used for optimisation of the cycloaddition of amino acrylate **11** (Reaction D), which had previously been carried out under acetophenone sensitisation.³³ Nearly all the TX sensitizers proved to be very effective in the conversion of enamide **11** (Figure 6). However, unlike the related styrene reaction (Reaction A), the lowest energy sensitizers became ineffective ($E_T < 2$ -FTX).

The unoptimized cross [2+2] of the enamide **13** to **14** represented a more complex multi-chromophore system and proved to be consistently low yielding, requiring long reaction times, with both benzophenone and ITX sensitizers (Reaction E, Table 2, Entry 1&2). Using the NMR tube irradiation method we were able to screen the full sensitizer series in deuterated acetonitrile, using just 0.5 mmol of enamide **13**. It was found that there was a large variation in yield and productivity across the sensitizer range. The maximum yield was limited to just above 50% and obtained with the highest energy sensitizer 3,3'-MeOTX. Moving down in triplet energy it can be seen that the yields and productivity drop off rapidly (Figure 6).

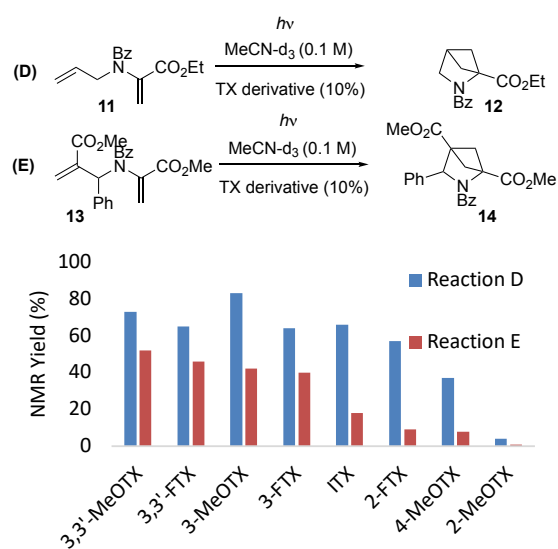


Figure 6. 0.5 ml NMR tube sensitizer screen (366 nm) for rapid optimization of reactions (D) and (E). Yield determined by adiponitrile internal standard after 15 min (D) and 30 min (E)

The value of this rapid NMR method can be seen in the translation of the screening results to the scale-up of Reaction E (Table 2). Using the conventional benzophenone sensitizer gave just over 1g of **14** after 9h irradiation. Conversely using the 3,3'-MeOTX sensitizer identified from above we were able to prepare 5.8g of product in 7 h and in the *same yield* as identified from screening. This result is of significance since the DFT calculations indicate both benzophenone and 3,3'-MeOTX share very similar triplet energies, yet 3,3'-MeOTX is a far superior sensitizer. Both 3-FTX and ITX showed the same drop off in yield and productivity as observed in the NMR screening reactions.

Table 2. Preparative scale reactions using 125 W medium-pressure Hg-lamp in a 150 ml batch reactor

Entry	Sensitizer	Conc. (M)	Time (h)	Yield	Mass (g)
1	BP	0.05	9	46	1.3
2	ITX	0.05	12	38	1.1
3	3-FTX	0.05	5	51	1.45
4	3,3'-MeOTX	0.1	3	56	3.2
5	3,3'-MeOTX	0.2	7	51	5.8

Development of a Visible Light Reactor for Preparative Photochemistry. We then turned our attention to the Group 3 sensitizers, which due to their longer wavelengths of absorption (> 400 nm) should be capable of facilitating triplet state photochemistry in the visible region. Our aim was to enable preparative scale photochemistry with low sensitizer loadings (≤ 1 mol%) using readily available powerful visible light LED sources. Reported visible light mediated photoredox reactions are often driven by a 40 W Kessil lamp or a flexible LED strip placed side-on and a few centimetres away from a vial containing the reaction solution. The overall light capture is poor and as a result the reactions are often left on overnight to drive a successful reaction to completion (Figure 7A). The side-on method of irradiation is necessary since the vials are stirred over a magnetic stirrer and there is no room below for a commercial light source. A successful (4×1.1 W) device for addressing this problem was recently described by McMillan *et al*³⁴ for optimizing photoredox chemistry and has been commercialised and utilised in a number of labs worldwide.

For our present triplet sensitizer focussed chemistry we required significantly higher-powered devices to take productivities from mg/h to multi-grams/h. We have recently shown that excited state photochemistry can be scaled-up predictably with increasing lamp power since the reactions are often photon limited and have a linear relationship with photon-flux.³⁵

Our past experience with the design of UV flow reactors for excited state photochemistry^{14,35,36} demonstrated that much higher productivity levels (\geq kg per day) could be achieved if careful attention was paid to light capture by the photosylate. We therefore sought to engineer a visible light system for sensitised photochemistry at input powers of at least 30 W, which could exploit the high-power density of modern visible LED's in conjunction with readily available lab components such as hotplate stirrer (Figure 7B). To achieve this, we designed a high-intensity blue light reactor system based around *chip-on-board* (COB) LEDs with peak emissions at 455 nm. As these COBs have an output of 36 W from a circular area of only 22 mm diameter, they are ideal for delivering a high photon flux to a standard round bottom flask (50-100 ml). Figures 7C and D show a 36 W COB attached to a standard magnetic stirrer in close proximity to a round bottom flask. The magnetic stirrer surface acts as a heat sink and a small fan prevents hot air stagnating around the flask.

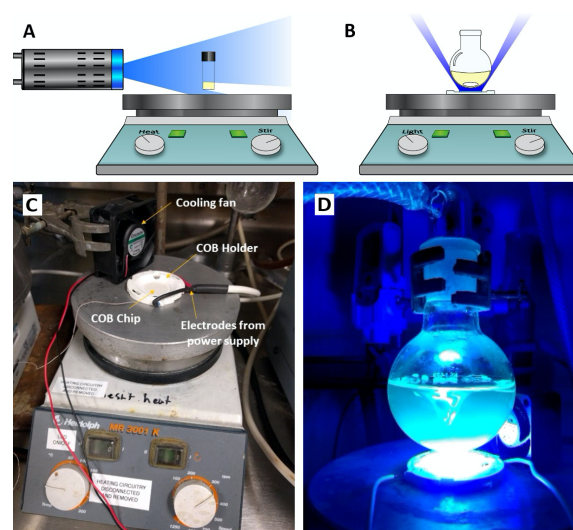


Figure 7. (A) Inefficient side-on irradiation with external lamp over magnetic stirrer. (B) Novel integrated COB LED and magnetic stirrer for maximum light capture. (C) Prototype 455 nm 36 W COB reactor system. (D) Trial reaction, demonstrating irradiation of a stirred vessel

Scale-up of Triplet Sensitized Photochemistry with Visible Light. Simple alkene [2+2] cycloadditions cannot be achieved by direct UV irradiation as alkene absorption is normally ≤ 200 nm. Conjugated alkenes such as styrene undergo sensitized photochemistry from an easily accessible triplet. The cinnamyl alcohol derived diene **15** was chosen as a test substrate. Yoon^{11a} was the first to demonstrate that this substrate underwent [2+2] cycloaddition to the cyclobutene ether **16** in 80% yield after irradiation with white light (23 W) for 28 h with 1 mol% $(\text{Ir}[\text{dF}(\text{CF}_3)\text{ppy}]_2(\text{dtbpy}))\text{PF}_6$ catalyst. We repeated this useful reaction using 2,2'-MeOTX (1 mol%) as sensitizer in a MeCN solution of **15** (0.5 M) with the 455 nm 36 W COB reactor. Remarkably, after just 3 h irradiation (Table 3, Entry 1) the reaction was complete allowing for the isolation of 1.5g (89%) of **16** (0.5 g/h). The aza analogue **17**³⁷ performed even better, providing a high yield (87%) of the bicyclic amine **18** with a productivity of 1.43 g/h.

Interestingly, Oderinde *et al* recently reported^{37b} that the cycloaddition of **17** proceeded using 450 nm irradiation (34 W) and 5 mole % $(\text{Ir}[\text{dF}(\text{CF}_3)\text{ppy}]_2(\text{dtbpy}))\text{PF}_6$ to give 152 mg of **18** in over 24 h. As a like for like comparison this demonstrates that, in conjunction with the 36 W COB reactor, 2,2'-MeOTX at just 1 mol% loading is over 225 times more productive (g/h). As this is the most commonly¹¹ used Iridium based sensitizer for cycloaddition, 2,2'-MeOTX and related sensitizers may find use as convenient and low cost alternatives.

The intramolecular cross [2+2] cycloaddition of amino styrenes has previously been carried out by us in the UV at high

concentrations (0.1-0.4 M) with a 400 W Hg lamp, ITX sensitizer in a Pyrex immersion well batch reactor.^{3a} In this work we first chose to study these reactions with the visible light absorbing Group 3 sensitizers using the blue 36 W COB and enamide **1**. As can be seen from Figure 8 all three sensitizers (1 mol %) were highly effective at 455 nm. In particular 2,2'-MeOTX gave complete conversion to **2** in under 2 h (0.5 M), presumably due to the more optimal overlap of the absorption bands with the emission of the COB at 455 nm.

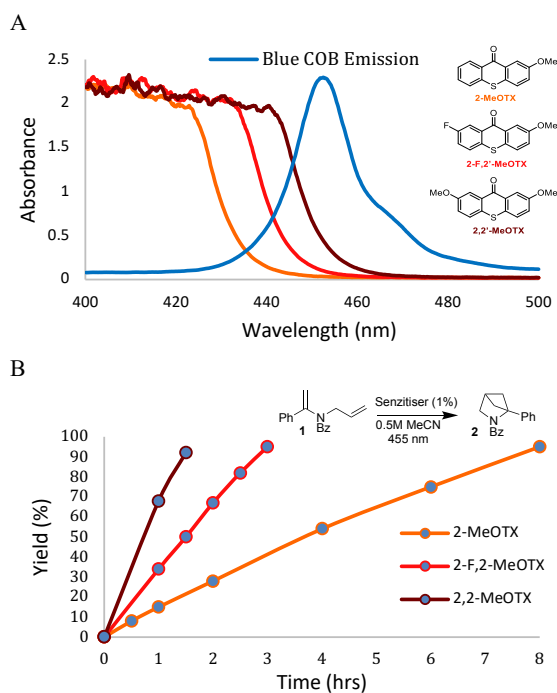


Figure 8. A comparison of (A) UV-Vis absorption spectra and (B) reaction profiles for 3-different visible light sensitizers at 455 nm with the blue COB LED reactor.

We then undertook a preparative study of 5 different enamides using the absorption matched 2,2'-MeOTX/COB system (Table 3, entries 3-7). In all cases this proved to be a remarkably efficient combination, with their productivities exceeding all expectations e.g. up to 6 g/h of **20**. To put this in context, for entries 4 and 7, a single 36 W COB system approached the productivity of the much larger and more powerful 400 W Hg lamp. For this reaction class the visible light COB /2,2'-MeOTX combination was 6 - 9× more energy efficient than the ITX/Hg lamp reaction. Unlike the NH cinnamate **8** the Boc protected derivative **25** undergoes cycloaddition without degradation with the low energy sensitizer 2,2'-MeOTX. Compared to the UV conditions this reaction also showed a 9× increase in energy efficiency when carried out with 2,2'-MeOTX and the blue COB reactor.

Moving away from styrene chromophores we studied the performance of the alkoxy-maleimide **27** which proved to be a

productive cycloaddition using a 125 W Hg UV lamp when irradiated directly (no sensitizer). Pleasingly, carrying out the same reaction at 455 nm with 2,2'-MeOTX gave the product **28** but with more than twice the energy efficiency (productivity per W). Finally, the well-studied Cookson's dione³⁸ **30** was produced in high yield at 455 nm with 2,2'-MeOTX and with more than twice the productivity per W compared to the customary direct irradiation with UV. As with all the other examples the reaction was repeated with 455 nm in the absence of sensitizer and surprisingly was observed to proceed with identical productivity (6 g/h). This interesting observation has not been previously reported in the literature and close inspection of the UV-Vis spectra of the pale yellow starting dione revealed a weak, but significant absorption tail overlapping with the output of the 455 nm COB. This move to the visible should prove to be a useful observation for a variety of Cookson's dione type cycloadditions³⁹ which have previously thought to have been restricted to the UV.

CONCLUSION

This study has demonstrated that modern DFT methods can be used to inform the design (pre-synthesis) of a family of thioxanthone sensitizers that span the UV-Vis region (300-450 nm). Based on this design **9** previously untested sensitizers were synthesised and their DFT calculated triplet energies (E_T) found to be in excellent agreement with those measured by phosphorescence. A rapid NMR screening method was developed to test the efficacy of the entire sensitizer range and proved very effective in optimizing conditions for the scale-up of [2+2] cycloadditions. A new 36 W COB reactor system was developed for the optimal visible light (455 nm) irradiation of stirred vessels. The lower triplet energy sensitizers were found to perform as outstanding sensitizers at 455 nm for a variety of photocycloaddition reactions previously attempted in the UV. For example, on a W per W basis the 2,2'-MeOTX sensitizer, at just 1% loading, proved to be 2-9 times more productive than the corresponding UV reactions. Furthermore, for the same power input 2,2'-MeOTX outperformed Iridium based visible light sensitization of [2+2] cycloadditions by over 200 times (g/h). These outstanding results pave the way for the rational computational design of low-cost, non-metal based organic sensitizers. This should enable the transfer of a range of useful preparative photochemical reactions from the UV to the visible region of the spectra, where modern, compact, powerful and efficient LED based sources are available.

Table 3. Visible light 2,2'-MeOTX triplet sensitized [2+2] cycloadditions of alkenes with a 36 W 455 nm COB and comparison to ITX sensitized process in UV

#	Starting Material	Product	Time h	36 W Blue / 2,2'-MeOTX		UV/ ITX	Efficiency Blue vs. UV
				Yield % (g)	Productivity g/h (mg/h/W)	Productivity g/h (mg/h/W)	
1			3	89 (1.54)	0.51 (14.2)	0.85 (6.8)	2.1x
2			5	87 (7.13)	1.43 (39.7)	1.15 (9.2)	4.3x
3			3	83 (6.58)	2.19 (60.8)	3.89 (9.7)	6.3x
4			1.5	91 (9.05)	6.03 (167.5)	7.11 (17.8)	9.4x
5			3.5	88 (7.78)	2.22 (61.7)	3.51 (8.8)	7.0x
6			6	68 (5.87)	0.98 (27.2)	1.98 (5.0)	5.5x
7			3.75	84 (7.98)	2.13 (59.2)	2.63 (6.6)	9.0x
8			1.5	92 (2.38)	1.59 (44.1)	2.38 (19.0) ^a	2.3x
9			0.4	92 (2.41)	6.0 (166.7)	9.52 (76.2) ^a	2.2x

^aUV results (125W) using no sensitizer

ASSOCIATED CONTENT

Supporting Information

The Supporting Information is available free of charge at <https://pubs.acs.org/doi/xxxxxxx>

Experimental and spectral details for all new compounds and all reactions reported (PDF)

AUTHOR INFORMATION

Corresponding Authors

Luke D. Elliott – [a] School of Chemistry, Cantocks's Close, University of Bristol, Bristol, UK, BS8 1TS; Email: luke.elliott@bristol.ac.uk

Kevin I. Booker-Milburn – [a] School of Chemistry, Cantocks's Close, University of Bristol, Bristol, UK, BS8 1TS; orcid.org/0000-0001-6789-6882; Email: k.booker-milburn@bristol.ac.uk

Authors

Surajit Kayal- [b] School of Chemistry, University of Nottingham, University Park, Nottingham, UK, NG7 2RD; orcid.org/0000-0002-4239-455X; Email: Surajit.Kayal@nottingham.ac.uk

Michael W. George- [b] School of Chemistry, University of Nottingham, University Park, Nottingham, UK, NG7 2RD; [c] Department of Chemical and Environmental Engineering, The University of Nottingham Ningbo China, Ningbo 315100, China orcid.org/0000-0002-7844-1696; Email: Mike.George@nottingham.ac.uk

ACKNOWLEDGMENT

We thank the EPSRC for funding (EP/P013341/1; EP/L003325/1). We thank Dr. Hazel Sparkes for X-ray crystallography of compounds **25** and **26** and Dr Xue Zhong Sun for helpful discussions and assistance with the TRIR measurements.

REFERENCES

- (1) (a) Hoffmann, N. Photochemical Reactions as Key Steps in Organic Synthesis. *Chem. Rev.* **2008**, *108*, 1052-1103. (b) Bach, T.; Hehn, J. P. Photochemical Reactions as Key Steps in Natural Product Synthesis. *Angew. Chem. Int. Ed.* **2011**, *50*, 1000-1045. (c) Kärkäs, M. D.;

- Porco, Jr., J. A.; Stephenson, C. R. J. Photochemical Approaches to Complex Chemotypes: Applications in Natural Product Synthesis. *Chem. Rev.* **2016**, *116*, 9683–9747. (d) Poplata, S.; Tröster, A.; Zou, Y-Q.; Bach, T. Recent Advances in the Synthesis of Cyclobutanes by Olefin [2 + 2] Photocycloaddition Reactions. *Chem. Rev.* **2016**, *116*, 9748–9815. (e) Remy, R.; Bochet, C. G. Arene–Alkene Cycloaddition. *Chem. Rev.* **2016**, *116*, 9816–9849.
- (2) Cox, B.; Booker-Milburn, K. I.; Elliott, L. D.; Robertson-Ralph, M.; Zdorichemko, V. Escaping from Flatland: [2 + 2] Photocycloaddition; Conformationally Constrained sp³-rich Scaffolds for Lead Generation. *ACS Med. Chem. Lett.* **2019**, *10*, 1512–1517
- (3) (a) Elliott, L. D.; Booker-Milburn, K. I. Photochemically Produced Aminocyclobutanes as Masked Dienes in Thermal Electrocyclic Cascade Reactions. *Org. Lett.* **2019**, *21*, 1463–1466. (b) Donnelly, B. L.; Elliott, L. D.; Willis, C.; Booker-Milburn, K. I. Sequential Photochemical and Prins Reactions for the Diastereoselective Synthesis of Tricyclic Scaffolds. *Angew. Chem. Int. Ed.* **2019**, *58*, 9095–9098
- (4) Hammond, G. S.; Turro, N. J.; Leermakers, P. A. The Mechanisms of Photoreactions in Solution. IX. Energy Transfer from the Triplet States of Aldehydes and Ketones to Unsaturated Compounds. *J. Phys. Chem.* **1962**, *66*, 1144–1147
- (5) Denisenko, A. V.; Druzenko, T.; Skalenko, Y.; Samoilenko, M.; Grygorenko, O. O.; Zozulya, S.; Mykhailiuk, P. K. Photochemical Synthesis of 3-Azabicyclo[3.2.0]heptanes: Advanced Building Blocks for Drug Discovery. *J. Org. Chem.* **2017**, *82*, 9627–9636.
- (6) (a) Engel, P. S.; Schexnayder, M. A.; Ziffer, H.; Seeman, J. I. Effect of α -methyl groups on the photochemistry of 3,4,5,6,7,8-hexahydronaphthalen-2(1H)-one. *J. Am. Chem. Soc.* **1974**, *96*, 924–925. (b) Roscini, C.; Cabbage, K. L.; Berry, M.; Orr-Ewing, A. J.; Booker-Milburn, K. I. Reaction Control in Synthetic Organic Photochemistry: Switching between [5+2] and [2+2] Modes of Cycloaddition. *Angew. Chem. Int. Ed.* **2009**, *48*, 8716–8720
- (7) (a) Ravelli, D.; Protti, S.; Neri, P.; Fagnoni, M.; Albini, A. Photochemical technologies assessed: the case of rose oxide. *Green Chem.* **2011**, *13*, 1876. (b) Beatty, J. W.; Douglas, J. J.; Miller, R.; McAtee, R. C.; Cole, K. P.; Stephenson, C. R. J. Photochemical Perfluoroalkylation with Pyridine N-Oxides: Mechanistic Insights and Performance on a Kilogram Scale. *Chem.* **2016**, *1*, 456–472. (c) Harper, K. C.; Moschetta, E. G.; Bordawekar, S. V.; Wittenberger, S. J. A Laser Driven Flow Chemistry Platform for Scaling Photochemical Reactions with Visible Light. *ACS Cent. Sci.* **2019**, *5*, 109–115
- (8) (a) Prier, C. K.; Rankic, D. A.; MacMillan, D. W. C. Visible Light Photoredox Catalysis with Transition Metal Complexes: Applications in Organic Synthesis. *Chem. Rev.* **2013**, *113*, 5322–5363. (b) Romero, N. A.; Nicewicz, D. A. Organic Photoredox Catalysis. *Chem. Rev.* **2016**, *116*, 10075–10166. (c) Shaw, M. H.; Twilton, J.; MacMillan, D. W. C. Photoredox Catalysis in Organic Chemistry. *J. Org. Chem.* **2016**, *81*, 6898–6926. (d) Twilton, J.; Le, C.; Zhang, P.; Shaw, M. H.; Evans, R. W.; MacMillan, D. W. C. The merger of transition metal and photocatalysis. *Nat. Rev. Chem.* **2017**, *1*, 0052
- (9) (a) Rillema, D. P.; Allen, G.; Meyer, T. J.; Conrad, D. Redox properties of ruthenium(II) tris chelate complexes containing the ligands 2,2'-bipyrazine, 2,2'-bipyridine, and 2,2'-bipyrimidine. *Inorg. Chem.* **1983**, *22*, 1617–1622. (b) Lowry, M. S.; Hudson, W. R.; Pascal, Jr., R. A.; Bernhard, S. Accelerated Luminophore Discovery through Combinatorial Synthesis. *J. Am. Chem. Soc.* **2014**, *126*, 14129–14135. (c) Singh, A.; Teegardin, K.; Kelly, M.; Prasad, K. S.; Krishnan, S.; Weaver, J. D. Facile synthesis and complete characterization of homoleptic and heteroleptic cyclometalated Iridium(III) complexes for photocatalysis. *J. Organomet. Chem.* **2015**, *776*, 51–59
- (10) (a) Clennan, E. L.; Liao, C. Synthesis, Characterization, Photochemistry and Photochemistry of Pyrrolyl Electron Transfer Sensitizers. *Photochem. Photobiol.* **2014**, *90*, 344–357. (b) Alfonso, E.; Alfonso, F. S.; Beeler, A. B. Redesign of a Pyrrolyl Photoredox Catalyst and Its Application to the Generation of Carbonyl Ylides. *Org. Lett.* **2017**, *19*, 2989–2992. (c) White, A. R.; Wang, L.; Nicewicz, D. A. Synthesis and Characterization of Acridinium Dyes for Photoredox Catalysis. *Synlett* **2019**, *30*, 827–832
- (11) (a) Lu, Z.; Yoon, T. P. Visible Light Photocatalysis of [2+2] Styrene Cycloadditions by Energy Transfer. *Angew. Chem. Int. Ed.* **2012**, *51*, 10329–10332. (b) Zou, Y-Q.; Duan, S-W.; Meng, X-G.; Hu, X-Q.; Gao, S.; Chen, J-R.; Xiao, W-J. Visible light induced intermolecular [2+2]-cycloaddition reactions of 3-ylideneoxindoles through energy transfer pathway. *Tetrahedron*, **2012**, *68*, 6914–6919. (c) Skubi, K. L.; Kidd, J. B.; Jung, H.; Guzei, I. A.; Baik, M-H.; Yoon, T. P. Enantioselective Excited-State Photoreactions Controlled by a Chiral Hydrogen-Bonding Iridium Sensitizer. *J. Am. Chem. Soc.* **2017**, *139*, 17186–17192. (d) Hörmann, F. M.; Chung, T. S.; Rodriguez, E.; Jakob, M.; Bach, T. Evidence for Triplet Sensitization in the Visible-Light-Induced [2+2] Photocycloaddition of Eniminium Ions. *Angew. Chem. Int. Ed.* **2018**, *57*, 827–831 (e) James, M. J.; Schwarz, J. L.; Strieth-Kalthoff, F.; Wibbeling, B.; Glorius, F. Dearomative Cascade Photocatalysis: Divergent Synthesis through Catalyst Selective Energy Transfer. *J. Am. Chem. Soc.* **2018**, *140*, 8624–8628. (f) Zhu, M.; Zheng, C.; Zhang, X.; You, S-L. Synthesis of Cyclobutane-Fused Angular Tetracyclic Spiroindolines via Visible-Light-Promoted Intramolecular Dearomatization of Indole Derivatives. *J. Am. Chem. Soc.* **2019**, *141*, 2636–2644. (g) Becker, M. R.; Richardson, A. D.; Schindler, C. S. Functionalized azetidines via visible light-enabled aza Paternò-Büchi reactions. *Nat. Commun.* **2019**, *10*, 5095
- (12) Hörmann, F. M.; Kerzig, C.; Chung, T. S.; Bauer, A.; Wenger, O. S.; Bach, T. Triplet Energy Transfer from Ruthenium Complexes to Chiral Eniminium Ions: Enantioselective Synthesis of Cyclobutane-carbaldehydes by [2+2] Photocycloaddition. *Angew. Chem. Int. Ed.* **2020**, *59*, 9659–9668
- (13) Triplet sensitizers are more commonly designed for optoelectronic processes for triplet-triplet annihilation, optical sensors or ¹O₂ generation for photodynamic therapy. See Zhao, J.; Wu, W.; Sun, J.; Guo, S. Triplet photosensitizers: from molecular design to applications. *Chem. Soc. Rev.* **2013**, *42*, 5323–5351
- (14) Elliott, L. D.; Berry, M.; Harji, B.; Klauber, D.; Leonard, J.; Booker-Milburn, K. I. A Small-Footprint, High-Capacity Flow Reactor for UV Photochemical Synthesis on the Kilogram Scale. *Org. Process Res. Dev.* **2016**, *20*, 1806–1811
- (15) Williams, J. D.; Nakano, M.; Gerardy, R.; Rincon, J. A.; de Frutos, O.; Mateos, C.; Monbaliu, J-C. M.; Kappe, C. O. Finding the Perfect Match: A Combined Computational and Experimental Study toward Efficient and Scalable Photosensitized [2 + 2] Cycloadditions in Flow. *Org. Process Res. Dev.* **2019**, *23*, 78–87
- (16) (a) Alonso, R.; Bach, T. A Chiral Thioxanthone as an Organocatalyst for Enantioselective [2+2] Photocycloaddition Reactions Induced by Visible Light. *Angew. Chem. Int. Ed.* **2014**, *53*, 4368–4371. (b) Kumarasamy, E.; Raghunathan, R.; Jockusch, S.; Ugrinov, A.; Sivaguru, J. Tailoring Atropisomeric Maleimides for Stereospecific [2 + 2] Photocycloaddition-Photochemical and Photophysical Investigations Leading to Visible-Light Photocatalysis. *J. Am. Chem. Soc.* **2014**, *136*, 8729–8737. (c) Tröster, A.; Alonso, R.; Bauer, A.; Bach, T. Enantioselective Intermolecular [2 + 2] Photocycloaddition Reactions of 2(1H)-Quinolones Induced by Visible Light Irradiation. *J. Am. Chem. Soc.* **2016**, *138*, 7808–7811. (d) Hölzl-Hobmeier, A.; Bauer, A.; Silva, A. V.; Huber, S. M.; Bannwarth, C.; Bach, T. Catalytic deraacemization of chiral allenes by sensitized excitation with visible light. *Nature*, **2018**, *564*, 240–243. (e) Tröster, A.; Bach, T. Triplet-sensitized di- π -methane rearrangement of N-substituted 2-azabarrelenones. *Chem. Commun.*, **2019**, *55*, 302–305
- (17) Iyer, A.; Clay, A.; Jockusch, S.; Sivaguru, J.; J. Evaluating brominated thioxanthenes as organo-photocatalysts. *Phys. Org. Chem.* **2017**, *30*, e3738
- (18) Qiu, G.; Li, Y.; Wu, J. Recent developments for the photoinduced Ar–X bond dissociation reaction. *Org. Chem. Front.*, **2016**, *3*, 1011–1027
- (19) (a) Pitts, J. N., Jr; Letsinger, R. L.; Taylor, R. P.; Patterson, J. M.; Recktenwald, G.; Martin, R. B. Photochemical Reactions of Benzophenone in Alcohols. *J. Am. Chem. Soc.* **1959**, *81*, 1068–1077. (b) Lathioer, E. C.; Leigh, W. J. Bimolecular hydrogen abstraction from phenols by aromatic ketone triplets. *Photochem. Photobiol.* **2006**, *82*, 291–300. (c) Kamijo, S.; Hoshikawa, T.; Inoue, M. Photochemically Induced Radical Transformation of C(sp³)-H Bonds to C(sp³)-CN Bonds. *Org. Lett.* **2011**, *13*, 5928–5931. (d) Gérardy, R.; Winter, M.; Horn, C. R.; Vizza, A.; Van Hecke, K.; Monbaliu, J-C. M. Continuous-Flow Preparation of γ -Butyrolactone Scaffolds from Renewable Fumaric and Itaconic Acids under Photosensitized Conditions. *Org. Process Res. Dev.* **2017**, *21*, 2012–2017

- (20) Ley, C.; Morlet-Savary, F.; Jacques, P.; Fouassier, J. P. Solvent dependence of the intersystem crossing kinetics of thioxanthone. *Chem. Phys.* **2000**, *255*, 335-346
- (21) Montalti, M.; Credi, A.; Prodi, L.; Gandolfi, M. T. *Handbook of Photochemistry*, 3rd ed.; CRC Press, **2006**
- (22) Herkstroeter, W. G.; Lamola, A. A.; Hammond, G. S. Mechanisms of Photochemical Reactions in Solution. XXVIII. Values of Triplet Excitation energies of Selected Sensitizers. *J. Am. Chem. Soc.* **1964**, *86*, 4537-4540
- (23) Lowry, M. S.; Goldsmith, J. I.; Slinker, J. D.; Rohl, R.; Pascal, Jr., R. A.; Malliaras, G. G.; Bernhard, S. Single-Layer Electroluminescent Devices and Photoinduced Hydrogen Production from an Ionic Iridium(III) Complex. *Chem. Mater.* **2005**, *17*, 5712-5719
- (24) Mündt, R.; Villnow, T.; Ziegenbein, C. T.; Gilch, P.; Marian, C.; Rai-Constapel, V. Thioxanthone in apolar solvents: ultrafast internal conversion precedes fast intersystem crossing. *Phys. Chem. Chem. Phys.* **2016**, *18*, 6637-6647
- (25) (a) Dalton, J. C.; Montgomery, F. C. Solvent effects on Thioxanthone Fluorescence. *J. Am. Chem. Soc.* **1974**, *96*, 6230-6232. (b) Lai, T. I.; Lim, E. C. Photophysical Behavior of Aromatic Carbonyl Compounds Related to Proximity Effect: Thioxanthone. *Chem. Phys. Lett.* **1980**, *73*, 244-248.
- (26) Junker, A. K. R.; Sørensen, T. J. Rationalizing substituent effects in 1-azathioxanthone photophysics. *Methods Appl. Fluoresc.* **2018**, *6*, 014002
- (27) (a) Salties, J.; Hammond, G. S. Mechanisms of Photochemical Reactions in Solution. XVII. *cis-trans* Isomerization of the Stilbenes by Excitation Transfer from Low Energy Sensitizers. *J. Am. Chem. Soc.* **1963**, *85*, 2515-2516. (b) Arai, T.; Sakuragi, H.; Tokumaru, K. Photosensitized *cis-trans* Isomerization of β -Alkylstyrenes. *Bull. Chem. Soc. Jpn.* **1982**, *55*, 2204-2207
- (28) Hammond, G. S.; Salties, J. Mechanisms of Photoreactions in Solution. XVIII. Energy Transfer with Nonvertical Transitions. *J. Am. Chem. Soc.* **1963**, *85*, 2516-2517.
- (29) (a) Singh, K.; Staig, S. J.; Weaver, J. D. Facile Synthesis of Z Alkenes via Uphill Catalysis. *J. Am. Chem. Soc.* **2014**, *136*, 5275-5278. (b) Metternich, J. B.; Gilmour, R. A Bio-Inspired, Catalytic $E \rightarrow Z$ Isomerization of Activated Olefins. *J. Am. Chem. Soc.* **2015**, *137*, 11254-11257. (c) Hou, J.; Ee, A.; Feng, W.; Xu, J.-H.; Zhao, Y.; Wu, J. Visible-Light-Driven Alkyne Hydro-/Carboxylation Using CO₂ via Iridium/Cobalt Dual Catalysis for Divergent Heterocycle Synthesis. *J. Am. Chem. Soc.* **2018**, *140*, 5257-5263. (d) Molloy, J. J.; Metternich, J. B.; Daniliuc, C. G.; Watson, A. J. B.; Gilmour, R. Contra-Thermodynamic, Photocatalytic $E \rightarrow Z$ Isomerization of Styrenyl Boron Species: Vectors to Facilitate Exploration of Two-Dimensional Chemical Space. *Angew. Chem. Int. Ed.* **2018**, *57*, 3168-3172. (e) Faßbender, S. I.; Molloy, J. J.; Mück-Lichtenfeld, C.; Gilmour, R. Geometric $E \rightarrow Z$ Isomerisation of Alkenyl Silanes by Selective Energy Transfer Catalysis: Stereodivergent Synthesis of Triarylethylenes via a Formal anti-Metallometallation. *Angew. Chem. Int. Ed.* **2019**, *58*, 18619 - 18626
- (30) Booker-Milburn, K. I.; Cowell, J. K.; Jiménez, D.; Sharpe, A.; White, A. J. Stereoselective Intermolecular [2+2] photocycloaddition reactions of tetrahydrophthalic anhydride and derivatives with alkenols and alkynols. *Tetrahedron*, **1999**, *55*, 5875-5888
- (31) For a similar sequence with a β -amino enone see (a) Kwak, Y.-S.; Winkler, J. D. Synthesis of 6-Aza-bicyclo[3,2,1]octan-3-ones via Vinyllogous Imide Photochemistry: An Approach to the Synthesis of the Hetisine Alkaloids. *J. Am. Chem. Soc.* **2001**, *123*, 7429-7430. The corresponding β -amino acrylate failed to react under direct irradiation and instead was prepared via oxidation of the ketone, see (b) Krow, G. R.; Lin, G.; Herzon, S. B.; Thomas, A. M.; Moore, K. P.; Huang, Q.; Carroll, P. J. Convenient Preparations of 2,4-Methanopyrrolidine and 5-Carboxy-2,4-methanopyrrolidines. *J. Org. Chem.* **2003**, *68*, 7562-7564
- (32) Allushi, A.; Kutahya, C.; Aydongan, C.; Kreutzer, J.; Yilmaz, G.; Yagci, Y. Conventional Type II photoinitiators as activators for photoinduced metal-free atom transfer radical polymerization. *Polym. Chem.*, **2017**, *8*, 1972-1977
- (33) (a) Pirrung, M. C. Total Synthesis of 2,4-Methanoproline. *Tetrahedron Lett.* **1980**, *21*, 4577-4578. (b) Varnes, J. G.; Lehr, G. S.; Moore, G. L.; Hulsizer, J. M.; Albert, J. S. Efficient preparation of 2,4-methanoproline. *Tetrahedron Lett.* **2010**, *51*, 3756-3758 (c) Levterov, V. V.; Michurin, O.; Borysko, P. O.; Zozulya, S.; Sadkova, I. V.; Tolmachev, A. A.; Mykhailiuk, P. K. Photochemical In-Flow Synthesis of 2,4-Methanopyrrolidines: Pyrrolidine Analogues with Improved Water Solubility and Reduced Lipophilicity. *J. Org. Chem.* **2018**, *83*, 14350-14361
- (34) Le, C.; Wismer, M. K.; Shi, Z.-C.; Zhang, R.; Conway, D. V.; Li, G.; Vachal, P.; Davies, I. W.; MacMillan, D. W. C. A General Small-Scale Reactor To Enable Standardization and Acceleration of Photocatalytic Reactions. *ACS Cent. Sci.* **2017**, *3*, 647-653
- (35) Elliott, L. D.; Knowles, J. P.; Stacey, C. S.; Klauber, D. J.; Booker-Milburn, K. I. Using batch reactor results to calculate optimal flow rates for the scale-up of UV photochemical reactions. *React. Chem. Eng.* **2018**, *3*, 86-93
- (36) (a) Hook, B. D. A.; Dohle, W.; Hirst, P. R.; Pickworth, M.; Berry, M. B.; Booker-Milburn, K. I. *J. Org. Chem.* **2005**, *70*, 7558-7564. (b) Elliott, L. D.; Knowles, J. P.; Koovits, P. J.; Maskill, K. G.; Ralph, M. J.; Lejeune, G.; Edwards, L. J.; Robinson, R. I.; Clemens, I. R.; Cox, B.; Pascoe, D. D.; Koch, G.; Eberle, M.; Berry, M. B.; Booker-Milburn, K. I. *Chem.-Eur. J.* **2014**, *20*, 15226-15232.
- (37) (a) Bach, T.; Krüger, C.; Harms, K. The Stereoselective Synthesis of 2-Substituted 3-Azabicyclo[3.2.0]heptanes by Intramolecular [2+2]-Photocycloaddition Reactions. *Synthesis*, **2000**, *2*, 305-320. (b) Oderinde, M. S.; Kempson, J.; Smith, D.; Meanwell, N. A.; Mao, E.; Pawluczyk, J.; Vetrichevan, M.; Pitchai, M.; Karmakar, A.; Rampulla, R.; Li, J.; Dhar, T. G. M.; Mathur, A. Intramolecular [2+2] Cycloaddition of *N*-Allylcinnamamines and *N*-Allylcinnamamides by Visible-Light Photocatalysis. *Eur. J. Org. Chem.* **2020**, 41-46
- (38) Cookson, R. C.; Crundwell, E.; Hill, R.R.; Hudec, J. Photochemical Cyclisation of Diels-Alder Adducts. *J. Chem. Soc.* **1964**, *0*, 3062-3075
- (39) (a) Kenwright, A. M.; Sellars, J. D. Preparation and complete ¹H and ¹³C assignment of some pentacyclo [5.4.0.0^{2,6}.0^{3,10}.0^{5,9}]undecane-8,11-dione (PCUD) derivatives. *Magn. Reson. Chem.* **2012**, *50*, 803-808. (b) Kotha, S.; Rao, S.; Cheekatla, S. R.; Meshram, M.; Bandi, V.; Seema, V. Realization of Photo-Thermal Metathesis Under Microwave Irradiation Conditions: An Entry to Triquinane Frameworks. *Asian J. Org. Chem.* **2019**, *8*, 2097-2104

Supporting Information

Rational Design of Triplet Sensitizers for the Transfer of Excited State Photochemistry from UV to Visible

Luke D. Elliott,^{*[a]} Surajit Kayal,^[b] Michael W. George^[b]
and Kevin Booker-Milburn^{*[a]}

[a] School of Chemistry, University of Bristol, Cantock's Close, Bristol, BS8 1TS, UK

[b] School of Chemistry, University of Nottingham, University Park, NG7 2RD, UK

Table of Contents

General Details.....	4
General Batch Irradiation Procedure.....	4
Synthesis of Thioxanthone Derivatives	4
Newman-Kwart Rearrangements.....	4
4-methoxythiosalicylic acid.....	5
4-fluorothiosalicylic acid.....	5
5-methoxythiosalicylic acid.....	6
5-fluorothiosalicylic acid.....	6
Ullmann-Coupling / Friedel-Crafts Cyclization to Thioxanthenes.....	7
4-methoxythioxanthone (4-MeOTX).....	7
3-methoxythioxanthone (3-MeOTX).....	8
2-methoxythioxanthone (2-MeOTX).....	8
3-fluorothioxanthone (3-FTX).....	9
2-fluorothioxanthone (2-FTX).....	9
3,6-dimethoxythioxanthone (3,3'-MeOTX).....	10
3,6-difluorothioxanthone (3,3'-FTX).....	10
2-methoxy,7-fluorothioxanthone (2-F,2'-MeOTX).....	11
2,7-dimethoxythioxanthone (2,2'-MeOTX).....	11
UV-Vis Spectra of Thioxanthone Derivatives.....	12
Triplet Measurements of Thioxanthone Derivatives.....	14
Low temperature (77 K) emission measurement:.....	14
ps and ns TRIR Studies.....	16
Instrumentation.....	16
ps (400 nm excitation) TRIR spectra and kinetics of ITX.....	17
Estimation of triplet quantum yield for ITX from the parent bleach recovery kinetics.....	18
TD-DFT Calculations of Thioxanthone Derivatives.....	20
Optimised co-ordinates.....	20
3,3'-MeOTX.....	20
3,3'-FTX.....	21
3-MeOTX.....	22
3-FTX.....	23
TX.....	24
ITX.....	25
2-FTX.....	26
4-MeOTX.....	27
2-MeOTX.....	28

2-F,2'-MeOTX.....	29
2,2'-MeOTX	30
Excited State Energies	31
Synthesis of Novel Photochemical Precursors.....	33
Amino cinnamate 8	33
Boc protection to 25.....	34
α -amido acrylate 13.....	34
Amido styrene 23.....	35
<i>N</i> -Bn-3-(but-3-en-1-yloxy)-maleimide (27).....	36
Novel Reactor Configurations	36
Parallel NMR Tube Irradiations.....	36
36 W Blue COB Reactor Configuration	37
36 W Blue COB Reactor Construction	37
TX Sensitizer Screening Studies.....	38
Alkene Isomerization Studies in NMR Tubes	38
Sensitizer Screen with 125 W, 150 ml Immersion Well Reactor	40
Enamide (1) to 2,4-methanopyrrolidine (2).....	40
THPA (3) to Cyclobutene (7).....	40
Cross [2+2] / retro-Mannich of (8) to (10).....	41
Cross [2+2] Sensitizer Screen in NMR Tubes.....	42
α -amido acrylate (11) to 2,4-methanoproline (12).....	42
α -amido acrylate (13) to 2,4-methanoproline (14).....	42
Preparative Scale Synthesis of 2,4-methanoproline (14).....	43
Blue Light Mediated Reactions with 36 W, 455 nm COB Reactor	44
General procedure.....	44
Intramolecular [2+2] of Styrene 15.....	44
Intramolecular [2+2] of Styrene 17.....	44
Cross [2+2] of Enamide 1	45
Cross [2+2] of Enamide 19	45
Cross [2+2] of Enamide 21	45
Cross [2+2] of Enamide 23	46
Cross [2+2] of Amino Cinnamate 25	46
Intramolecular [2+2] of Alkoxy-maleimide 27.....	47
Cookson's Dione [2+2].....	47
X-Ray Data for 24 and 26.....	49
Copies of ¹ H and ¹³ C NMR Spectra.....	52

General Details

All reagents and solvents were used as purchased and no special precautions were taken to dry or otherwise further purify. For the purposes of thin layer chromatography (tlc), Merck silica-aluminium plates were used, visualising with UV light (254 nm) and/or dipping in potassium permanganate followed by heating. For column chromatography, Sigma Aldrich technical grade 60Å silica gel was used. All NMR data was collected using either a Jeol Eclipse 400 MHz, Varian 400 MHz or Varian 500 MHz instruments. Data was processed directly using MestReNova (version 11.0.2). Chemical shifts (δ) are given in parts per million (ppm). Reference values for residual solvents were taken as $\delta = 7.27$ (CDCl_3), 2.50 (DMSO-d_6) and 2.05 (acetone-d_6) for ^1H NMR and $\delta = 77.16$ ppm (CDCl_3), 39.52 (DMSO-d_6) and 206.26 (acetone-d_6) for ^{13}C NMR. Multiplicities for coupled signals were denoted as: s = singlet, d = doublet, t = triplet, q = quartet, m = multiplet, br. = broad, app. = apparent and dd = double doublet etc. Coupling constants (J) are given in Hz and are quoted to the nearest 0.1 Hz. Where appropriate, COSY, DEPT, HMQC and NOE NMR experiments were carried out to aid assignment. Mass spectrometry data was collected was carried out by the University of Bristol mass spectrometry service using Fisons Autospec or Bruker Daltonics MicrOTOF II instruments. Infrared data was collected using a Perkin-Elmer Spectrum One FTIR machine as thin films or solids compressed on a diamond plate. Melting points are uncorrected and were recorded on Stuart Scientific apparatus.

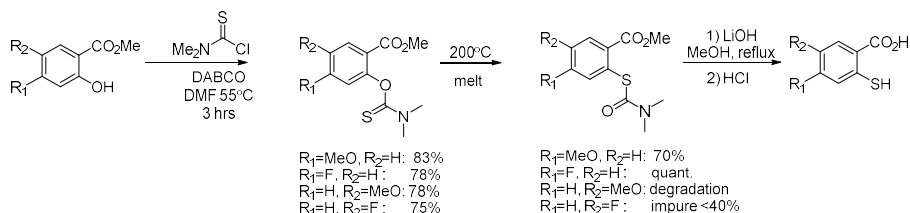
General Batch Irradiation Procedure

For all photochemical reactions, solvents were “degassed” by evacuating a stirred vessel under vacuum and re-filling with N_2 . For the duration of the reaction, N_2 was bubbled through the solution. When photochemical reactions were followed for their duration by NMR, 1,3,5-trimethoxybenzene was used as an internal standard. In all cases, a stock solution (0.05 M) of this was added to aliquots of the reaction mixture prior to NMR sample preparation. Batch reactors, 125 W and 400 W medium pressure mercury lamps were purchased from Photochemical Reactors Ltd. Reading. In all cases, Pyrex immersion wells were used for irradiations.

Synthesis of Thioxanthone Derivatives

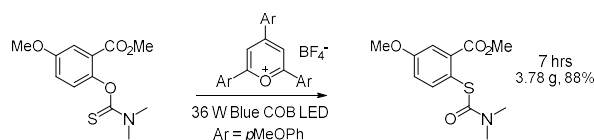
Newman-Kwart Rearrangements

Substituted thiosalicylic acids were prepared from the corresponding methyl thiosalicylic acids via a Newman-Kwart rearrangement as shown (Scheme S1). The thermal Newman-Kwart rearrangement was successfully carried out as a melt for 4-substituted derivatives but the 5-substituted derivatives resulted in extensive degradation.



Scheme S1: Synthesis of thiosalicylic acids

A modification of the photoredox mediated Newman-Kwart rearrangement developed by Nicewicz¹ gave the 5-methoxysalicylate derivative in excellent yield (Scheme S2). Unfortunately, the 5-fluoro derivative failed to react under the photoredox conditions.

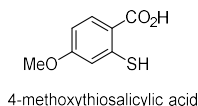


Scheme S2: Photoredox mediated Newman-Kwart

Synthesis of *O*-aryl thiocarbamates

To a solution of the relevant methyl salicylate derivative (200 mmol) and dimethylthiocarbamoyl chloride (37.1 g, 300 mmol) in DMF (100 ml) was added DABCO (33.7 g, 300 mmol) before heating at 55°C for 3 hrs. The mixture was poured over water (500 ml) and extracted with EtOAc (3×300 ml). The combined extracts were dried (MgSO₄), filtered and evaporated to a yellow solid which was washed with Et₂O and dried to give the thiocarbamate as a colourless powder.

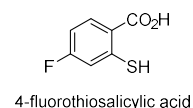
4-methoxythiosalicylic acid



The general procedure for *O*-aryl thiocarbamate synthesis was first followed using methyl 4-methoxysalicylate (45 g, 247 mmol), dimethylthiocarbamoyl chloride (42.7 g, 346 mmol) and DABCO (38.8 g, 346 mmol). After heating at 55°C for 3 hrs the work-up procedure was followed to give methyl 2-((dimethylcarbamothioyl)oxy)-4-methoxybenzoate as a colourless powder (55.2 g, 83%); m.p. 128-129°C (lit. 122-124 °C)²

The *O*-aryl thiocarbamate (57.8 g, 215 mmol) was then heated as a melt at 200°C under N₂ for 5.5 hrs. The cooled mixture was purified by chromatography on silica (40 – 50% EtOAc in petrol) and the concentrated fractions were triturated with Et₂O and filtered to give methyl 2-((dimethylcarbamoyl)thio)-4-methoxybenzoate as a pale orange solid (40.4 g, 70%). To a solution of the *S*-aryl thiocarbamate (40.0 g, 149 mmol) in MeOH (110 ml) was added LiOH (8.91 g, 372 mmol) and the mixture heated at reflux for 2.5 hrs. The cooled solution was quenched with 3M HCl (130 ml), diluted with water (100 ml) and the resulting slurry extracted with EtOAc (500 ml and 2×250 ml). The combined extracts were dried (MgSO₄), filtered and evaporated to give 4-methoxythiosalicylic acid as a white solid (28.0 g) of sufficient purity for further use: δ_H (400 MHz, DMSO-d₆) 7.88 (1H, d, *J* = 8.8 Hz, Ar.H), 7.11 (1H, d, *J* = 2.6 Hz, Ar.H), 6.75 (1H, dd, *J* = 8.8, 2.6 Hz, Ar.H), 3.79 (3H, s, OCH₃); δ_C (101 MHz, DMSO-d₆) 167.3 (C), 161.7 (C), 140.8 (C), 133.3 (CH), 118.8 (C), 115.0 (CH), 110.9 (CH), 55.5 (CH₃)

4-fluorothiosalicylic acid

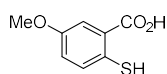


The general procedure for *O*-aryl thiocarbamate synthesis was first followed using methyl 4-fluorosalicylate (29.8 ml, 200 mmol), dimethylthiocarbamoyl chloride (37.1 g, 300 mmol) and DABCO (33.7 g, 300 mmol). After heating at 55°C for 3 hrs the work-up procedure was followed to give methyl 2-((dimethylcarbamothioyl)oxy)-4-fluorobenzoate as a colourless powder (42.3 g, 78%); m.p. 106-107°C (lit. 106.8-107.2°C)³

The *O*-aryl thiocarbamate (41.0 g, 159 mmol) was heated as a melt at 200°C under N₂ for 2.5 hrs to give methyl 2-((dimethylcarbamoyl)thio)-4-fluorobenzoate. The resulting material was of sufficient

purity for subsequent hydrolysis. To a solution of the *S*-aryl thiocarbamate (41.0 g, 159 mmol) in MeOH (110 ml) was added LiOH (9.53 g, 398 mmol) and the mixture heated at reflux for 2.5 hrs. The cooled solution was quenched with 3M HCl (140 ml), diluted with water (100 ml) and the resulting slurry extracted with EtOAc (3×250 ml). The combined extracts were washed (1 M HCl, brine), dried (MgSO₄), filtered and evaporated to give 4-fluorothiosalicylic acid as a white solid (27.6 g) of sufficient purity for further use: δ_{H} (500 MHz, DMSO-d₆) 8.11 (1H, dd, $J = 8.7, 6.0$ Hz, Ar.H), 7.33 (1H, dd, $J = 10.2, 2.5$ Hz, Ar.H), 7.20 (1H, app. td, $J = 8.2, 2.5$ Hz, Ar.H); δ_{C} (126 MHz, DMSO-d₆) 166.8 (C), 164.8 (d, $J = 253.1$ Hz, C), 142.4 (d, $J = 7.7$ Hz, C), 134.7 (d, $J = 9.8$ Hz, CH), 124.8 (d, $J = 2.8$ Hz, C), 113.5 (d, $J = 21.9$ Hz, CH), 111.7 (d, $J = 26.8$ Hz, CH); δ_{F} (377 MHz, CDCl₃) -105.1

5-methoxythiosalicylic acid

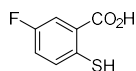


5-methoxythiosalicylic acid

The general procedure for *O*-aryl thiocarbamate synthesis was first followed using methyl 5-methoxysalicylate (29.8 ml, 200 mmol), dimethylthiocarbamoyl chloride (37.1 g, 300 mmol) and DABCO (33.7 g, 300 mmol). After heating at 55°C for 3 hrs the work-up procedure was followed to give methyl 2-((dimethylcarbamoithiyl)oxy)-5-methoxybenzoate as a colourless powder (42.3 g, 78%); m.p. 103-104°C (lit. 99.5-100.5°C)⁴

A solution of the *O*-aryl thiocarbamate (4.31 g, 16 mmol) and 2, 4, 6-tris(4-methoxyphenyl)pyrylium tetrafluoroborate (0.08 mmol, 39 mg) in MeCN (80 ml) was irradiated with a 36 W blue COB LED for 7 hrs. The solvent was removed *in vacuo* and chromatography on silica (10% Et₂O in DCM) yielded methyl 2-((dimethylcarbamoithiyl)thio)-5-methoxybenzoate as a pale yellow solid (3.78 g, 88%). To a solution of the *S*-aryl thiocarbamate (23.0 g, 85.5 mmol) in MeOH (60 ml) was added LiOH (5.13 g, 214 mmol) and the mixture heated at reflux for 2.5 hrs. The cooled solution was quenched with 3M HCl (80 ml) and the resulting slurry extracted with EtOAc (250 ml and 3×100 ml). The combined extracts were washed (1 M HCl, brine), dried (MgSO₄), filtered and evaporated to give 5-methoxythiosalicylic acid (15.7 g) as a pale yellow solid of sufficient purity for further use: δ_{H} (400 MHz, DMSO-d₆) 7.42 (1H, d, $J = 3.0$ Hz, Ar.H), 7.41 (1H, d, $J = 8.7$ Hz, Ar.H), 7.04 (dd, $J = 8.7, 3.0$ Hz, Ar.H), 3.75 (3H, s, OCH₃); δ_{C} (101 MHz, DMSO-d₆) 167.4 (C), 156.4 (C), 131.9 (CH), 128.4 (C), 127.5 (C), 119.6 (CH), 115.4 (CH), 55.3 (CH₃)

5-fluorothiosalicylic acid



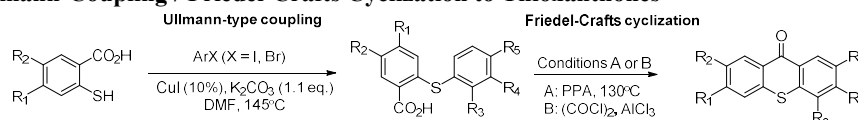
5-fluorothiosalicylic acid

The general procedure for *O*-aryl thiocarbamate synthesis was first followed using methyl 5-fluorosalicylate (40 g, 235 mmol), dimethylthiocarbamoyl chloride (34.9 g, 282 mmol) and DABCO (31.6 g, 282 mmol). After heating at 55°C for 3 hrs the work-up procedure was followed to give methyl 2-((dimethylcarbamoithiyl)oxy)-5-fluorobenzoate as a colourless powder (45.3 g, 75%); m.p. 120-121°C

The *O*-aryl thiocarbamate (43.1 g, 168 mmol) was then heated as a melt at 215 °C under N₂ for 5.5 hrs. The cooled mixture was purified by chromatography on silica (30% EtOAc in petrol) to give a dark oil (25.8 g) which contained the *S*-aryl thiocarbamate in approximately 60% purity due to a significant unknown by-product. To the crude mixture in MeOH (100 ml) was added LiOH (6.36 g, 265 mmol) and the solution heated at reflux for 3 hrs. The cooled solution was quenched with 3M HCl (100 ml), extracted with DCM (3×150 ml), the organic extracts concentrated *in vacuo* and re-dissolved in water (150 ml) with K₂CO₃ (25 g, 181 mmol). The aqueous solution was washed with DCM (2×50 ml) and

acidified with HCl (12 M, 30 ml) to give a pale yellow suspension which was extracted with DCM (3×50 ml). The combined extracts were dried (MgSO₄), filtered and evaporated to give 5-fluorothiosalicylic acid (9.3 g) containing significant impurities, but of sufficient purity for further use

Ullmann-Coupling / Friedel-Crafts Cyclization to Thioxanthenes



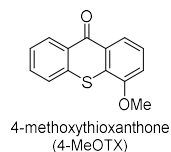
Entry	Thiosalicylic acid		ArX				Product
	R ₁	R ₂	X	R ₃	R ₄	R ₅	
1	H	H	I	MeO	H	H	93%
2	H	H	Br	H	MeO	H	85%
3	H	H	Br	H	H	MeO	92%
4	H	H	I	H	F	H	95%
5	H	H	I	H	H	F	84%
6	MeO	H	I	H	MeO	H	87%
7	F	H	I	H	F	H	78%
8	H	F	Br	H	H	MeO	55%
9	H	MeO	Br	H	H	MeO	62%

Table S1: Ullmann-type coupling of thiosalicylic acids with aryl bromides and iodides

Entry	Conditions	R ₁	R ₂	R ₃	R ₄	R ₅	Product
1	A	H	H	MeO	H	H	81%
2	B	H	H	H	MeO	H	76%
3	A	H	H	H	H	MeO	49%
4	B	H	H	H	F	H	83%
5	A	H	H	H	H	F	94%
6	B	MeO	H	H	MeO	H	69%
7	B	F	H	H	F	H	84%
8	A	H	F	H	H	MeO	62%
9	A	H	MeO	H	H	MeO	80%

Table S2: Intramolecular Friedel-Crafts cyclization to thioxanthenes

4-methoxythioxanthone (4-MeOTX)

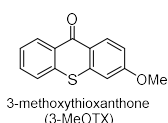


Thiosalicylic acid (30.8 g, 200 mmol) and K₂CO₃ (30.4 g, 220 mmol) were added to DMF (300 ml) in a 1 L flask. CuI (3.8 g, 20 mmol) and 2-iodoanisole (28.6 ml, 220 mmol) were then added and the mixture heated at 145°C for 19 hrs before cooling and pouring over water (500 ml). The aqueous mixture was filtered before acidifying with 3 M HCl (80 ml). The resulting slurry was filtered and the residue washed with water, stirred in EtOH, filtered again and dried to give 2-((2-methoxyphenyl)thio)benzoic acid as a grey power (48.3 g, 93%).

A mixture of the thioether (52 g, 200 mmol) and polyphosphoric acid (100 g) was heated at 130°C for 1 hr before allowing to cool and quenching with water (150 ml). The mixture was mechanically broken up to a suspension which was extracted with DCM (500 ml). The aqueous solution was further extracted

with DCM (2×250 ml) and the combined extracts washed with sat. aq. NaHCO₃ (2×100 ml), dried (MgSO₄), filtered and evaporated to a beige solid (41.5 g) which was recrystallized from MeCN (600 ml) to give 4-methoxythioxanthone as a fluffy solid (39.3 g, 81%): m.p. 168 – 169 °C (lit. 165 °C)⁵; λ_{max} (MeCN)/nm 385 ($\epsilon/M^{-1}\text{cm}^{-1}$ 5,940); δ_{H} (400 MHz, CDCl₃) 8.60 (1H, app. d, $J = 8.1$ Hz), 8.25 (1H, app. d, $J = 8.4$ Hz), 7.66 – 7.58 (2H, m), 7.50 – 7.41 (2H, m), 7.13 (1H, app. d, $J = 7.9$ Hz), 4.03 (3H, s, OCH₃); δ_{C} (101 MHz, CDCl₃) 180.2 (C), 154.5 (C), 137.5 (C), 132.3 (CH), 130.4 (C), 129.8 (CH), 129.1 (C), 127.7 (C), 126.8 (CH), 126.4 (CH), 126.1 (CH), 121.8 (CH), 112.33 (CH) 56.6 (CH₃); ESI-HRMS m/z 243.0474 (MH⁺ C₁₄H₁₁O₂S requires 243.0474)

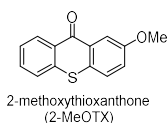
3-methoxythioxanthone (3-MeOTX)



Thiosalicylic acid (30.8 g, 200 mmol) and K₂CO₃ (30.4 g, 220 mmol) were added to DMF (400 ml) in a 1 L flask. CuI (3.8 g, 20 mmol) and 3-bromoanisole (27.9 ml, 220 mmol) were then added and the mixture heated at 145°C for 20 hrs before cooling and pouring over water (600 ml). The aqueous mixture was filtered before acidifying with 3 M HCl (90 ml). The resulting slurry was filtered and the residue washed with water, stirred in EtOH, filtered again and dried to give 2-((3-methoxyphenyl)thio)benzoic acid as a grey power (44.2 g, 85%).

A mixture of the thioether (10 g, 38.4 mmol) in anhydrous DCM (70 ml) with a few drops of DMF was cooled in an ice bath before the addition of (COCl)₂ (3.9 ml, 46 mmol). The stirred mixture was removed from the ice bath until the reaction had reached completion before removing the solvent *in vacuo*. The residue was re-dissolved in anhydrous DCM (100 ml) and the solution cooled in an ice bath before the addition of AlCl₃ (6.13 g, 46 mmol). After stirring overnight the mixture was quenched with water, extracted with DCM (3×150 ml), washed with sat. aq. NaHCO₃, dried (MgSO₄), filtered and evaporated to a beige solid (9 g) which was recrystallized from MeCN (50 ml) to give 3-methoxythioxanthone as an off-white powder (7.1 g, 76%): m.p. 133 – 134 °C (lit. 129 °C)⁴; λ_{max} (MeCN)/nm 367 ($\epsilon/M^{-1}\text{cm}^{-1}$ 5,550); δ_{H} (400 MHz, CDCl₃) 8.62 – 8.58 (1H, m), 8.55 (1H, d, $J = 9.0$ Hz), 7.62 – 7.51 (2H, m), 7.49 – 7.44 (1H, m), 7.03 (1H, dd, $J = 9.0, 2.5$ Hz), 6.96 (1H, d, $J = 2.4$ Hz), 3.92 (3H, s, OCH₃); δ_{C} (101 MHz, CDCl₃) 179.2 (C), 162.7 (C), 139.7 (C), 137.1 (C), 132.1 (CH), 132.1 (CH), 129.9 (CH), 129.5 (C), 126.4 (CH), 125.9 (CH), 123.2 (C), 115.3 (CH), 108.2 (CH), 55.8 (CH₃); ESI-HRMS m/z 243.0475 (MH⁺ C₁₄H₁₁O₂S requires 243.0474)

2-methoxythioxanthone (2-MeOTX)

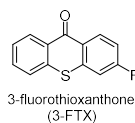


Thiosalicylic acid (30.8 g, 200 mmol) and K₂CO₃ (30.4 g, 220 mmol) were added to DMF (300 ml) in a 1 L flask. CuI (3.8 g, 20 mmol) and 4-bromoanisole (27.9 ml, 220 mmol) were then added and the mixture heated at 145°C for 20 hrs before cooling and pouring over water (600 ml). The aqueous mixture was filtered before acidifying with 3 M HCl (90 ml). The resulting slurry was filtered and the residue washed with water, stirred in MeOH, filtered again and dried to give 2-((4-methoxyphenyl)thio)benzoic acid as a grey power (47.8 g, 92%).

A mixture of the thioether (46 g, 177 mmol) and polyphosphoric acid (180 g) was heated at 130°C for 4.5 hrs before allowing to cool and quenching with water (150 ml). The mixture was mechanically broken up to a suspension which was extracted with DCM, washed with sat. aq. NaHCO₃, dried (MgSO₄), filtered and evaporated to a yellow solid (25) which was recrystallized from MeCN (200 ml)

to give 2-methoxythioxanthone as a fluffy yellow solid (20.8 g, 49%): m.p. 128 – 129 °C (lit. 129 °C)⁶; λ_{max} (MeCN)/nm 399 ($\epsilon/M^{-1}\text{cm}^{-1}$ 6,050); δ_{H} (400 MHz, CDCl_3) 8.65 – 8.61 (1H, m), 8.08 (1H, d, $J = 2.9$ Hz), 7.64 – 7.56 (2H, m), 7.51 – 7.45 (2H, m), 7.26 (1h, dd, $J = 8.8, 3.0$ Hz), 3.94 (3H, s, OCH_3); δ_{C} (101 MHz, CDCl_3) 179.8 (C), 158.6 (C), 137.7 (C), 132.2 (CH), 130.4 (C), 130.0 (CH), 129.3 (C), 128.8 (C), 127.4 (CH), 126.2 (CH), 126.1 (CH), 122.9 (CH), 110.5 (CH), 55.9 (CH_3); ESI-HRMS m/z 243.0476 (MH^+ $\text{C}_{14}\text{H}_{11}\text{O}_2\text{S}$ requires 243.0474)

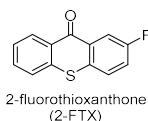
3-fluorothioxanthone (3-FTX)



Thiosalicyclic acid (30.8 g, 200 mmol) and K_2CO_3 (30.4 g, 220 mmol) were added to DMF (300 ml) in a 1 L flask. CuI (3.8 g, 20 mmol) and 3-fluoroiodobenzene (25.8 ml, 220 mmol) were then added and the mixture heated at 145°C for 19 hrs before cooling and pouring over water (500 ml). The aqueous mixture was filtered before acidifying with 3 M HCl (90 ml). The resulting slurry was filtered and the residue washed with water, stirred in hot MeOH (70 ml), filtered again and dried to give 2-((3-fluorophenyl)thio)benzoic acid as a grey power (47.1 g, 95%).

To a stirred mixture of the thioether (10 g, 40.3 mmol) in anhydrous DCM (90 ml) with a few drops of DMF was added $(\text{COCl})_2$ (4.1 ml, 48.5 mmol). When the reaction had reached full conversion after 3 hrs the solvent was removed *in vacuo*, the residue was re-dissolved in anhydrous DCM (130 ml) and the solution cooled in an ice bath before the addition of AlCl_3 (6.5 g, 48.7 mmol). After stirring for 1 hr the mixture was quenched with water (80 ml) and extracted with DCM (3×150 ml). The combined organic extracts were washed with sat. aq. NaHCO_3 , dried (MgSO_4), filtered and evaporated to a beige solid which was recrystallized from MeCN (90 ml) to give 3-fluorothioxanthone as a colourless powder (7.7 g, 83%): m.p. 166 – 167 °C; λ_{max} (MeCN)/nm 370 ($\epsilon/M^{-1}\text{cm}^{-1}$ 5,710); δ_{H} (400 MHz, CDCl_3) 8.63 (1H, dd, $J = 9.0, 6.0$ Hz), 8.61 – 8.57 (1H, m), 7.62 (1H, ddd, $J = 8.4, 7.0, 1.5$ Hz), 7.56 – 7.52 (1H, m), 7.49 (1H, ddd, $J = 8.2, 7.0, 1.3$ Hz), 7.24 (1H, dd, $J = 8.8, 2.5$ Hz), 7.17 (1H, ddd, $J = 9.0, 8.0, 2.5$ Hz); δ_{C} (101 MHz, CDCl_3) 179.1 (C), 164.8 (d, $J = 256.8$ Hz, C), 139.8 (d, $J = 10.2$ Hz, C), 136.9 (C), 133.2 (d, $J = 9.9$ Hz, CH), 132.5 (CH), 130.0 (CH), 129.2 (C), 126.8 (CH), 126.1 (d, $J = 2.1$ Hz, C), 126.0 (CH), 115.1 (d, $J = 22.5$ Hz, CH), 112.0 (d, $J = 24.6$ Hz, CH); δ_{F} (376 MHz, CDCl_3) -104.8; ESI-HRMS m/z 231.0271 (MH^+ $\text{C}_{13}\text{H}_8\text{OFS}$ requires 231.0274)

2-fluorothioxanthone (2-FTX)

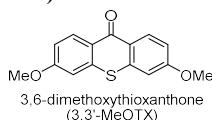


Thiosalicyclic acid (30.8 g, 200 mmol) and K_2CO_3 (30.4 g, 220 mmol) were added to DMF (400 ml) in a 1 L flask. CuI (3.8 g, 20 mmol) and 4-fluoroiodobenzene (24.2 ml, 220 mmol) were then added and the mixture heated at 145°C for 12 hrs before cooling and pouring over water (500 ml). The aqueous mixture was filtered before acidifying with 3 M HCl (90 ml). The resulting slurry was filtered and the residue washed with water, stirred in hot MeOH (70 ml), filtered again and dried to give 2-((4-fluorophenyl)thio)benzoic acid as a grey power (41.9 g, 84%).

A mixture of the thioether (40.5 g, 163 mmol) and polyphosphoric acid (150 g) was heated at 130°C for 11 hrs before allowing to cool and quenching with water (150 ml). The mixture was mechanically broken up to a suspension which was extracted with DCM (500 ml). The aqueous solution was further extracted with DCM (2×250 ml) and the combined extracts washed with sat. aq. NaHCO_3 (2×100 ml), dried (MgSO_4), filtered and evaporated to give 2-fluorothioxanthone as an off white solid (35.4 g, 94%):

m.p. 170 – 171 °C (lit. 171 °C)⁷; λ_{max} (MeCN)/nm 388 ($\epsilon/M^{-1}\text{cm}^{-1}$ 6,310); δ_{H} (400 MHz, CDCl_3) 8.63 – 8.58 (1H, m), 8.29 (1H, dd, $J = 9.6, 2.9$ Hz), 7.66 – 7.54 (3H, m), 7.49 (1H, ddd, $J = 8.2, 6.9, 1.4$ Hz), 7.38 (1H, ddd, $J = 8.8, 7.5, 2.9$ Hz); δ_{C} (101 MHz, CDCl_3) 179.3 (d, $J = 2.4$ Hz, C), 161.3 (d, $J = 247.6$ Hz, C), 137.3 (C), 132.7 (d, $J = 2.4$ Hz, C), 132.6 (CH), 131.0 (d, $J = 6.5$ Hz, C), 130.1 (CH), 128.43 (C), 128.1 (d, $J = 7.4$ Hz, CH), 126.7 (CH), 126.1 (CH), 121.2 (d, $J = 24.2$ Hz, CH), 115.5 (d, $J = 22.9$ Hz, CH); δ_{F} (376 MHz, CDCl_3) -113.6; ESI-HRMS m/z 231.0270 (MH^+ $\text{C}_{13}\text{H}_8\text{OFS}$ requires 231.0274)

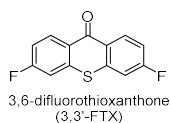
3,6-dimethoxythioxanthone (3,3'-MeOTX)



4-Methoxythiosalicylic acid (17.6 g, 96 mmol) and K_2CO_3 (14.6 g, 106 mmol) were added to DMF (200 ml) in a 1 L flask. CuI (1.83 g, 9.6 mmol) and 3-bromoanisole (13.4 ml, 106 mmol) were then added and the mixture heated at 145°C for 2.5 hrs before cooling and pouring over water (300 ml). The aqueous mixture was filtered before acidifying with 3 M HCl (40 ml). The resulting slurry was filtered and the residue washed with water, dissolved in EtOAc (300 ml), washed with brine, dried (MgSO_4) and filtered. The solution was evaporated *in vacuo* to give 4-methoxy-2-((3-methoxyphenyl)thio)benzoic acid as a white power (24.2 g, 87%).

To a stirred mixture of the thioether (10 g, 34.4 mmol) in anhydrous DCM (70 ml) with a few drops of DMF was added $(\text{COCl})_2$ (3.5 ml, 41.3 mmol). When the reaction had reached full conversion after 1 hr the solvent was removed *in vacuo*, the residue was re-dissolved in anhydrous DCM (130 ml) and the solution cooled in an ice bath before the addition of AlCl_3 (5.51 g, 41.3 mmol). After stirring for 1 hr the mixture was quenched with water (50 ml) and extracted with DCM (3×150 ml). The combined organic extracts were washed with sat. aq. NaHCO_3 , dried (MgSO_4), filtered and evaporated to a beige solid (9.2 g) which was recrystallized from MeCN (90 ml) to give 3,6-dimethoxythioxanthone as a colourless powder (6.5 g, 69%): m.p. 175°C; λ_{max} (MeCN)/nm 354 ($\epsilon/M^{-1}\text{cm}^{-1}$ 5,850); δ_{H} (400 MHz, CDCl_3) 8.52 (2H, d, $J = 9.0$ Hz), 7.00 (2H, dd, $J = 9.0, 2.5$ Hz), 6.92 (2H, d, $J = 2.5$ Hz), 3.91 (6H, s, OCH_3); δ_{C} (101 MHz, CDCl_3) 178.5 (C), 162.4 (C), 139.3 (C), 132.0 (CH), 123.3 (C), 114.9 (CH), 108.2 (CH), 55.8 (CH_3); ESI-HRMS m/z 273.0572 (MH^+ $\text{C}_{15}\text{H}_{13}\text{O}_3\text{S}$ requires 273.0580)

3,6-difluorothioxanthone (3,3'-FTX)

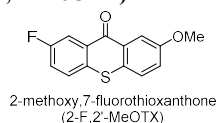


4-Fluorothiosalicylic acid (27 g, 157 mmol) and K_2CO_3 (24.2 g, 175 mmol) were added to DMF (250 ml) in a 1 L flask. CuI (3.1 g, 16 mmol) and 3-fluoroiodobenzene (20.6 ml, 175 mmol) were then added and the mixture heated at 145°C for 3 hrs before cooling and pouring over water (400 ml). The aqueous mixture was filtered before acidifying with 3 M HCl (70 ml). The resulting slurry was filtered and the residue washed with water, stirred in hot MeOH (80 ml), filtered again and dried to give 4-fluoro-2-((3-fluorophenyl)thio)benzoic acid as a white power (32.5 g, 78%).

To a stirred mixture of the thioether (10 g, 37.6 mmol) in anhydrous DCM (90 ml) with a few drops of DMF was added $(\text{COCl})_2$ (3.8 ml, 45 mmol). When the reaction had reached full conversion after 2 hrs the solvent was removed *in vacuo*, the residue was re-dissolved in anhydrous DCM (130 ml) and the solution cooled in an ice bath before the addition of AlCl_3 (6.0 g, 45 mmol). After stirring for 1 hr the mixture was quenched with water (80 ml) and extracted with DCM (3×150 ml). The combined organic extracts were washed with sat. aq. NaHCO_3 , dried (MgSO_4), filtered and evaporated to a pale orange solid (9.0 g) which was recrystallized from MeCN (100 ml) to give 3,6-difluorothioxanthone as a

colourless powder (7.8 g, 84%); m.p. 207 – 208 °C; $\lambda_{\max}(\text{MeCN})/\text{nm}$ 361 ($\epsilon/\text{M}^{-1}\text{cm}^{-1}$ 5,290); δ_{H} (400 MHz, CDCl_3) 8.62 (2H, dd, $J = 9.0, 5.8$ Hz), 7.25 – 7.16 (4H, m); δ_{C} (101 MHz, CDCl_3) 178.0 (C), 164.8 (d, $J = 257.2$ Hz, C), 139.2 (d, $J = 10.0$ Hz, C), 133.3 (d, $J = 10.0$ Hz, CH), 125.9 (d, $J = 2.5$ Hz, C), 115.4 (d, $J = 22.3$ Hz, CH), 112.0 (d, $J = 24.8$ Hz, CH); δ_{F} (376 MHz, CDCl_3) -104.5; ESI-HRMS m/z 249.0174 (MH^+ $\text{C}_{13}\text{H}_7\text{OF}_2\text{S}$ requires 249.0180)

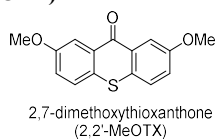
2-methoxy,7-fluorothioxanthone (2-F,2'-MeOTX)



5-Fluorothiosalicylic acid (9.3 g, 54 mmol) and K_2CO_3 (7.5 g, 54 mmol) were added to DMF (100 ml) in a 250 ml flask. CuI (0.95 g, 5.0 mmol) and 4-bromoanisole (6.8 ml, 54 mmol) were then added and the mixture heated at 145°C for 23 hrs before cooling and pouring over water (200 ml). The aqueous mixture was filtered through celite before acidifying with 3 M HCl (25 ml). The resulting slurry was filtered and the residue dissolved in EtOAc (200 ml), dried (MgSO_4) and filtered. The solution was evaporated *in vacuo* to a slurry which was washed with Et_2O and dried to give 5-fluoro-2-((4-methoxyphenyl)thio)benzoic acid as a white powder (8.2 g, 55%).

A mixture of the thioether (1.0 g, 3.6 mmol) and polyphosphoric acid (5 ml) was heated at 120°C for 1 hr before allowing to cool and quenching with water (10 ml). The mixture was mechanically broken up to a suspension which was extracted with DCM and Et_2O . The combined extracts were dried (MgSO_4), filtered and evaporated to a yellow solid (0.68 g) which was recrystallized from MeCN (12 ml) to give 2-methoxy,7-fluorothioxanthone as a fluffy yellow powder (858 mg, 62%); m.p. 160 - 161°C; $\lambda_{\max}(\text{MeCN})/\text{nm}$ 408 ($\epsilon/\text{M}^{-1}\text{cm}^{-1}$ 6,220); δ_{H} (400 MHz, CDCl_3) 8.29 (1H, dd, $J = 9.7, 2.9$ Hz), 8.04 (1H, d, $J = 2.9$ Hz), 7.57 (1H, dd, $J = 8.8, 4.8$ Hz), 7.49 (1H, d, $J = 8.8$ Hz), 7.41 – 7.33 (1H, m), 7.30 – 7.24 (1H, m), 3.94 (3H, s); δ_{C} (101 MHz, CDCl_3) 179.0 (d, $J = 2.3$ Hz, C), 161.2 (d, $J = 247.3$ Hz, C), 158.7 (C), 132.94 (d, $J = 2.4$ Hz, C), 130.3 (d, $J = 6.5$ Hz, C), 129.5 (C), 129.2 (C), 128.1 (d, $J = 7.5$ Hz, CH), 127.4 (CH), 123.2 (CH), 121.0 (d, $J = 24.2$ Hz, CH), 115.4 (d, $J = 22.8$ Hz, CH), 110.4 (d, $J = 1.5$ Hz, CH), 55.8 (CH₃); δ_{F} (376 MHz, CDCl_3) -113.9; ESI-HRMS m/z 261.0376 (MH^+ $\text{C}_{14}\text{H}_{10}\text{O}_2\text{FS}$ requires 261.0380)

2,7-dimethoxythioxanthone (2,2'-MeOTX)



5-Methoxythiosalicylic acid (15.5 g, 84 mmol) and K_2CO_3 (12.8 g, 93 mmol) were added to DMF (200 ml) in a 1 L flask. CuI (1.6 g, 8.4 mmol) and 4-bromoanisole (13.4 ml, 93 mmol) were then added and the mixture heated at 145°C for 23 hrs before cooling and pouring over water (300 ml). The aqueous mixture was filtered before acidifying with 3 M HCl (40 ml). The resulting slurry was filtered and the residue, dissolved in EtOAc (200 ml), washed with brine, dried (MgSO_4) and filtered. The solution was evaporated *in vacuo* to a slurry which was washed with Et_2O and dried to give 5-methoxy-2-((4-methoxyphenyl)thio)benzoic acid as an off white solid (15.1 g, 62%).

A mixture of the thioether (13.9 g, 48 mmol) and polyphosphoric acid (130 g) was heated at 120°C for 1 hr before allowing to cool and quenching with water (100 ml). The mixture was mechanically broken up to a suspension which was extracted with DCM, washed with sat. aq. NaHCO_3 , dried (MgSO_4), filtered and evaporated to a yellow solid (11.8 g) which was recrystallized from MeCN (155 ml) to give 2,7-dimethoxythioxanthone as a fluffy yellow solid (10.5 g, 80%); m.p. 155 – 157 °C; $\lambda_{\max}(\text{MeCN})/\text{nm}$

415 ($\epsilon/M^{-1}cm^{-1}$ 6,270); δ_H (400 MHz, $CDCl_3$) 8.08 (2H, d, $J = 2.9$ Hz), 7.49 (2H, d, $J = 8.9$ Hz), 7.25 (2H, dd, $J = 8.9, 2.9$ Hz), 3.94 (6H, s); δ_C (101 MHz, $CDCl_3$) 179.5 (C), 158.4 (C), 129.7 (C), 129.6 (C), 127.5 (CH), 122.8 (CH), 110.4 (CH), 55.8 (CH₃); ESI-HRMS m/z 273.0573 (MH⁺ C₁₅H₁₃O₃S requires 273.0580)

UV-Vis Spectra of Thioxanthone Derivatives

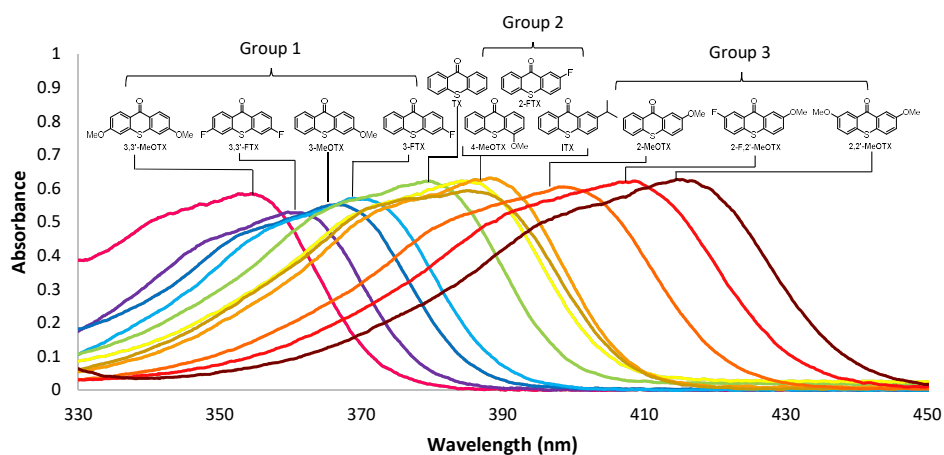
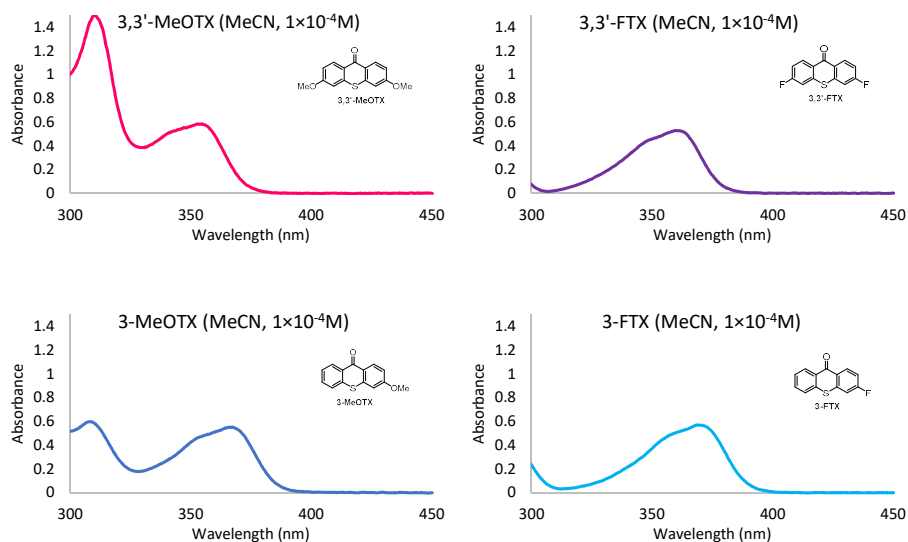


Figure S1: Composite UV-vis spectra of TX derivatives (MeCN, 1×10^{-4} M)



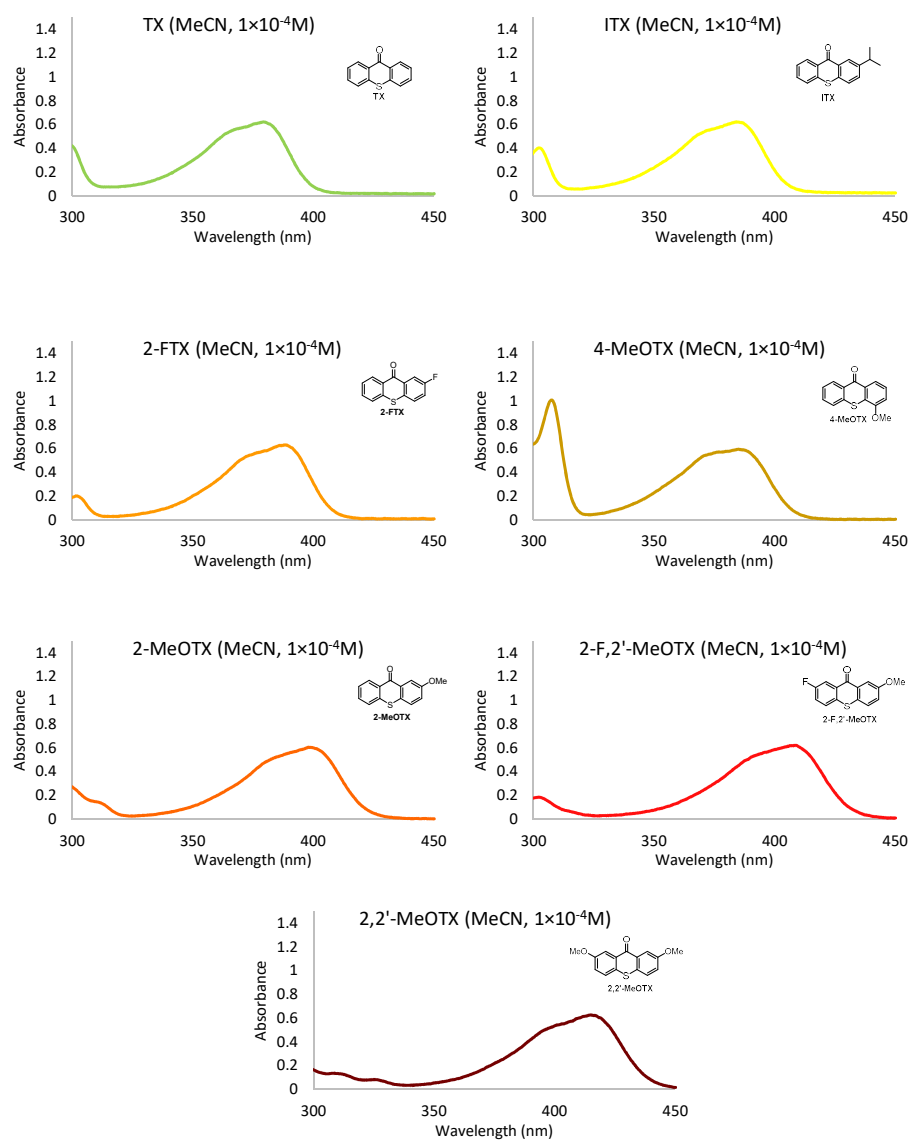


Figure S2: Individual UV-vis absorption spectra of TX derivatives

Triplet Measurements of Thioxanthone Derivatives

Low temperature (77 K) emission measurement:

The low temperature emission spectra were measured in FLS900 Fluorescence spectrometer (Edinburgh Instrument). The room temperature absorption spectra were measured in UV-Vis spectrometer (Agilent Cary 60). For all the measurements 10 μM concentration was used. Methylcyclohexane (Alfa Aesar), 2-methyl tetrahydrofuran (Alfa Aesar) were used as received.

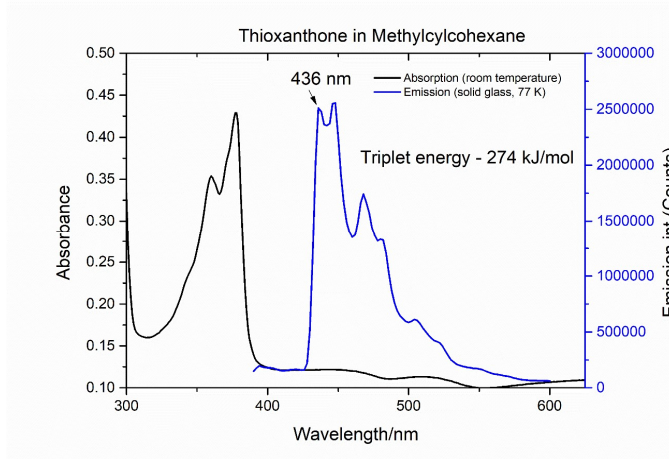


Figure S3: Room temperature absorption and glass temperature emission spectra of thioxanthone in methylcyclohexane. The excitation wavelength was 380 nm.

In Figure S3, the room temperature absorption and glass temperature emission spectra are presented for the thioxanthone. It is well known that the thioxanthone is nonemissive in nonpolar solvents at room temperature. Therefore, the strong red-shifted emission observed in nonpolar solvent (Methylcyclohexane) at glass temperature is safely assigned to the emission from the triplet state. The highest energy emission band (436 nm) is used as the lowest triplet energy and it matches well with the reported triplet energy of thioxanthone. The emission and absorption spectra of other molecules are presented in Figure S4

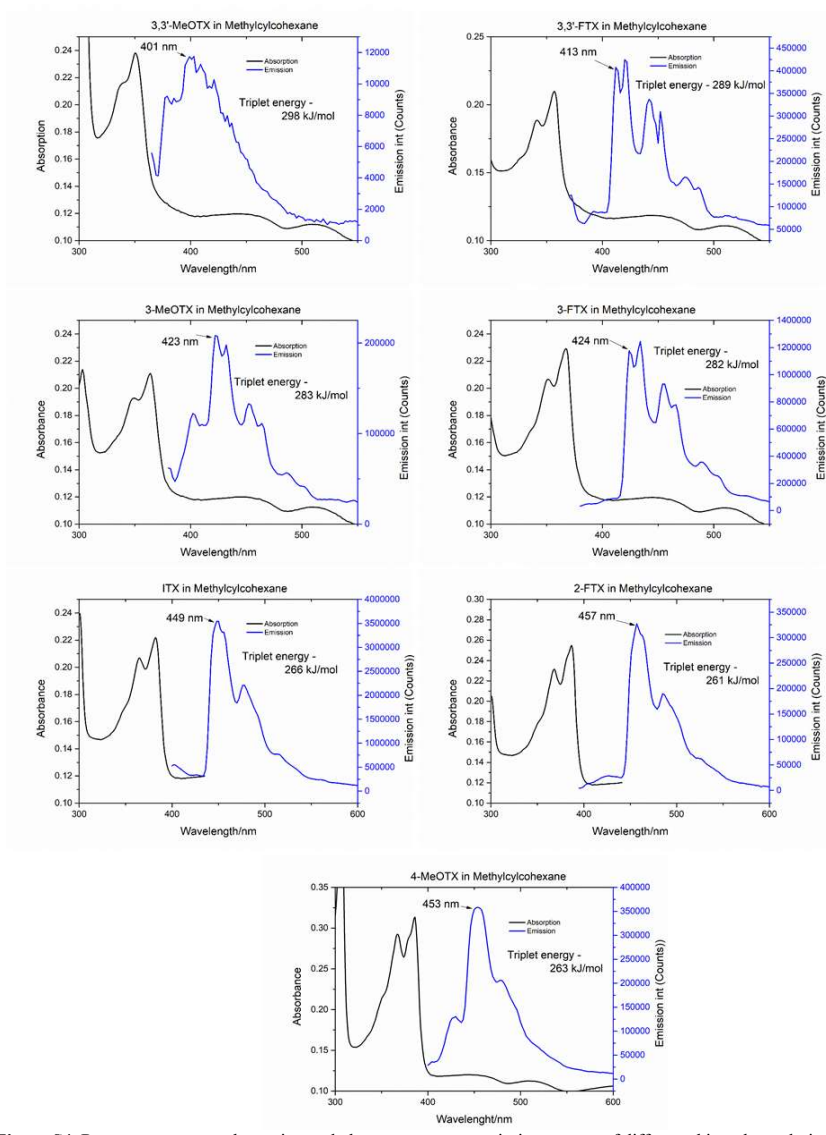


Figure S4. Room temperature absorption and glass temperature emission spectra of different thioxathone derivatives in methylcyclohexane. The lowest energy bands are mentioned and the calculated triplet energies are reported. The excitation wavelengths are: 350 nm (3,3'- MeOTX), 360 nm (3,3'-FTX), 370 nm (3-MeOTX), 375 nm (3-FTX), 380 nm (ITX), 385 nm (2-FTX), 390 nm (4-MeOTX) respectively.

The emission results at 77K in 2-MeTHF for the last three derivatives, 2-MeOTX, 2-F,2'-MeOTX, 2,2'-MeOTX are shown in Figure S5

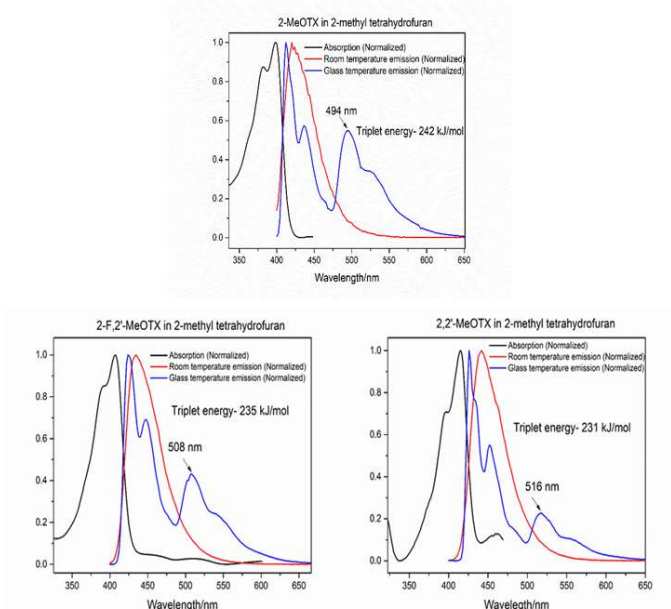


Figure S5. Room temperature absorption, room temperature emission and 77K emission of the thioxanthone derivatives in 2-methyl tetrahydrofuran. For all the measurements 390 nm excitation wavelength was used. Here we have plotted all the spectra with x-axis normalized.

ps and ns TRIR Studies

Instrumentation

We performed ps and ns time-resolved infrared (TRIR) measurements in order to measure the singlet and triplet lifetimes. All the measurements were performed in CD_3CN (1 mM). Each solution was degassed using three freeze pump thaw cycles before time-resolved measurements. The sample Harrick cell (path length 400 μm) with CaF_2 windows was continuously raster scan in order to avoid photodamage. The detailed description of the TRIR measurements at the Nottingham has been discussed in detail elsewhere.⁸ Briefly, 800 nm, 100 fs, 80 MHz fundamental pulses are generated with a commercial Ti:Sapphire oscillator (MaiTai). The input pulses are amplified in a Ti:Sapphire amplifier (Spitfire Pro/Spectra Physics) to produce 800 nm, 100 fs, 1 kHz, 2 mJ pulses. Half of the output is used to pump a TOPAS-C (Light Conversion) that produces tunable IR pulses using a difference frequency generator. The other part of the amplifier output is used to pump a harmonic generator (Timeplate tripler, Minioptic Technology) to produce 400 nm, 100 fs pump pulses. For 355 nm picosecond experiments, we have used a second TOPAS output pumped by the 800 nm fundamental. The IR beam passes through a Ge beam splitter and half of the IR beam is reflected onto a single element MCT detector (Kolmar Technology) to serve as a reference and the other half is focused and overlaps with the pump beam at the sample position. The pump pulse was delayed relative to the probe pulse by using a translation stage (LMA Actuator, Aerotech, USA). The polarization of the pump pulse was set at the magic angle (54.7°) relative to the probe pulse to avoid rotational diffusion. For a measurement with a longer time delays a Q-switched Nd:YVO ns-laser (ACE- 25QSPXHP/MOPA, Advanced Optical Technology, UK) was employed as a pump source and this was synchronized relative to the Spitfire Pro amplifier output. The IR probe beam was dispersed with a spectrograph and detected with a 128 element HgCdTe linear array detector (Infrared Associates, USA).

ps (400 nm excitation) TRIR spectra and kinetics of ITX

The ps and ns TRIR spectra of ITX in CD₃CN as the photophysical properties (singlet lifetime, triplet quantum yield) are well known. The ps TRIR spectra of ITX in the 1650-1450 cm⁻¹ region for selected time delays after 400 nm excitation were presented in Figure S6. The negative peaks at 1637 and 1592 cm⁻¹ are associated with the ground state bleach and are assigned to $\nu(\text{C}=\text{O})$ and $\nu(\text{C}=\text{C})$ bands respectively. The transient peak at 1477 cm⁻¹ appears immediately after the flash and is assigned to the singlet excited state. The 1477 cm⁻¹ band decays at the same rate (240 ± 10 ps) as a new band at 1518 cm⁻¹ grows in and this peak is assigned to the triplet state.

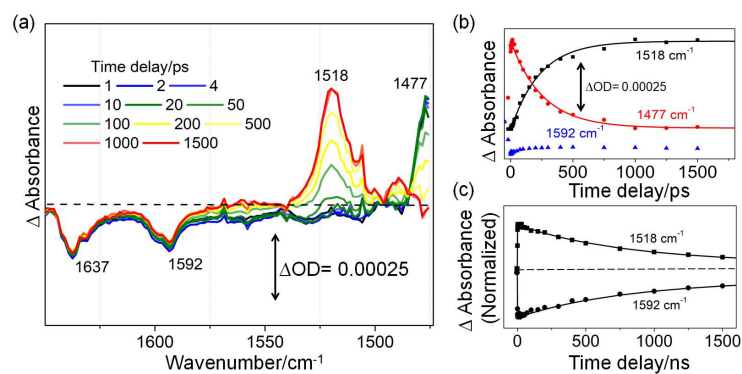


Figure S6. (a) ps-TRIR spectra of ITX for selected time delays in CD₃CN following photoexcitation (400 nm). (b) and (c) show selected TRIR kinetic traces associated with the formation and decay of the parent (1592 cm⁻¹), singlet (1477 cm⁻¹) and triplet (1518 cm⁻¹) excited state bands obtained from TRIR spectra.

Estimation of triplet quantum yield for ITX from the parent bleach recovery kinetics

The triplet quantum yield (Φ_{ISC}) is estimated from the parent bleach recovery kinetics using the approximation that triplet quantum yield is given by the $\Delta A^{max} / \Delta A^{\infty}$ ratio.

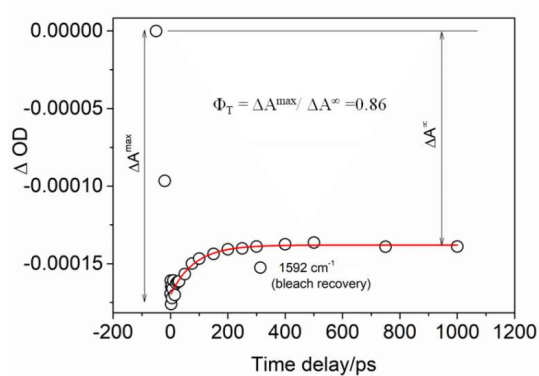


Figure S7. ps intensity kinetics of 1592 cm^{-1} band. The initial bleach recovery is associated with ground state recovery due to radiative (fluorescence) and nonradiative (internal conversion) decays. The bleach recovery at longer time is used to calculate the triplet quantum yield.

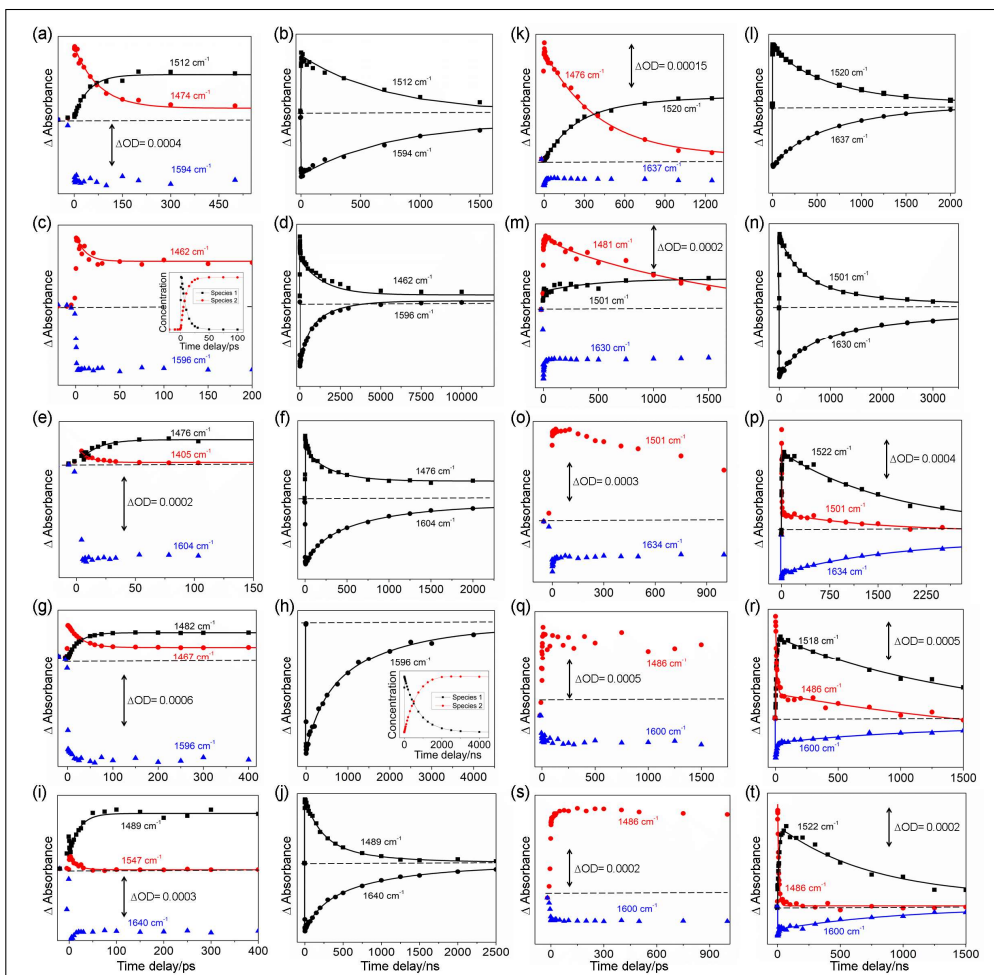


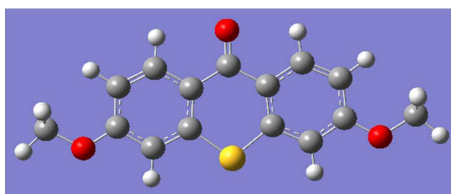
Figure S8. Selected TRIR kinetic traces associated with the singlet, triplet excited states and ground state displaying decay of the singlet state, formation and decay of the triplet state, and ground state recovery for the thioxathone derivatives in CD₃CN. The characteristic transient IR peaks associated with excited state singlet, triplet state and parent of TX {(a) and (b)}; 3,3'-MeOTX {(c) and (d)} – please note the insert to (c) which shows the results from global analysis to more clearly show the decay of the singlet and the growth of the triplet; 3,3'-FTX (e) and (f)}; 3-MeOTX {(g) and (h)} – please note the insert to (h) which shows the results from global analysis to clearly show the recovery of parent; 3-FTX {(i) and (j)-FTX {(k) and (l)}; 4-MeOTX {(m) and (n)}; 2-MeOTX {(o) and (p)}; 2-F,2'-MeOTX {(q) and (r)}; 2,2'-MeOTX {(s) and (t)} are shown.

TD-DFT Calculations of Thioxanthone Derivatives

Calculations were carried out with Gaussian09W on a standard desktop PC (Octo-Core Intel i7-9700, 16 GB RAM)⁹

Optimised co-ordinates

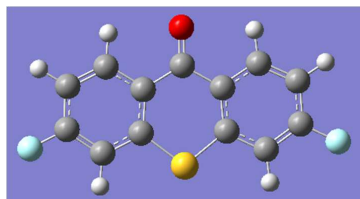
3,3'-MeOTX



Charge = 0 Multiplicity = 1

# opt b3lyp/6-31g(d,p) geom=connectivity				# opt b3lyp/6-31g(d,p) scrf=(cpcm,solvent=acetonitrile) geom=connectivity			
C	2.62616	-1.20095	-0.00017	C	2.62328	-1.20037	-0.00502
C	1.39402	-0.55507	0	C	1.39404	-0.55274	-0.01169
C	1.28285	0.84041	0.00005	C	1.28096	0.84344	-0.00732
C	2.47053	1.60535	0.00005	C	2.47416	1.60622	0.0044
C	3.72255	1.00171	-0.00003	C	3.7217	1.00077	0.01178
C	3.78835	-0.40397	-0.00007	C	3.79028	-0.4068	0.00703
H	2.72348	-2.28645	-0.00043	H	2.7164	-2.2876	-0.00855
H	2.38366	2.69979	0.00015	H	2.39494	2.70044	0.00759
H	4.62038	1.61058	-0.0001	H	4.62526	1.60869	0.02098
C	0	1.58152	0.00001	C	0	1.57574	-0.01455
O	0	2.8042	-0.0001	O	0	2.80559	-0.02539
C	-1.28284	0.84041	0.0001	C	-1.28096	0.84344	-0.00723
C	-1.39401	-0.55506	0.00011	C	-1.39404	-0.55274	-0.01175
C	-2.47052	1.60536	0.00015	C	-2.47416	1.60621	0.00465
C	-2.62617	-1.20095	0.00004	C	-2.62328	-1.20037	-0.00519
C	-3.72255	1.00172	0.00011	C	-3.7217	1.00076	0.01197
H	-2.38365	2.69979	0.00022	H	-2.39494	2.70044	0.00801
C	-3.78835	-0.40397	-0.00004	C	-3.79028	-0.40681	0.00702
H	-2.72348	-2.28644	0.00004	H	-2.7164	-2.2876	-0.00895
H	-4.62037	1.61059	0.00022	H	-4.62526	1.60869	0.02126
S	0	-1.61602	0.00032	S	0	-1.61508	-0.02879
O	4.93884	-1.14594	0.00012	O	4.93565	-1.14493	0.01343
O	-4.93884	-1.14593	-0.00039	O	-4.93564	-1.14493	0.01336
C	6.20772	-0.44281	-0.00029	C	6.21232	-0.4448	0.02703
H	6.30771	0.15996	0.90692	H	6.30693	0.15462	0.93764
H	6.92256	-1.27695	0.00003	H	6.92471	-1.2814	0.03003
H	6.30746	0.15922	-0.90801	H	6.32249	0.16143	-0.87729
C	-6.20774	-0.44282	-0.00018	C	-6.21231	-0.44479	0.02696
H	-6.30761	0.1599	-0.90743	H	-6.3225	0.16135	-0.87741
H	-6.92257	-1.27696	-0.00055	H	-6.9247	-1.28139	0.0301
H	-6.30761	0.15926	0.90751	H	-6.3069	0.1547	0.93752

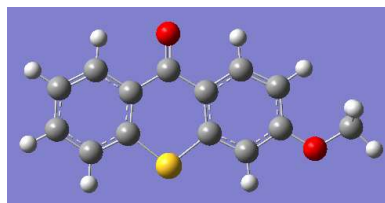
3,3'-FTX



Charge = 0 Multiplicity = 1

# opt b3lyp/6-31g(d,p) geom=connectivity				# opt b3lyp/6-31g(d,p) scrf=(cpcm,solvent=acetonitrile) geom=connectivity			
C	-1.26551	-0.00002	-2.63026	C	-0.00061	-1.26507	-2.62752
C	-0.61501	0.00023	-1.38956	C	-0.00005	-0.61344	-1.38777
C	0.77732	0.00019	-1.28649	C	0.00053	0.78027	-1.2855
C	1.54813	0	-2.47299	C	0.00052	1.54896	-2.47498
C	0.94041	-0.00028	-3.72298	C	-0.00005	0.93951	-3.7233
C	-0.46211	-0.00035	-3.77003	C	-0.0006	-0.46314	-3.76787
H	-2.35447	0.00006	-2.70765	H	-0.00104	-2.35651	-2.70291
H	2.64275	0.00013	-2.38499	H	0.00098	2.64344	-2.39519
H	1.53502	-0.00052	-4.63664	H	-0.00007	1.53631	-4.63782
C	1.52289	0.00026	0	C	0.00118	1.51891	0
O	2.74215	0.00029	0	O	0.00224	2.74415	0
C	0.77732	0.00019	1.28649	C	0.00053	0.78027	1.2855
C	-0.61501	0.00023	1.38956	C	-0.00005	-0.61344	1.38777
C	1.54813	0	2.47299	C	0.00052	1.54896	2.47498
C	-1.26551	-0.00002	2.63026	C	-0.00061	-1.26507	2.62752
C	0.94041	-0.00028	3.72298	C	-0.00005	0.93951	3.7233
H	2.64275	0.00013	2.38499	H	0.00098	2.64344	2.39519
C	-0.46211	-0.00035	3.77003	C	-0.0006	-0.46314	3.76787
H	-2.35447	0.00006	2.70765	H	-0.00104	-2.35651	2.70291
H	1.53502	-0.00052	4.63664	H	-0.00007	1.53631	4.63782
S	-1.6754	0.0007	0	S	-0.00005	-1.67511	0
F	-1.0552	-0.00064	-4.96142	F	-0.00115	-1.05758	-4.95934
F	-1.0552	-0.00064	4.96142	F	-0.00115	-1.05758	4.95934

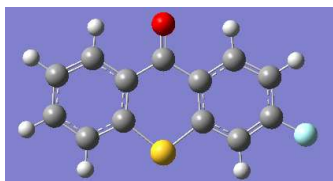
3-MeOTX



Charge = 0 Multiplicity = 1

# opt b3lyp/6-31g(d,p) geom=connectivity				# opt b3lyp/6-31g(d,p) scrf=(cpcm,solvent=acetonitrile) geom=connectivity			
C	3.24792	-1.5541	-0.00014	C	3.24499	-1.55372	0.02514
C	2.05814	-0.81243	0.00008	C	2.05806	-0.81065	-0.0122
C	2.06601	0.582	0.00002	C	2.06497	0.58505	-0.00471
C	3.31133	1.24643	-0.00026	C	3.31209	1.24684	0.04361
C	4.50088	0.52347	-0.00049	C	4.49912	0.52204	0.08203
C	4.46827	-0.87943	-0.00044	C	4.46598	-0.88101	0.07231
H	3.22775	-2.64447	-0.0001	H	3.22702	-2.64668	0.01852
H	3.31948	2.34256	-0.00027	H	3.32918	2.34163	0.04977
H	5.45727	1.04449	-0.00073	H	5.45822	1.04176	0.11952
H	5.40137	-1.44374	-0.00063	H	5.39999	-1.44787	0.10233
C	0.8388	1.42904	0.00021	C	0.83809	1.42323	-0.04614
O	0.9423	2.64574	0.00033	O	0.94303	2.64581	-0.09475
C	-0.49608	0.79217	0.00022	C	-0.49369	0.79517	-0.02423
C	-0.71805	-0.5909	0.00025	C	-0.71684	-0.5888	-0.0329
C	-1.61995	1.64938	0.00017	C	-1.62312	1.65052	0.00432
C	-1.99818	-1.13565	0.00013	C	-1.9945	-1.13542	-0.0152
C	-2.91551	1.14761	0.00005	C	-2.91401	1.14628	0.02423
H	-1.44646	2.73346	0.00022	H	-1.45745	2.735	0.01046
C	-3.09324	-0.24887	-0.0001	C	-3.0942	-0.25196	0.01417
H	-2.18157	-2.21006	0.00022	H	-2.17371	-2.21179	-0.0226
H	-3.76227	1.82586	0.00009	H	-3.76642	1.82359	0.04673
S	0.5868	-1.75802	0.0005	S	0.58746	-1.75608	-0.07694
O	-4.29878	-0.89621	-0.00054	O	-4.29463	-0.89578	0.03144
C	-5.50802	-0.09444	-0.00037	C	-5.51113	-0.09611	0.06727
H	-5.5598	0.514	-0.90783	H	-5.58576	0.52173	-0.83281
H	-6.28674	-0.86938	-0.00053	H	-6.28803	-0.87308	0.07763
H	-5.55979	0.51373	0.90726	H	-5.5443	0.50399	0.98176

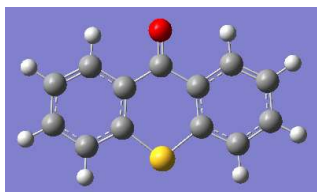
3-FTX



Charge = 0 Multiplicity = 1

# opt b3lyp/6-31g(d,p) geom=connectivity				# opt b3lyp/6-31g(d,p) scrf=(cpcm,solvent=acetonitrile) geom=connectivity			
C	-2.86991	-1.53686	-0.00021	C	-2.86544	-1.53659	-0.02403
C	-1.67411	-0.80513	0.00014	C	-1.6725	-0.8033	0.01751
C	-1.67041	0.58961	0.00013	C	-1.66888	0.59281	0.00869
C	-2.91065	1.26464	-0.00011	C	-2.91098	1.26483	-0.04561
C	-4.10568	0.55125	-0.00055	C	-4.10302	0.54922	-0.08867
C	-4.08461	-0.852	-0.00066	C	-4.08074	-0.85427	-0.07726
H	-2.85925	-2.62765	-0.0001	H	-2.85644	-2.62987	-0.01613
H	-2.91039	2.36092	0.00012	H	-2.91949	2.35985	-0.05244
H	-5.05828	1.07997	-0.00097	H	-5.05817	1.07618	-0.13098
H	-5.02275	-1.40858	-0.00105	H	-5.01927	-1.41379	-0.11078
C	-0.43878	1.42617	0.00025	C	-0.43875	1.42123	0.05625
O	-0.52455	2.6425	0.0003	O	-0.52457	2.64199	0.12211
C	0.89759	0.77425	0.00025	C	0.89627	0.77738	0.01898
C	1.09923	-0.60766	0.00022	C	1.09749	-0.60588	0.02967
C	2.02619	1.62759	0.00019	C	2.02721	1.62867	-0.02528
C	2.38416	-1.16727	-0.00009	C	2.38107	-1.16681	0.00034
C	3.31644	1.11109	-0.00014	C	3.31542	1.11016	-0.05696
H	1.86006	2.71291	0.00047	H	1.86937	2.71441	-0.03347
C	3.46303	-0.28469	-0.00038	C	3.46	-0.28584	-0.04238
H	2.53818	-2.24783	-0.00004	H	2.53377	-2.24981	0.00965
H	4.18511	1.76908	-0.00031	H	4.1845	1.7701	-0.09151
S	-0.2112	-1.76292	0.00073	S	-0.21112	-1.76066	0.09169
F	4.69422	-0.79091	-0.00074	F	4.69081	-0.79357	-0.07176

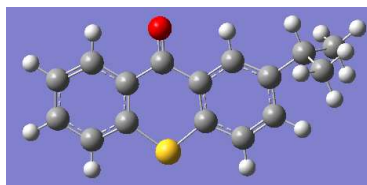
TX



Charge = 0 Multiplicity = 1

# opt b3lyp/6-31g(d,p) geom=connectivity				# opt b3lyp/6-31g(d,p) scrf=(cpcm,solvent=acetonitrile) geom=connectivity			
C	1.40696	-0.00037	2.63682	C	1.4066	-0.04575	2.62959
C	0.76295	0.00015	1.39092	C	0.76095	0.03354	1.38872
C	-0.62817	0.00023	1.28808	C	-0.63164	0.02252	1.28548
C	-1.38992	0.00003	2.47735	C	-1.39091	-0.07579	2.4732
C	-0.76414	-0.00058	3.72009	C	-0.76236	-0.15809	3.71129
C	0.63742	-0.00089	3.7991	C	0.63923	-0.14175	3.79008
H	2.4956	-0.00032	2.70314	H	2.49737	-0.03504	2.69853
H	-2.48318	0.00046	2.39839	H	-2.48344	-0.08476	2.40279
H	-1.3591	-0.00103	4.63242	H	-1.35592	-0.23467	4.62405
H	1.12515	-0.00145	4.77459	H	1.12987	-0.20574	4.76472
C	-1.3748	0.00037	0	C	-1.36714	0.11568	0
O	-2.59423	0.00055	0	O	-2.58404	0.26102	0
C	-0.62817	0.00023	-1.28808	C	-0.63164	0.02252	-1.28548
C	0.76295	0.00015	-1.39092	C	0.76095	0.03354	-1.38872
C	-1.38992	0.00003	-2.47735	C	-1.39091	-0.07579	-2.4732
C	1.40696	-0.00037	-2.63682	C	1.4066	-0.04575	-2.62959
C	-0.76414	-0.00058	-3.72009	C	-0.76236	-0.15809	-3.71129
H	-2.48318	0.00046	-2.39839	H	-2.48344	-0.08476	-2.40279
C	0.63742	-0.00089	-3.7991	C	0.63923	-0.14175	-3.79008
H	2.4956	-0.00032	-2.70314	H	2.49737	-0.03504	-2.69853
H	-1.3591	-0.00103	-4.63242	H	-1.35592	-0.23467	-4.62405
H	1.12515	-0.00145	-4.77459	H	1.12987	-0.20574	-4.76472
S	1.82154	0.00095	0	S	1.81481	0.17012	0

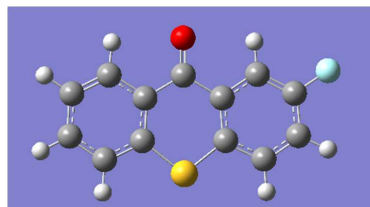
ITX



Charge = 0 Multiplicity = 1

# opt b3lyp/6-31g(d,p) geom=connectivity				# opt b3lyp/6-31g(d,p) scrf=(cpcm,solvent=acetonitrile) geom=connectivity			
C	-3.86202	-1.09679	-0.00092	C	-3.84902	-1.09621	-0.12531
C	-2.5326	-0.64939	0.00003	C	-2.52821	-0.64821	0.00957
C	-2.22007	0.71015	0.00029	C	-2.21578	0.71264	0.03803
C	-3.28036	1.64321	-0.00047	C	-3.27133	1.64512	-0.07844
C	-4.60361	1.21337	-0.00142	C	-4.58626	1.21357	-0.21635
C	-4.89413	-0.16011	-0.00163	C	-4.87622	-0.16002	-0.23825
H	-4.0924	-2.16274	-0.00114	H	-4.08201	-2.16382	-0.14503
H	-3.03659	2.71181	-0.00026	H	-3.03714	2.71427	-0.05672
H	-5.41494	1.93979	-0.00199	H	-5.39569	1.9401	-0.30683
H	-5.93216	-0.49441	-0.00235	H	-5.91091	-0.49561	-0.34545
C	-0.83396	1.25346	0.00144	C	-0.83847	1.24228	0.19279
O	-0.65069	2.45916	0.00282	O	-0.66079	2.43983	0.38222
C	0.32743	0.31998	0.00075	C	0.32557	0.32283	0.10696
C	0.21571	-1.06966	0.00052	C	0.21418	-1.06767	0.08471
C	1.61587	0.89362	0.00041	C	1.61359	0.897	0.05205
C	1.35208	-1.89101	0.00001	C	1.34809	-1.88822	0.01289
C	2.76016	0.09366	-0.00007	C	2.75539	0.09753	-0.02251
H	1.69462	1.9871	0.00058	H	1.6995	1.98855	0.07048
C	2.61642	-1.30745	-0.00027	C	2.61082	-1.30429	-0.04104
H	1.25493	-2.97748	-0.00019	H	1.25312	-2.97735	-0.00295
H	3.50455	-1.94049	-0.00065	H	3.49901	-1.93894	-0.09973
S	-1.31843	-1.90637	0.001	S	-1.31964	-1.90218	0.16437
C	4.13389	0.73704	-0.0004	C	4.12897	0.73921	-0.08418
H	4.00983	1.85258	0.00059	H	4.0111	1.85389	-0.0226
C	4.90791	0.35186	1.26616	C	4.9852	0.29286	1.10624
H	5.86527	0.88214	1.31935	H	5.94784	0.81769	1.11809
H	4.33999	0.6033	2.16976	H	4.48712	0.50128	2.06004
H	5.12718	-0.72033	1.30552	H	5.20478	-0.78064	1.07933
C	4.90628	0.35387	-1.26855	C	4.80897	0.41248	-1.41863
H	4.33779	0.60804	-2.17103	H	4.19339	0.72527	-2.26987
H	5.86423	0.88312	-1.32142	H	5.7736	0.9264	-1.50582
H	5.12424	-0.71849	-1.31061	H	5.00388	-0.66009	-1.53178

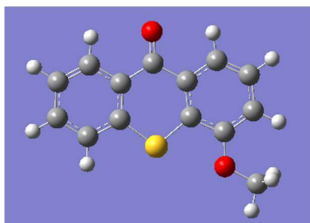
2-FTX



Charge = 0 Multiplicity = 1

# opt b3lyp/6-31g(d,p) geom=connectivity				# opt b3lyp/6-31g(d,p) scrf=(cpcm,solvent=acetonitrile) geom=connectivity			
C	-3.08091	-1.24277	-0.00041	C	-3.06901	-1.24197	-0.08992
C	-1.7846	-0.70758	-0.00006	C	-1.78015	-0.70545	0.02753
C	-1.56353	0.66987	0.00018	C	-1.55921	0.67385	0.03305
C	-2.68384	1.53054	0.00038	C	-2.67528	1.53284	-0.08703
C	-3.97517	1.01293	0.00011	C	-3.95936	1.0124	-0.20742
C	-4.1733	-0.37686	-0.00032	C	-4.1571	-0.37762	-0.20767
H	-3.24037	-2.32191	-0.00076	H	-3.23094	-2.32309	-0.09247
H	-2.51239	2.6133	0.00076	H	-2.51271	2.6155	-0.08222
H	-4.83368	1.68364	0.00033	H	-4.8164	1.68199	-0.30094
H	-5.18705	-0.77983	-0.00075	H	-5.16794	-0.7831	-0.30179
C	-0.21906	1.30439	-0.0001	C	-0.22099	1.29491	0.16717
O	-0.10883	2.51738	-0.00052	O	-0.11086	2.49963	0.35134
C	1.00592	0.4461	0.0001	C	1.0032	0.44832	0.06471
C	0.98425	-0.94877	-0.00004	C	0.98112	-0.94695	0.06601
C	2.24925	1.11072	0.00017	C	2.24426	1.11272	-0.03002
C	2.16926	-1.7056	-0.00036	C	2.16281	-1.70509	-0.01961
C	3.41112	0.34554	-0.00002	C	3.40036	0.34546	-0.11682
H	2.27317	2.20757	0.00038	H	2.27354	2.20738	-0.03058
C	3.40132	-1.0592	-0.00036	C	3.39112	-1.05992	-0.11246
H	2.13159	-2.79755	-0.00065	H	2.12674	-2.79999	-0.01592
H	4.3327	-1.62712	-0.0007	H	4.3198	-1.63261	-0.18156
S	-0.49077	-1.88201	0.00052	S	-0.49179	-1.87473	0.19617
F	4.59052	0.9688	0.0002	F	4.57699	0.97018	-0.20767

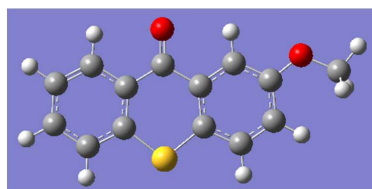
4-MeOTX



Charge = 0 Multiplicity = 1

# opt b3lyp/6-31g(d,p) geom=connectivity				# opt b3lyp/6-31g(d,p) scrf=(cpcm,solvent=acetonitrile) geom=connectivity			
C	-2.60603	-1.85527	0.00018	C	-2.57423	-1.86103	-0.07486
C	-1.60776	-0.86795	-0.00003	C	-1.59993	-0.86837	0.08282
C	-1.92972	0.49051	-0.00004	C	-1.9252	0.49054	0.03345
C	-3.29452	0.85874	0.00007	C	-3.27223	0.85165	-0.18823
C	-4.29152	-0.11016	0.0002	C	-4.24862	-0.1262	-0.35237
C	-3.94477	-1.47141	0.00029	C	-3.8998	-1.48434	-0.29345
H	-2.34187	-2.91343	0.00028	H	-2.31035	-2.92077	-0.03224
H	-3.54782	1.925	0.00005	H	-3.53705	1.91297	-0.22716
H	-5.34022	0.18248	0.00023	H	-5.28753	0.16009	-0.52565
H	-4.72876	-2.22942	0.00046	H	-4.66961	-2.24969	-0.42163
C	-0.93247	1.5929	-0.00013	C	-0.93536	1.5808	0.2141
O	-1.29479	2.75645	-0.00021	O	-1.29926	2.71921	0.47094
C	0.52766	1.26635	-0.00007	C	0.5186	1.27555	0.06017
C	1.00919	-0.03601	-0.00012	C	1.00701	-0.02706	0.11686
C	1.44515	2.33899	0.00007	C	1.41659	2.33818	-0.14709
C	2.40661	-0.27098	0	C	2.39059	-0.26996	-0.03354
C	2.81541	2.09764	0.0002	C	2.78247	2.08898	-0.29642
H	1.05408	3.36104	0.00008	H	1.03481	3.36092	-0.18881
C	3.31614	0.78584	0.00021	C	3.28576	0.78451	-0.2419
H	3.5152	2.93417	0.00028	H	3.47141	2.92258	-0.45741
H	4.38801	0.61371	0.00043	H	4.35402	0.60526	-0.36206
S	0.03342	-1.47152	-0.00039	S	0.0296	-1.43686	0.39568
O	2.69715	-1.61553	-0.00016	O	2.69578	-1.60522	0.05453
C	4.09499	-1.99939	0.00025	C	4.07968	-1.99726	-0.16293
H	4.02185	-3.09565	-0.00003	H	4.02166	-3.08965	-0.06086
H	4.58823	-1.63963	-0.90703	H	4.40306	-1.71393	-1.16907
H	4.58757	-1.64002	0.90804	H	4.72194	-1.56581	0.6106

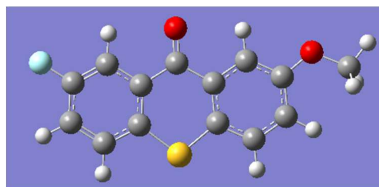
2-MeOTX



Charge = 0 Multiplicity = 1

# opt b3lyp/6-31g(d,p) geom=connectivity				# opt b3lyp/6-31g(d,p) scrf=(cpcm,solvent=acetonitrile) geom=connectivity			
C	-3.50144	-1.18383	-0.00018	C	-3.45545	-1.17913	-0.24409
C	-2.19039	-0.68401	0.00001	C	-2.17633	-0.68085	0.0274
C	-1.93311	0.68723	0.00007	C	-1.91848	0.69274	0.05914
C	-3.03054	1.5772	-0.00005	C	-2.98146	1.58504	-0.19642
C	-4.33516	1.0948	-0.00028	C	-4.25694	1.10086	-0.47359
C	-4.57008	-0.28953	-0.00035	C	-4.49473	-0.28182	-0.49522
H	-3.68865	-2.25826	-0.0002	H	-3.64811	-2.2545	-0.26524
H	-2.83012	2.65478	0.00006	H	-2.7899	2.66205	-0.17133
H	-5.17514	1.78787	-0.0004	H	-5.07508	1.79541	-0.67262
H	-5.59398	-0.66512	-0.00055	H	-5.49806	-0.6576	-0.71179
C	-0.57273	1.28704	0.00023	C	-0.58397	1.26067	0.36613
O	-0.43445	2.49723	0.00047	O	-0.46493	2.41909	0.73578
C	0.63328	0.39803	0.00008	C	0.62604	0.39789	0.19653
C	0.571	-1.00042	0.00014	C	0.56207	-0.99959	0.18341
C	1.88423	1.02421	-0.00005	C	1.86542	1.03002	0.05057
C	1.73405	-1.78002	0.00008	C	1.71676	-1.77888	0.03362
C	3.04999	0.23546	-0.00012	C	3.02163	0.24216	-0.10465
H	1.9586	2.11728	-0.00009	H	1.94201	2.11937	0.06004
C	2.98724	-1.1672	-0.00011	C	2.95762	-1.16229	-0.11126
H	1.67292	-2.87084	0.00022	H	1.65694	-2.87228	0.02629
H	3.88781	-1.77444	-0.00025	H	3.85584	-1.76898	-0.22951
S	-0.9292	-1.89228	0.00025	S	-0.94074	-1.86877	0.38675
O	4.20166	0.98774	-0.00022	O	4.16404	0.99116	-0.23989
C	5.46883	0.28653	-0.00019	C	5.42337	0.28963	-0.42325
H	5.57235	-0.31474	-0.90772	H	5.40349	-0.29435	-1.34844
H	6.18253	1.12212	-0.00017	H	6.1343	1.1236	-0.50136
H	5.57231	-0.3147	0.90739	H	5.64427	-0.33302	0.44886

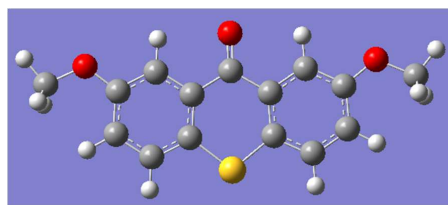
2-F,2'-MeOTX



Charge = 0 Multiplicity = 1

# opt b3lyp/6-31g(d,p) geom=connectivity				# opt b3lyp/6-31g(d,p) scrf=(cpcm,solvent=acetonitrile) geom=connectivity			
C	3.07115	1.524	-0.09087	C	3.04169	1.51588	-0.1918
C	1.80549	0.92801	0.04938	C	1.79663	0.92938	0.08902
C	1.64984	-0.45835	0.08347	C	1.64127	-0.45671	0.1657
C	2.79029	-1.27946	-0.02751	C	2.75755	-1.28847	-0.0508
C	4.03352	-0.67114	-0.16898	C	3.9802	-0.68679	-0.3335
C	4.20333	0.72289	-0.20218	C	4.15238	0.70524	-0.40755
H	3.17288	2.61146	-0.11585	H	3.14749	2.60445	-0.24679
H	2.67577	-2.36943	0.00659	H	2.64779	-2.37558	0.0105
H	5.19426	1.16503	-0.3131	H	5.12861	1.14368	-0.63103
C	0.33341	-1.14607	0.24519	C	0.33967	-1.10807	0.48679
O	0.28972	-2.34254	0.45711	O	0.30526	-2.2469	0.92216
C	-0.92881	-0.35156	0.12152	C	-0.92107	-0.34487	0.24461
C	-0.96363	1.04778	0.08877	C	-0.95422	1.05222	0.17433
C	-2.1276	-1.06703	0.04126	C	-2.10712	-1.0704	0.09018
C	-2.17438	1.74152	-0.02182	C	-2.15563	1.73971	-0.043
C	-3.3423	-0.36358	-0.07142	C	-3.31037	-0.37395	-0.13182
H	-2.1271	-2.16186	0.07242	H	-2.10762	-2.16119	0.1437
C	-3.37754	1.03975	-0.10244	C	-3.34453	1.03022	-0.19724
H	-2.18992	2.83374	-0.04819	H	-2.17249	2.83344	-0.09637
H	-4.31576	1.58065	-0.18861	H	-4.279	1.5658	-0.36822
S	0.46843	2.03933	0.20395	S	0.47523	2.03342	0.39294
F	5.11687	-1.4423	-0.27704	F	5.04258	-1.46814	-0.54258
O	-4.43388	-1.19619	-0.14374	O	-4.39219	-1.20745	-0.267
C	-5.74428	-0.58858	-0.25334	C	-5.69156	-0.60639	-0.51701
H	-5.82137	-0.01218	-1.17942	H	-5.68397	-0.06298	-1.46678
H	-6.39456	-1.47394	-0.28738	H	-6.33897	-1.49206	-0.57712
H	-5.9586	0.01867	0.63053	H	-5.98276	0.03578	0.31957

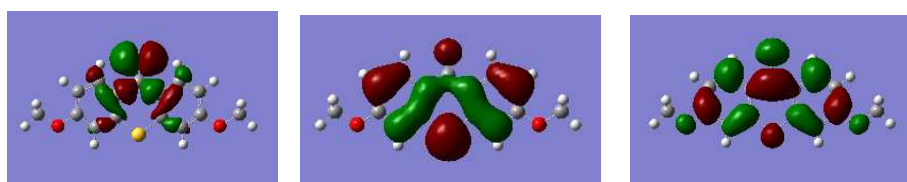
2,2'-MeOTX



Charge = 0 Multiplicity = 1

# opt b3lyp/6-31g(d,p) geom=connectivity				# opt b3lyp/6-31g(d,p) scrf=(cpcm,solvent=acetonitrile) geom=connectivity			
C	-2.60279	1.6956	0.1087	C	1.6896	-0.1593	2.58229
C	-1.37967	1.06855	-0.14868	C	1.07892	0.18936	1.37233
C	-1.28633	-0.32548	-0.25178	C	-0.30958	0.34479	1.27956
C	-2.43522	-1.10423	-0.09299	C	-1.10484	0.14191	2.41043
C	-3.66339	-0.46574	0.16932	C	-0.4838	-0.21425	3.62393
C	-3.75976	0.93066	0.26958	C	0.91013	-0.36353	3.7202
H	-2.66408	2.78318	0.18941	H	2.77595	-0.27772	2.64689
H	-2.39049	-2.19378	-0.18177	H	-2.18917	0.25873	2.36493
H	-4.70839	1.41987	0.4702	H	1.38576	-0.63771	4.66227
C	-0.00002	-1.03663	-0.53895	C	-0.97786	0.73148	0
O	0	-2.17301	-0.96643	O	-2.04035	1.32729	0
C	1.28631	-0.32548	-0.2518	C	-0.30958	0.34479	-1.27956
C	1.37973	1.06858	-0.14919	C	1.07892	0.18936	-1.37233
C	2.43515	-1.10426	-0.09277	C	-1.10484	0.14191	-2.41043
C	2.60297	1.69567	0.10754	C	1.6896	-0.1593	-2.58229
C	3.66339	-0.46574	0.16917	C	-0.4838	-0.21425	-3.62393
H	2.39034	-2.19383	-0.18108	H	-2.18917	0.25873	-2.36493
C	3.75992	0.93072	0.26857	C	0.91013	-0.36353	-3.7202
H	2.66438	2.78328	0.18766	H	2.77595	-0.27772	-2.64689
H	4.70866	1.41997	0.46857	H	1.38576	-0.63771	-4.66227
S	-0.00002	2.11726	-0.37774	S	2.12649	0.47819	0
O	-4.70436	-1.35473	0.30762	O	-1.3799	-0.3848	4.64982
O	4.70424	-1.35479	0.30811	O	-1.3799	-0.3848	-4.64982
C	-6.02452	-0.81706	0.56332	C	-0.86366	-0.77361	5.95137
H	-6.34731	-0.18572	-0.26928	H	-1.78463	-0.83412	6.54753
H	-6.62872	-1.73322	0.61737	H	-0.37277	-1.74972	5.89116
H	-6.04027	-0.28217	1.51695	H	-0.19347	-0.00235	6.34247
C	6.02441	-0.81719	0.56398	C	-0.86366	-0.77361	-5.95137
H	6.03988	-0.2817	1.51732	H	-0.37277	-1.74972	-5.89116
H	6.62843	-1.73342	0.61884	H	-1.78463	-0.83412	-6.54753
H	6.34764	-0.18643	-0.26886	H	-0.19347	-0.00235	-6.34247

Excited State Energies



n-orbital

HOMO (π -orbital)

LUMO (π^* -orbital)

Figure S9: Representative MOs for the lowest energy transitions of interest, 3,3'-MeOTX shown

Thioxanthone		Gaseous				CPCM			
3,3'-MeOTX		S ₁	S ₂	T ₁	T ₂	S ₁	S ₂	T ₁	T ₂
 3,6-dimethoxythioxanthone (3,3'-MeOTX)	Energy (kJ/mol)	355	363	292	313	356	364	291	308
	Character	$n\pi^*$	$\pi\pi^*$	$\pi\pi^*$	$n\pi^*$	$\pi\pi^*$	$\pi\pi^*$	$\pi\pi^*$	$\pi\pi^*$
	$\Delta n-p$	-8 kJ/mol		21 kJ/mol		8 kJ/mol		33 kJ/mol	

Table S3

Thioxanthone		Gaseous				CPCM			
3,3'-FTX		S ₁	S ₂	T ₁	T ₂	S ₁	S ₂	T ₁	T ₂
 3,6-difluorothioxanthone (3,3'-FTX)	Energy (kJ/mol)	353	365	290	310	355	360	286	319
	Character	$n\pi^*$	$\pi\pi^*$	$\pi\pi^*$	$n\pi^*$	$\pi\pi^*$	$\pi\pi^*$	$\pi\pi^*$	$\pi\pi^*$
	$\Delta n-p$	-12 kJ/mol		21 kJ/mol		5 kJ/mol		33 kJ/mol	

Table S4

Thioxanthone		Gaseous				CPCM			
3-MeOTX		S ₁	S ₂	T ₁	T ₂	S ₁	S ₂	T ₁	T ₂
 3-methoxythioxanthone (3-MeOTX)	Energy (kJ/mol)	349	354	284	307	346	358	280	306
	Character	$n\pi^*$	$\pi\pi^*$	$\pi\pi^*$	$n\pi^*$	$\pi\pi^*$	$\pi\pi^*$	$\pi\pi^*$	$\pi\pi^*$
	$\Delta n-p$	-5 kJ/mol		23 kJ/mol		12 kJ/mol		38 kJ/mol	

Table S5

Thioxanthone		Gaseous				CPCM			
3-FTX		S ₁	S ₂	T ₁	T ₂	S ₁	S ₂	T ₁	T ₂
 3-fluorothioxanthone (3-FTX)	Energy (kJ/mol)	349	356	282	306	346	357	278	316
	Character	$n\pi^*$	$\pi\pi^*$	$\pi\pi^*$	$n\pi^*$	$\pi\pi^*$	$\pi\pi^*$	$\pi\pi^*$	$\pi\pi^*$
	$\Delta n-p$	-7 kJ/mol		23 kJ/mol		11 kJ/mol		38 kJ/mol	

Table S6

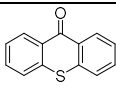
Thioxanthone		Gaseous				CPCM			
TX		S ₁	S ₂	T ₁	T ₂	S ₁	S ₂	T ₁	T ₂
 Thioxanthone (TX)	Energy (kJ/mol)	345	347	274	302	338	353	269	312
	Character	$\pi\pi^*$	$\pi\pi^*$	$\pi\pi^*$	$\pi\pi^*$	$\pi\pi^*$	$\pi\pi^*$	$\pi\pi^*$	$\pi\pi^*$
$\Delta n-p$		-2 kJ/mol		28 kJ/mol		15 kJ/mol		43 kJ/mol	

Table S7

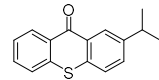
Thioxanthone		Gaseous				CPCM			
ITX		S ₁	S ₂	T ₁	T ₂	S ₁	S ₂	T ₁	T ₂
 Isopropylthioxanthone (ITX)	Energy (kJ/mol)	343	345	270	302	333	353	264	312
	Character	$\pi\pi^*$	$\pi\pi^*$	$\pi\pi^*$	$\pi\pi^*$	$\pi\pi^*$	$\pi\pi^*$	$\pi\pi^*$	$\pi\pi^*$
$\Delta n-p$		2 kJ/mol		32 kJ/mol		20 kJ/mol		48 kJ/mol	

Table S8

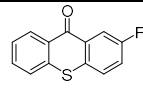
Thioxanthone		Gaseous				CPCM			
2-FTX		S ₁	S ₂	T ₁	T ₂	S ₁	S ₂	T ₁	T ₂
 2-fluorothioxanthone (2-FTX)	Energy (kJ/mol)	337	344	263	301	329	353	258	311
	Character	$\pi\pi^*$	$\pi\pi^*$	$\pi\pi^*$	$\pi\pi^*$	$\pi\pi^*$	$\pi\pi^*$	$\pi\pi^*$	$\pi\pi^*$
$\Delta n-p$		7 kJ/mol		38 kJ/mol		24 kJ/mol		53 kJ/mol	

Table S9

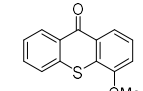
Thioxanthone		Gaseous				CPCM			
4-MeOTX		S ₁	S ₂	T ₁	T ₂	S ₁	S ₂	T ₁	T ₂
 4-methoxythioxanthone (4-MeOTX)	Energy (kJ/mol)	336	346	267	302	325	354	261	303
	Character	$\pi\pi^*$	$\pi\pi^*$	$\pi\pi^*$	$\pi\pi^*$	$\pi\pi^*$	$\pi\pi^*$	$\pi\pi^*$	$\pi\pi^*$
$\Delta n-p$		10 kJ/mol		35 kJ/mol		29 kJ/mol		52 kJ/mol	

Table S10

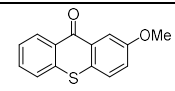
Thioxanthone		Gaseous				CPCM			
2-MeOTX		S ₁	S ₂	T ₁	T ₂	S ₁	S ₂	T ₁	T ₂
 2-methoxythioxanthone (2-MeOTX)	Energy (kJ/mol)	320	343	252	300	310	353	243	312
	Character	$\pi\pi^*$	$\pi\pi^*$	$\pi\pi^*$	$\pi\pi^*$	$\pi\pi^*$	$\pi\pi^*$	$\pi\pi^*$	$\pi\pi^*$
$\Delta n-p$		23 kJ/mol		48 kJ/mol		43 kJ/mol		69 kJ/mol	

Table S11

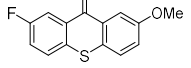
Thioxanthone	Gaseous				CPCM				
2-MeO,2'-FTX	S ₁	S ₂	T ₁	T ₂	S ₁	S ₂	T ₁	T ₂	
 2-methoxy,7-fluorothioxanthone (2-MeO,2'-FTX)	Energy (kJ/mol)	311	342	242	299	301	352	234	311
	Character	$\pi\pi^*$	$n\pi^*$	$\pi\pi^*$	$n\pi^*$	$\pi\pi^*$	$n\pi^*$	$\pi\pi^*$	$n\pi^*$
$\Delta n-p$	31 kJ/mol		57 kJ/mol		51 kJ/mol		77 kJ/mol		

Table S12

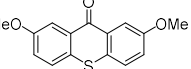
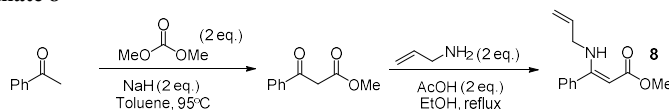
Thioxanthone	Gaseous				CPCM				
2,2'-MeOTX	S ₁	S ₂	T ₁	T ₂	S ₁	S ₂	T ₁	T ₂	
 2,7-dimethoxythioxanthone (2,2'-MeOTX)	Energy (kJ/mol)	302	342	235	299	291	352	225	310
	Character	$\pi\pi^*$	$n\pi^*$	$\pi\pi^*$	$n\pi^*$	$\pi\pi^*$	$n\pi^*$	$\pi\pi^*$	$\pi\pi^*$
$\Delta n-p$	40 kJ/mol		64 kJ/mol		61 kJ/mol		86 kJ/mol		

Table S13

Synthesis of Novel Photochemical Precursors

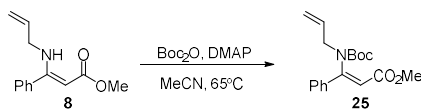
Amino cinnamate **8**



Scheme S3

A stirred suspension of NaH (60% on oil, 32 g, 800 mmol) in toluene (300 ml) with dimethyl carbonate (68 ml, 808 mmol) was heated to 95°C in a 1 L flask with an overhead stirrer and condenser. A solution of acetophenone (46.6 ml, 400 mmol) in toluene (100 ml) was added dropwise to allow for a controlled exotherm and H₂ evolution. After the addition was complete, heating was continued for 1 hour before the solution was cooled in an ice bath and quenched with acetic acid (23 ml, 400 mmol) and 1 M HCl (400 ml). The biphasic mixture was separated and the aqueous layer further extracted with EtOAc (2×150 ml) before the pooled organic extracts were washed with brine, dried (MgSO₄), filtered and concentrated *in vacuo*. The resulting oil was filtered through silica with pet. ether 40/60, then Et₂O and the solution evaporated under reduced pressure to give the 1,3-keto ester as an oil (71.5 g, 100%). 53.5 g (300 mmol) of this oil, along with allylamine (45 ml, 600 mmol) and acetic acid (34 ml, 600 mmol) was added to EtOH (300 ml) in a 1 L flask and the solution refluxed for 3 hours until all keto-ester had been consumed. The cooled solution was concentrated, purified by chromatography on silica (10-20% Et₂O in petrol) and concentrated to an oil (52 g) which was re-dissolved in petrol (50 ml), cooled in a freezer at -20°C and the resulting suspension rapidly filtered to give **8** as a white solid (47.5 g, 73%): m.p. 35 – 36 °C; δ_{H} (400 MHz, CDCl₃) 8.61 (1H, s, NH), 7.43 – 7.32 (5H, m, Ar.H), 5.78 (1H, ddt, J = 17.1, 10.1, 4.9 Hz, CH=CHH), 5.21 (1H, app. dq, J = 17.1, 1.7 Hz, CH=CHH), 5.11 (1H, app. dq, J = 10.3, 1.6 Hz, CH=CHH), 4.64 (1H, s, CH=C), 3.72 – 3.64 (5H, m, NCH₂, OCH₃); δ_{C} (101 MHz, CDCl₃) 170.9 (C), 165.1 (C), 136.0 (C), 135.5 (CH), 129.5 (CH), 128.5 (2×CH), 127.9 (2×CH), 116.0 (CH₂), 85.5 (CH), 50.4 (CH₂), 46.9 (CH₃); ESI-HRMS m/z 218.1180 (MH⁺ C₁₃H₁₆NO₂ requires 218.1176)

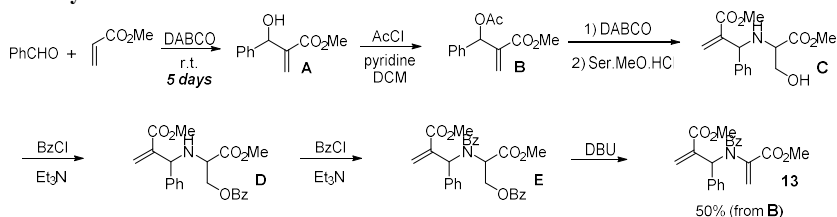
Boc protection to 25



Scheme S4

To a solution of amino cinnamate **8** (21.7 g, 100 mol) in MeCN (100 ml) was added Boc₂O (28.3 g, 130 mmol) and DMAP (0.61 g, 5 mmol) and the mixture heated to 65°C. After gas evolution had ceased, additional Boc₂O (16.7 g, 77 mmol) was added portionwise. The solution was concentrated and purified by chromatography on silica (10-20% Et₂O in petrol) to give **25** as a solid (19.0 g, 60%): m.p. 60 – 61 °C; δ_H (400 MHz, CDCl₃) 7.40 – 7.29 (5H, m, Ar.H), 5.92 (1H, ddt, *J* = 17.0, 10.6, 5.4 Hz, CH=CHH), 5.86 (1H, s, CH=C), 5.25 – 5.16 (2H, m, CH=CHH), 4.24 (2H, app. dt, *J* = 5.4, 1.6 Hz, NCH₂), 3.56 (3H, s, OCH₃), 1.15 (9H, s, 3×CH₃); δ_C (101 MHz, CDCl₃) 167.0 (C), 156.1 (C), 153.7 (C), 136.9 (C), 133.6 (CH), 129.4 (CH), 128.8 (2×CH), 127.8 (2×CH), 117.1 (CH₂), 109.7 (CH), 81.8 (C), 53.3 (CH₂), 51.3 (CH₃), 27.8 (3×CH₃); ESI-HRMS *m/z* 318.1699 (MH⁺ C₁₈H₂₄NO₄ requires 318.1700)

α-amido acrylate 13



Scheme S5

Solvent-free Baylis-Hillman : A mixture of methyl acrylate (333 mmol, 1.0 eq.), benzaldehyde (333 mmol, 1.0 eq.) and DABCO (20 mol %) was stirred at room temp for 5 days before pouring over 1 M HCl (250 ml) and extracting with EtOAc (3×200 ml). The organic extracts were dried (MgSO₄), filtered and evaporated to an oil (62.9 g) containing ~15 mol. % benzaldehyde. The product **A** was of sufficient purity to use in next step.

Acylation: To an ice cooled solution of the above Baylis-Hillman adduct **A** in DCM (~300 mmol; 2M), and pyridine (1.15 eq), was added acetyl chloride (1.15 eq.) dropwise. The mixture was allowed to warm to room temperature and stirring continued until the alcohol was fully consumed (monitored by tlc). The concentration was halved by the addition of more DCM and the mixture washed with 1 M HCl (×2) and water. The solution was dried (MgSO₄), filtered and evaporated to give **B** as an oil containing residual benzaldehyde as an impurity (~15%). Yield ≈ 83% (2-steps)

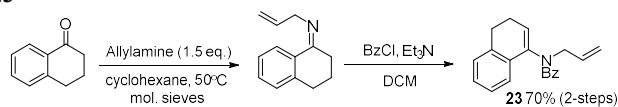
Ser-OMe.HCl: Acetyl chloride (2.5 eq) was added dropwise to MeOH (600 ml) before the portionwise addition of DL-serine (0.5 mol, 1.0 eq.) and the mixture refluxed for 2 hrs. The solvent was evaporated, the product was triturated with Et₂O, filtered and washed (Et₂O) before drying to a free-flowing powder (76 g, 98%)

Serine Adduct C: To a 1:1 THF/Water solution of crude allylic acetate **B** (200 mmol, 1 M) cooled in an ice bath was added DABCO (2.5 eq.) The ice bath was removed and the mixture stirred for 15 min before the portionwise addition of Ser-OMe.HCl (1.2 eq.). The mixture was stirred, until the reaction had gone to completion, before removal of THF under reduced pressure. The remaining mixture was extracted with EtOAc, dried (MgSO₄) and chromatography on silica (gradient elution 30% -80% EtOAc in hexane) yielded the product **C** as an oil (49g), free from benzaldehyde and as a mix of diastereomers.

Benzoylation to E: To a solution of **C** (~167 mmol) in DCM (1 M) was added Et₃N (1.15 eq.) and the solution cooled in an ice bath after which was added BzCl (1.15 eq.) dropwise. The solution was stirred at room temperature for approx. 1 hr. before washing with 1 M HCl (×2) and brine. The solution was dried (MgSO₄), filtered and evaporated to **D** an oil which was used directly for the second benzoylation. To solution of **D** in MeCN (1 M) and Et₃N (1.2 eq.) was added BzCl (1.2 eq) and the mixture then heated at reflux with stirring until full consumption of the starting material (tlc monitoring). After cooling to room temperature the slurry was filtered and the solution concentrated *in vacuo* before re-dissolving in DCM and washing with 1 M HCl and brine. The solution was dried (MgSO₄), filtered and evaporated to an oil which was purified by chromatography on silica (20 – 30% EtOAc in hexane) to give **E** as an oil (75g, mixture of diastereomers).

Benzoate Elimination to 13: To an ice cooled solution of **E** (~150 mmol) in DCM (0.6 M) was added neat DBU (1 eq.) dropwise. The ice bath was removed and stirring continued until the reaction had gone to completion (tlc monitoring). The solution was washed (sat. NaHCO₃), brine and dried (MgSO₄). Chromatography on silica (30% EtOAc in hexane) yielded product **13** as a white solid (40.5g, 50% from **B**): m.p. 110 – 112 °C; δ_H (400 MHz, CDCl₃) 7.55 – 7.50 (2H, m, Ar.**H**), 7.38 – 7.23 (8H, m, Ar.**H**), 6.71 (1H, br. s, Ph**CH**), 6.56 (1H, app. t, *J* = 1.0 Hz, CHH=C), 5.99 – 5.97 (1H, m, CHH=C), 5.96 (1H, d, *J* = 0.7 Hz, CHH=C), 5.45 (1H, d, *J* = 0.7 Hz, CHH=C), 3.70 (3H, s, CH₃), 3.43 (3H, s, CH₃); δ_C (101 MHz, CDCl₃) 171.1 (C), 166.6 (C), 164.8 (C), 139.5 (C), 139.4 (C), 136.5 (C), 136.3 (C), 130.5 (CH), 129.7 (2×CH), 128.4 (2×CH), 128.3 (2×CH), 128.2 (2×CH), 128.1 (CH), 127.8 (CH₂), 124.8 (CH₂), 62.5 (CH), 52.3 (CH₃), 52.2 (CH₃); ESI-HRMS *m/z* 380.1496 (MH⁺ C₂₂H₂₂NO₅ requires 380.1498)

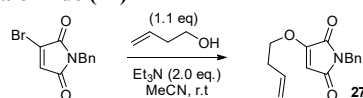
Amido styrene **23**



Scheme S6

A solution of α-tetralone (100g, 684 mmol) and allylamine (77 ml, 1.03 mol) in cyclohexane (250 ml) was stirred over 3 Å molecular sieves, 3-5 mm beads, (140 g) in a 1 L flask, heated at 50°C for 90 hrs (95% conversion). The mixture was filtered through celite, concentrated *in vacuo* and the resulting oil poured over DCM (500 ml), cooled in an ice bath, before the addition of benzoyl chloride (79 ml, 684 mmol) then triethylamine (95 ml, 684 mmol) over about 20 mins. The fully charged vessel was allowed to warm to room temperature and stirred for 17 hrs before filtering and the filtrate washed (1M HCl, sat. aq. NaHCO₃ and brine), dried (MgSO₄) and filtered before concentrating under reduced pressure. To the resulting oil was added hexane to allow trituration of the product before filtering to give enamide **23** as an off-white solid (139 g, 70%): m.p. 86 – 87 °C; δ_H (400 MHz, CDCl₃) 7.49 – 7.11 (9H, m, Ar.**H**), 5.99 (1H, dddd, *J* = 17.3, 10.2, 7.3, 5.4 Hz, CH₂=CH), 5.52 (1H, dd, *J* = 6.0, 3.5 Hz, C=CHCH₂), 5.22 – 5.09 (2H, m, CH₂=CH), 4.83 (1H, dd, *J* = 14.5, 5.4 Hz, NCHHCH), 3.68 (1H, dd, *J* = 14.5, 7.3 Hz, NCHHCH), 2.73 (1H, app. td, *J* = 14.3, 6.7 Hz, CCHHCH₂), 2.60 (1H, app. dt, *J* = 15.5, 5.9 Hz, CCHHCH₂), 2.18 (1H, app. dq, *J* = 17.6, 6.1 Hz, CH₂CHHCH), 2.00 (1H, dddd, *J* = 17.0, 13.5, 6.7, 3.5 Hz, CH₂CHHCH); δ_C (101 MHz, CDCl₃) 171.2 (C), 138.8 (C), 137.3 (C), 136.2 (C), 133.1 (CH), 131.8 (C), 130.0 (CH), 129.4 (CH), 128.1 (CH), 128.1 (CH), 127.8 (2×CH), 127.6 (2×CH), 127.0 (CH), 122.8 (CH), 118.4 (CH₂), 50.2 (CH₂), 27.3 (CH₂), 22.9 (CH₂); ESI-HRMS *m/z* 290.1549 (MH⁺ C₂₀H₂₀NO requires 290.1539)

N-Bn-3-(but-3-en-1-yloxy)-maleimide (**27**)



Scheme S7

A mixture of *N*-benzyl-3-bromomaleimide (16.9 g, 63.5 mmol), 3-buten-1-ol (6 ml, 70 mmol) and triethylamine (17.6 ml, 127 mmol) in MeCN (65 ml) was stirred at room temperature for 4 days. The mixture was concentrated, re-dissolved in DCM (100 ml) and washed with water (2×50 ml), dried (MgSO_4), filtered and concentrated to an oil which was filtered through silica with Et_2O . The solvent was removed *in vacuo*, purified by chromatography on silica (70-100% DCM in petrol) and concentrated to an oil which was triturated with petrol / Et_2O , filtered and dried to give **27** as a white solid (10.3 g, 63%): m.p. 66 - 67°C; δ_{H} (400 MHz, CDCl_3) 7.35 – 7.22 (5H, m, Ar.H), 5.80 (1H, ddt, $J = 17.0, 10.2, 6.7$ Hz, CH=CHH), 5.36 (1H, s, CH=C), 5.20 – 5.10 (2H, m, CH=CH₂), 4.64 (2H, s, NCH₂Ph), 4.05 (2H, t, $J = 6.8$ Hz, OCH₂CH₂), 2.57 (2H, app. qt, $J = 6.8, 1.3$ Hz, OCH₂CH₂); δ_{C} (101 MHz, CDCl_3) 170.1 (C), 165.5 (C), 160.2 (C), 136.4 (C), 132.6 (CH), 128.8 (2×CH), 128.6 (2×CH), 127.9 (CH), 118.6 (CH₂), 96.6 (CH), 71.7 (CH₂), 41.3 (CH₂), 32.7 (CH₂); ESI-HRMS m/z 280.0940 (MNa^+ C₁₅H₁₅NO₃Na requires 280.0944)

Novel Reactor Configurations

Parallel NMR Tube Irradiations

For rapid screening of the sensitizer series, a simple new method was devised to save time and material. Irradiations were carried out directly in standard NMR tubes using deuterated acetonitrile. Stock solutions of the substrate (5 ml, 0.1 – 0.2 M) were prepared in a 5 ml volumetric flask, with adiponitrile (0.5 eq) as an internal standard if necessary, before dispensing 0.4 ml aliquots into individual NMR tubes containing the sensitizer of interest. The solutions were then irradiated in parallel with a 9 W PL-S UVA lamp by holding the tubes equidistant from the lamp (1-2 mm) using an improvised tube holder (Figure S10). The low power output of the lamp meant that external cooling was not required.

The reaction progress was monitored periodically by ¹H-NMR. By using this method, the entire sensitizer series could be screened within a working day, without the need for sample preparation, and using just 0.5 – 1.0 mmol of the substrate.

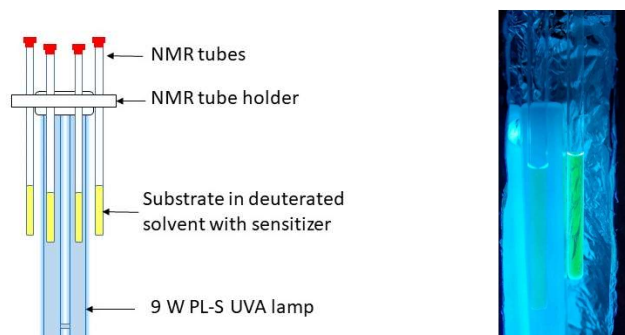


Figure S10: Parallel NMR tube irradiations with 9 W pl-s lamp

36 W Blue COB Reactor Configuration

To investigate the efficacy of the visible light absorbing TX derivatives as ‘energy transfer photocatalysts’ it was necessary to construct a novel reactor based around a high-intensity blue light source. Reported reactors for visible light photocatalysis are usually based around SMD (Surface Mount Device) LED chips. Single colour, high power SMD LEDs typically operate at about 1 – 3 W, have about 1- 3 individual diodes in a single housing and must be connected in arrays if more power / light intensity is required.

COB (Chip On board) LEDs have many more diodes (> 9) mounted on a single surface and can offer much higher power densities without having to connect multiple chips in an array. These devices can be commonly found in high power white LED spotlights. The white light is produced by a phosphor film over an LED chip which down-converts a higher energy light source to the full range of visible colours. . In the case of white COB LEDs the phosphor is driven by the much easier / cheaper to access emission from blue LEDs. As a result, all white COB chips have at their centre a powerful source of blue light which is ideal for many photoredox catalysts and lower energy triplet sensitizers which can be excited by visible light. Interestingly, ‘naked’ blue COB chips have only relatively recently become commercially available. LED manufacturer Citizen produce such chips for aquariums, swimming pools and architectural use.

A tray of the 34.6 V, 22 mm COB chips was ordered for initial investigations based on the convenient chip size and availability of a compact 36 W 1.05 A constant current driver. The peak wavelength is 455 nm and the emission spans from approximately 430 – 480 nm.

36 W Blue COB Reactor Construction

The key requirements of a photochemical batch reactor are:

- 1) light source in optimal position to ensure efficient light delivery to solution
- 2) a means of stirring solution and
- 3) effective heat management.

Reported visible light mediated photoredox reactions are often driven by a 40 W Kessil lamp or a flexible LED strip placed side-on and a few centimetres away from a vial containing the reaction solution (Figure S11, left). The overall light capture is poor and as a result the reactions are often left on overnight to drive a successful reaction to completion. The side-on method of irradiation is necessary since the vials are stirred over a magnetic stirrer and there is no room below for the bulky commercial light source.

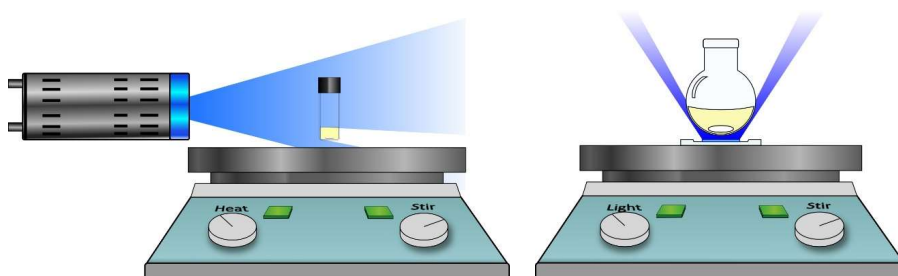


Figure S11 - *Left*: Inefficient side-on irradiation with external Kessil lamps over magnetic stirrer; *Right*: Novel integrated COB LED and magnetic stirrer for efficient light capture

The use of a COB LED allows for efficient stirring with simultaneous irradiation since the flat COB chip can be mounted directly onto the metal surface of a magnetic stirrer without affecting its ability to stir (Figure S11, right). In this way, a vessel can be magnetically stirred directly over the high intensity

discharge of the COB. In the case of the 36 W COB used, it was assumed the metal body of the stirrer should allow for sufficient heat dissipation and so prevent the COB chip overheating.

The reactor was based around a Heidolph stirrer hotplate with broken heating controls (Figure S12). The heating circuitry could be removed and replaced with the LED driver which fortuitously fit neatly within the resulting cavity. As a result, the driver could be wired internally onto the original heating switch allowing for a compact and safe design with minimal effort. The LED COB was fixed to the plate with a commercially available mount and a couple of screws tapped into the metal surface. Thermal contact was made with some thermal paste.

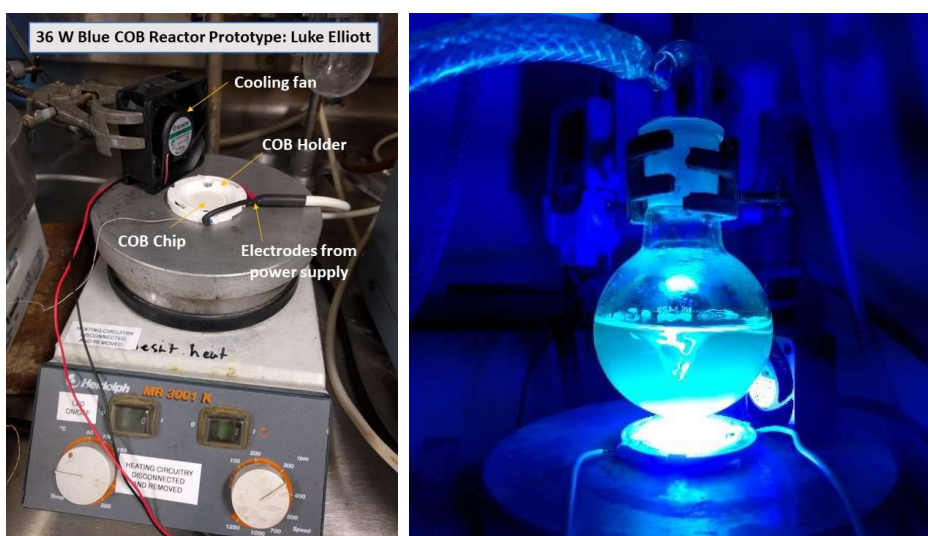
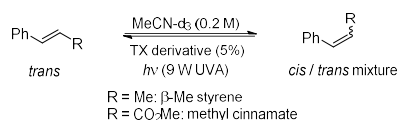


Figure S12: Working prototype of the 36 W blue COB reactor

Stirring acetonitrile in a 50 ml rbf over the 36 W COB resulted in rapid heating of the solvent to near reflux and so a fan was introduced to the side of the vessel. This allowed the temperature to be maintained below 40°C and also assisted in cooling the surface of the stirrer. Additional control over the temperature could involve a small double jacketed vessel or cold-finger.

TX Sensitizer Screening Studies

Alkene Isomerization Studies in NMR Tubes



Scheme S8

A stock solution was prepared in a 5 ml volumetric flask using 1 mmol of the relevant *trans*-styrene derivative and deuterated acetonitrile (0.2 M). For each irradiation, 0.5 ml aliquots were added to an NMR tube containing the relevant thioxanthone derivative (5 mol%) before gently warming to ensure the sensitizer was fully dissolved. The NMR tube was placed against a low pressure 9 W PL-S UVA lamp and the isomeric ratio was monitored every 15 mins by ¹H-NMR.

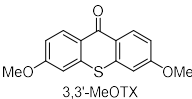
			<i>trans : cis</i>
Time / mins	β -Me styrene	Me-cinnamate	
15	1 : 1.09	1 : 0.87	 3,3'-MeOTX
30	1 : 1.15	1 : 1.03	
45	1 : 1.15	1 : 1.04	

Table S14: 3,3'-MeOTX

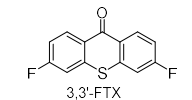
			<i>trans : cis</i>
Time / mins	β -Me styrene	Me-cinnamate	
15	1 : 0.97	1 : 0.76	 3,3'-FTX
30	1 : 1.13	1 : 1.00	
45	1 : 1.14	1 : 1.03	

Table S15: 3,3'-FTX

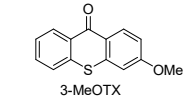
			<i>trans : cis</i>
Time / mins	β -Me styrene	Me-cinnamate	
15	1 : 1.03	1 : 1.02	 3-MeOTX
30	1 : 1.23		
60	1 : 1.23	1 : 1.05	

Table S16: 3-MeOTX

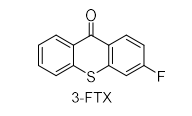
			<i>trans : cis</i>
Time / mins	β -Me styrene	Me-cinnamate	
15	1 : 0.88	1 : 0.77	 3-FTX
30	1 : 1.19	1 : 1.00	
45	1 : 1.24	1 : 1.04	
60	1 : 1.23		

Table S17: 3-FTX

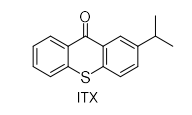
			<i>trans : cis</i>
Time / mins	β -Me styrene	Me-cinnamate	
15	1 : 1.22		 ITX
30	1 : 1.57	1 : 1.10	
45	1 : 1.64	1 : 1.11	
60	1 : 1.63		

Table S18: ITX

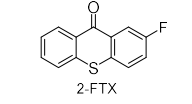
			<i>trans : cis</i>
Time / mins	β -Me styrene	Me-cinnamate	
15	1 : 1.50	1 : 0.83	 2-FTX
30	1 : 1.83	1 : 1.12	
45	1 : 1.86	1 : 1.15	
60	1 : 1.88		

Table S19: 2-FTX

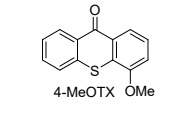
			<i>trans : cis</i>
Time / mins	β -Me styrene	Me-cinnamate	
15	1 : 1.05	1 : 0.78	 4-MeOTX
30	1 : 1.90	1 : 1.11	
45	1 : 2.09	1 : 1.18	
60	1 : 2.13	1 : 1.21	

Table S20: 4-MeOTX

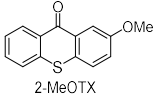
<i>trans</i> : <i>cis</i>			 2-MeOTX
Time / mins	β -Me styrene	Me-cinnamate	
15	1 : 2.32	1 : 1.06	
30	1 : 4.91	1 : 1.47	
45	1 : 4.82	1 : 1.52	
60	1 : 4.82		

Table S21: 2-MeOTX

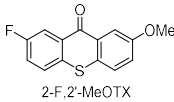
<i>trans</i> : <i>cis</i>			 2-F,2'-MeOTX
Time / mins	β -Me styrene	Me-cinnamate	
15	1 : 1.72	1 : 1.31	
30	1 : 4.66	1 : 1.73	
45	1 : 4.92	1 : 1.73	
60	1 : 4.97		

Table S22: 2-F,2'-MeOTX

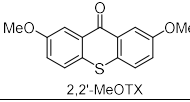
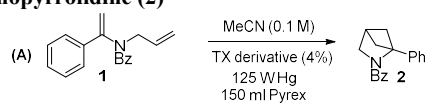
<i>trans</i> : <i>cis</i>			 2,2'-MeOTX
Time / mins	β -Me styrene	Me-cinnamate	
15	1 : 2.02	1 : 1.17	
30	1 : 3.70	1 : 1.48	
45	1 : 3.55	1 : 1.46	

Table S23: 2,2'-MeOTX

Sensitizer Screen with 125 W, 150 ml Immersion Well Reactor

Enamide (1) to 2,4-methanopyrrolidine (2)



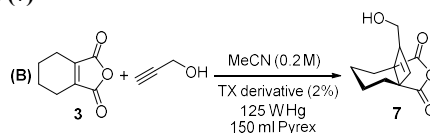
Scheme S9

The general immersion well batch irradiation procedure was followed using a 125 W Hg lamp and 150 ml Pyrex reactor. A solution of enamide **1** (3.95 g, 15 mmol) in degassed MeCN (150 ml) was irradiated with the relevant thioxanthone derivative (0.6 mmol) and the reaction monitored by quantitative $^1\text{H-NMR}$ using 1,3,5-trimethoxybenzene as an internal standard.

Time (min)	Sensitizer (4 mol %)								
	3,3'-MeO	3,3'-F	3-MeO	3-F	ITX	2-F	4-MeO	2-MeO	2,2'-MeO
30	20	21	21	23	23	26	28	28	24
60	36	41	46	42	45	52	55	49	
150	93	99	99	97	94	95	96	100	92
Initial productivity mmol/h	5.4	6.2	6.9	6.3	6.8	7.8	8.3	7.4	7.2

Table S24

THPA (3) to Cyclobutene (7)



Scheme S10

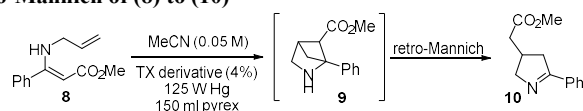
The general immersion well batch irradiation procedure was followed using a 125 W Hg lamp and 150 ml Pyrex reactor. A solution of THPA **3** (4.56 g, 30 mmol) and propargyl alcohol (2.62 ml, 45 mmol)

in degassed MeCN (150 ml) was irradiated with the relevant thioxanthone derivative (0.6 mmol) and the reaction monitored by quantitative ¹H-NMR using 1,3,5-trimethoxybenzene as an internal standard.

Time (min)	Sensitizer (4 mol %)								
	3,3'-MeO	3,3'-F	3-MeO	3-F	ITX	2-F	4-MeO	2-MeO	2,2'-MeO
20	24	29	23	28	27	28	9		/
40	48	58	47	55	58	59	17		/
60	70	74	68	70	75	74	26	6	/
Initial productivity mmol/h	22	26	21	25	24	25	8	1.8	0

Table S25

Cross [2+2] / retro-Mannich of (8) to (10)



Scheme S11

A solution of enamine **8** (1.63 g, 7.5 mmol) and the relevant TX derivative (0.3 mmol) in degassed MeCN (150 ml) was irradiated in a 150 ml Pyrex immersion well batch reactor with a 125 W Hg lamp. The reaction was followed by quantitative ¹H-NMR using 1,3,5-trimethoxybenzene as an internal standard. When at full conversion the concentrated reaction mixture was purified by chromatography on silica (30-40% EtOAc in petrol) to yield cyclic imine **10** as a pale orange oil.

δ_{H} (400 MHz, CDCl₃) 7.85 – 7.78 (2H, m, Ar.H), 7.45 – 7.36 (3H, m, Ar.H), 4.26 (1H, app. ddt, $J = 16.4, 8.0, 1.8$ Hz, NCHH), 3.74 (1H, ddt, $J = 16.4, 5.4, 1.9$ Hz, NCHH), 3.69 (3H, s, OCH₃), 3.21 (1H, app. ddt, $J = 17.0, 9.0, 1.8$ Hz, CHH), 2.94 – 2.82 (1H, m, CH), 2.70 (1H, app. ddt, $J = 17.0, 5.7, 1.9$ Hz, CHH), 2.53 – 2.40 (2H, m, CH₂); δ_{C} (101 MHz, CDCl₃) 173.0 (C), 172.6 (C), 134.5 (C), 130.6 (CH), 128.6 (2×CH), 127.6 (2×CH), 66.9 (CH₂), 51.8 (CH₃), 41.2 (CH₂), 39.3 (CH₂), 33.5 (CH); ESI-HRMS m/z 218.1175 (MH⁺ C₁₃H₁₆NO₂ requires 218.1176)

time / min	Sensitizer (4 mol%)							
	3,3'-MeOTX	3,3'-FTX	3-MeOTX	3-FTX*	ITX*	2-FTX*	4-MeO*	2-MeOTX*
0	0	0	0	0	0		0	0
30	22	25	24		31		30	22
60	38	43	41		50		53	30
90	56	54	57	47	50	40	56	30
120	72	63	64				44	30
150	78	62	62					
Isolated (g)	1.08	0.76	0.76	0.78	0.68	0.64	0.51	0.48
Isolated (%)	67%	47%	47%	48%	42%	39%	31%	29%

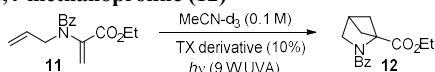
* Full consumption of starting enamine observed but product integration inaccurate due to significant degradation by-products

Table S26

Cross [2+2] Sensitizer Screen in NMR Tubes

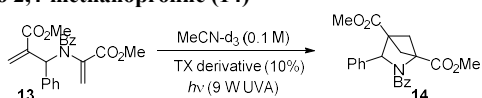
A stock solution was prepared in a 5 ml volumetric flask using 0.5 mmol of the relevant α -amido acrylate derivative and adiponitrile (0.25 mmol) in deuterated acetonitrile (0.1 M). For each irradiation, 0.4 ml aliquots were added to an NMR tube containing the relevant thioxanthone derivative (10 mol%) before gently warming to ensure the sensitizer was fully dissolved. The NMR tube was placed against a low pressure 9 W PL-S UVA lamp and reaction was monitored every 15 mins by $^1\text{H-NMR}$.

α -amido acrylate (11) to 2,4-methanoproline (12)



Scheme S12

α -amido acrylate (13) to 2,4-methanoproline (14)



Scheme S13

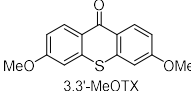
Time / min	Reaction D		Reaction E		 3,3'-MeOTX
	s.m. 11 (%)	prod 12 (%)	s.m. 13 (%)	prod 14 (%)	
15	9	73	30	36	
30	0	80	7	52	

Table S27

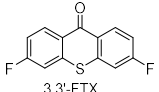
Time / min	Reaction D		Reaction E		 3,3'-FTX
	s.m. 11 (%)	prod 12 (%)	s.m. 13 (%)	prod 14 (%)	
15	22	65	33	33	
30	0	84	9	46	

Table S28

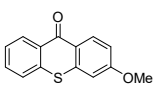
Time / min	Reaction D		Reaction E		 3-MeOTX
	s.m. 11 (%)	prod 12 (%)	s.m. 13 (%)	prod 14 (%)	
15	1	82	47	27	
30	0	83	17	42	

Table S29

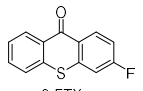
Time / min	Reaction D		Reaction E		 3-FTX
	s.m. 11 (%)	prod 12 (%)	s.m. 13 (%)	prod 14 (%)	
15	20	64	47	25	
30	3	78	17	40	

Table S30

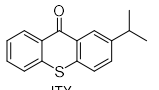
Time / min	Reaction D		Reaction E		 ITX
	s.m. 11 (%)	prod 12 (%)	s.m. 13 (%)	prod 14 (%)	
15	20	66	76	10	
30	2	80	56	18	

Table S31

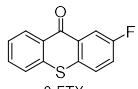
Time / min	Reaction D		Reaction E		 2-FTX
	s.m. 11 (%)	prod 12 (%)	s.m. 13 (%)	prod 14 (%)	
15	27	57	53	5	
30	2	76	73	9	

Table S32

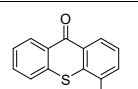
Time / min	Reaction D		Reaction E		 4-MeOTX OMe
	s.m. 11 (%)	prod 12 (%)	s.m. 13 (%)	prod 14 (%)	
15	47	37			
30	27	57	75	8	

Table S33

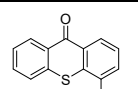
Time / min	Reaction D		Reaction E		 4-MeOTX OMe
	s.m. 11 (%)	prod 12 (%)	s.m. 13 (%)	prod 14 (%)	
15	47	37			
30	27	57	75	8	

Table S34

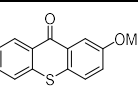
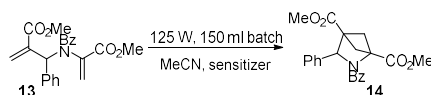
Time / min	Reaction D		Reaction E		 2-MeOTX
	s.m. 11 (%)	prod 12 (%)	s.m. 13 (%)	prod 14 (%)	
15	79	4			
60			86	2	

Table S35

Preparative Scale Synthesis of 2,4-methanoproline (**14**)



Entry	Sensitizer (mol %)	Conc. (M)	Time (h)	Yield (%)	Mass (g)
1	BP (10)	0.05	9	46	1.3
2	ITX (10)	0.05	12	38	1.1
3	3-FTX (10)	0.05	5	51	1.45
4	3,3'-MeOTX (5)	0.1	3	56	3.2
5	3,3'-MeOTX (2.5)	0.2	7	51	5.8

Table S36

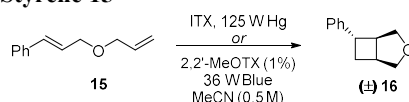
The general immersion well batch irradiation procedure was followed using a 125 W Hg lamp and 150 ml Pyrex reactor. In all cases the sensitizer concentration was fixed at 0.005 M. When the reaction had reached full conversion, the solution was concentrated and triturated with Et₂O, filtered and the residue washed with Et₂O to yield product **14** as a white solid: m.p. 170 – 171 °C; δ_H (400 MHz, CDCl₃) 7.43 – 7.29 (8H, m, Ar.H), 7.15 – 7.09 (2H, m, Ar.H), 4.95 (1H, s, NCH), 3.85 (3H, s, OCH₃), 3.61 (3H, s, OCH₃), 2.63 (1H, d, *J* = 7.3 Hz, CHH), 2.58 (1H, dd, *J* = 10.0, 8.3 Hz, CHH), 2.26 – 2.20 (2H, m, CHH, CHH); δ_C (101 MHz, CDCl₃) 177.0 (C), 169.2 (C), 168.3 (C), 138.4 (C), 134.1 (C), 131.6 (CH), 128.6 (2×CH), 128.4 (CH), 128.3 (2×CH), 128.0 (2×CH), 127.7 (2×CH), 67.6 (CH), 67.4 (C), 53.7 (C), 52.5 (CH₃), 52.1 (CH₃), 48.3 (CH₂), 38.8 (CH₂); ESI-HRMS *m/z* 380.1489 (MH⁺ C₂₂H₂₂NO₅ requires 380.1492)

Blue Light Mediated Reactions with 36 W, 455 nm COB Reactor

General procedure

A solution of the relevant substrate in degassed solvent was added to a multi-necked round bottom flask connected to a nitrogen line. The headspace was purged with N₂ several times before the addition of 2,2'-MeOTX. The solution was stirred over the modified hotplate COB reactor (see above) from a distance of approximately 15 mm, with fan cooling. Sample were taken periodically for quantitative analysis by ¹H-NMR using 1,3,6-trimethoxybenzene as an internal standard (see general batch irradiation procedure above) to determine the precise endpoint of the reaction for accurate reactor comparison.

Intramolecular [2+2] of Styrene 15

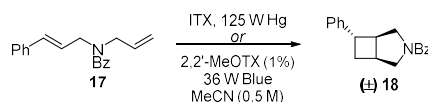


Scheme S14

125 W Batch Irradiation: The general immersion well batch procedure was followed using a 125 W Hg lamp and 150 ml Pyrex reactor to irradiate allylic ether **15** (2.61 g, 15 mmol) in degassed MeCN (0.1 M) with ITX (191 mg, 0.75 mmol). After 2.75 hrs the reaction mixture was concentrated *in vacuo* and chromatography on silica (10% Et₂O in DCM) yielded product **16** as a mixture of diastereomers (1 : 0.17), oil (2.34 g, 90%)

36 W Blue COB Irradiation: The general 36 W COB reactor procedure was followed by irradiating allylic ether **15** (1.74 g, 10 mmol) in degassed MeCN (0.5 M) with 2,2'-MeOTX (27 mg, 0.1 mmol) in a 50 ml flask for 3 hrs. The reaction mixture was concentrated *in vacuo* and chromatography on silica (10% Et₂O in DCM) yielded product **16** as a mixture of diastereomers (1 : 0.15), oil (1.54 g, 89%)

Intramolecular [2+2] of Styrene 17



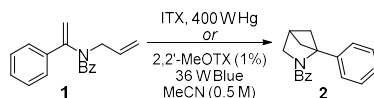
Scheme S15

125 W Batch Irradiation: The general immersion well batch procedure was followed using a 125 W Hg lamp and 150 ml Pyrex reactor to irradiate allylic amide **17** (4.16 g, 15 mmol) in degassed MeCN (0.1 M) with ITX (191 mg, 0.75 mmol). After 3.5 hrs the reaction mixture was concentrated *in vacuo* and chromatography on silica (30% EtOAc in petrol) yielded product **18** as a rotameric mixture of diastereomers, oil (4.02 g, 97%) Major diastereomer: δ_{H} (500 MHz, DMSO-d₆, 100°C) 7.57 – 7.44 (5H, m, Ar.H), 7.33 – 7.16 (5H, m, Ar.H), 3.90 – 3.70 (2H, m, 2×NCHH), 3.56 (1H, dd, $J = 12.3, 6.6$ Hz, NCHH), 3.45 (1H, dd, $J = 12.3, 5.2$ Hz, NCHH), 3.26 – 3.20 (1H, m, CH), 3.02 – 2.93 (2H, m, CH), 2.33 – 2.25 (1H, m, CHH), 2.17 – 2.09 (1H, m, CHH); δ_{C} (126 MHz, DMSO-d₆, 120°C) 168.6 (C), 144.4 (C), 137.2 (C), 128.8 (CH), 127.7 (2×CH), 127.6 (2×CH), 126.4 (2×CH), 125.6 (2×CH), 125.3 (CH), 52.7 (CH₂), 44.9 (CH), 41.5 (CH), 33.1 (CH), 31.0 (CH₂); ESI-HRMS m/z 278.1542 (MH⁺ C₁₉H₂₀NO requires 278.1539)

36 W Blue COB Irradiation: The general 36 W COB reactor procedure was followed by irradiating allylic amide **17** (8.32 g, 30 mmol) in degassed MeCN (0.5 M) with 2,2'-MeOTX (82 mg, 0.3 mmol) in a 100 ml flask for 5 hrs. The reaction mixture was concentrated *in vacuo* and chromatography on

silica (30% EtOAc in petrol) yielded product **18** as a rotameric mixture of diastereomers, oil (7.13 g, 86%)

Cross [2+2] of Enamide **1**

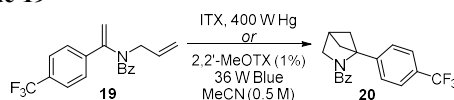


Scheme S16

400 W Batch Irradiation: Batch irradiation previously reported¹⁰ when enamide **1** (105 g, 400 mmol) was irradiated in MeCN (0.4 M) with ITX (1.0 g, 4 mmol) with a 400 W Hg lamp in a 1 L Pyrex reactor for 24 hrs. The product **2** was isolated as a pale yellow solid (93.4 g, 89%)

36 W Blue COB Irradiation: The general 36 W COB reactor procedure was followed by irradiating enamide **1** (7.90 g, 30 mmol) in degassed MeCN (0.5 M) with 2,2'-MeOTX (82 mg, 0.3 mmol) in a 100 ml flask for 3 hrs. The reaction mixture was concentrated *in vacuo* and triturated with hexane and filtered, washing with cold Et₂O to give **2** as a pale yellow solid (6.58 g, 83%)

Cross [2+2] of Enamide **19**

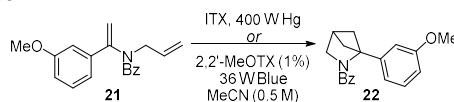


Scheme S17

400 W Batch Irradiation: Batch irradiation previously reported¹¹ when enamide **19** (265 g, 800 mmol) was irradiated in MeCN (0.4 M) with ITX (2.0 g, 8 mmol) with a 400 W Hg lamp in a 2 L Pyrex reactor for 35 hrs. The product **20** was isolated as a pale yellow solid (249 g, 94%)

36 W Blue COB Irradiation: The general 36 W COB reactor procedure was followed by irradiating enamide **19** (9.94 g, 30 mmol) in degassed MeCN (0.5 M) with 2,2'-MeOTX (82 mg, 0.3 mmol) in a 100 ml flask for 1.5 hrs. The reaction mixture was concentrated *in vacuo* and triturated with hexane and filtered, washing with cold Et₂O to give **20** as a pale yellow solid (9.05 g, 91%)

Cross [2+2] of Enamide **21**

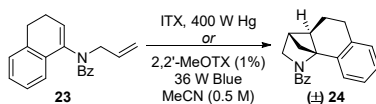


Scheme S18

400 W Batch Irradiation: Batch irradiation previously reported¹¹ when enamide **21** (117 g, 400 mmol) was irradiated in MeCN (0.2 M) with ITX (1.0 g, 4 mmol) with a 400 W Hg lamp in a 2 L Pyrex reactor for 29 hrs. The product **22** was isolated as a pale yellow solid (102 g, 87%)

36 W Blue COB Irradiation: The general 36 W COB reactor procedure was followed by irradiating enamide **21** (8.80 g, 30 mmol) in degassed MeCN (0.5 M) with 2,2'-MeOTX (82 mg, 0.3 mmol) in a 100 ml flask for 3.5 hrs. The reaction mixture was concentrated *in vacuo* and triturated with hexane and filtered, washing with cold Et₂O to give **22** as a pale yellow solid (7.78 g, 88%)

Cross [2+2] of Enamide **23**

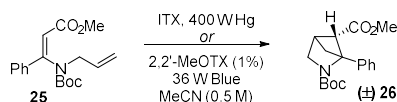


Scheme S19

400 W Batch Irradiation: The general immersion well batch procedure was followed using a 400 W Hg lamp and 1 L Pyrex reactor to irradiate enamide **23** (57.9 g, 200 mmol) in degassed MeCN (0.2 M) with ITX (1.0 g, 4 mmol). After 20 hrs the reaction mixture was concentrated *in vacuo* and triturated with hexane and filtered, washing with cold Et₂O to give **24** as a beige powder (39.5 g, 68%): m.p. 138–139°C; δ_{H} (500 MHz, DMSO-d₆, 80°C) 7.58 – 7.52 (2H, m, Ar.H), 7.44 – 7.32 (3H, m, Ar.H), 7.12 – 6.92 (4H, m, Ar.H), 3.90 (1H, d, $J = 8.0$ Hz, NCHH), 3.38 (1H, d, $J = 8.0$ Hz, NCHH), 2.85 – 2.73 (2H, m, CH₂), 2.70 (1H, s, CH), 2.42 – 2.37 (1H, m, CHH), 2.19 – 1.96 (4H, m, CH₂, CH, CHH); δ_{C} (126 MHz, DMSO-d₆, 80°C) 171.3 (C), 136.4 (C), 135.7 (C), 135.0 (C), 129.9 (CH), 128.0 (CH), 127.6 (2×CH), 127.4 (2×CH), 125.6 (CH), 125.1 (CH), 125.0 (CH), 71.1 (C), 56.7 (CH₂), 49.8 (CH), 45.8 (CH₂), 36.6 (CH), 28.7 (CH₂), 23.2 (CH₂); ESI-HRMS m/z 290.1544 (MH⁺ C₂₀H₂₀NO requires 290.1539)

36 W Blue COB Irradiation: The general 36 W COB reactor procedure was followed by irradiating enamide **23** (8.68 g, 30 mmol) in degassed MeCN (0.5 M) with 2,2'-MeOTX (82 mg, 0.3 mmol) in a 100 ml flask for 6 hrs. The reaction mixture was concentrated *in vacuo* and triturated with hexane and filtered, washing with cold Et₂O to give **24** as a beige solid (5.87 g, 68%)

Cross [2+2] of Amino Cinnamate **25**

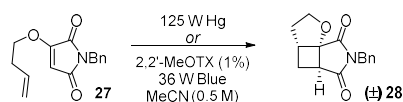


Scheme S20

400 W Batch Irradiation: The general immersion well batch procedure was followed using a 400 W Hg lamp and 400 ml Pyrex reactor to irradiate amino cinnamate **25** (12.7 g, 40 mmol) in degassed MeCN (0.1 M) with ITX (0.5 g, 2 mmol). After 3.5 hrs the reaction mixture was concentrated *in vacuo* and triturated with hexane and filtered, washing with petrol to give **26** as a pale yellow solid (9.2 g, 72%)

36 W Blue COB Irradiation: The general 36 W COB reactor procedure was followed by irradiating amino cinnamate **25** (9.52 g, 30 mmol) in degassed MeCN (0.5 M) with 2,2'-MeOTX (82 mg, 0.3 mmol) in a 100 ml flask for 3.75 hrs. The reaction mixture was concentrated *in vacuo* and triturated with hexane and filtered, washing with petrol to give **26** as a white solid (7.98 g, 84%): m.p. 73–74°C; δ_{H} (400 MHz, CDCl₃) 7.45 – 7.21 (5H, m, Ar.H), 3.92 (1H, d, $J = 8.9$ Hz, NCHH), 3.70 (3H, s, OCH₃), 3.56 (1H, d, $J = 8.9$ Hz, NCHH), 3.08 – 3.02 (2H, m, CH, CH), 1.92 – 1.84 (2H, m, CH₂), 1.07 (9H, s, 3×CH₃); δ_{C} (101 MHz, CDCl₃) 169.7 (C), 157.1 (C), 138.5 (C), 127.9 (2×CH), 127.3 (CH), 126.8 (2×CH), 79.1 (C), 76.5 (C), 51.7 (CH₃), 51.0 (CH), 50.9 (CH₂), 45.3 (CH₂), 38.0 (CH), 28.0 (3×CH₃); ESI-HRMS m/z 318.1693 (MH⁺ C₁₈H₂₄NO₄ requires 318.1700)

Intramolecular [2+2] of Alkoxy-maleimide **27**

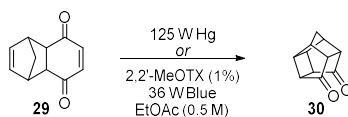


Scheme S21

125 W Batch Irradiation: The general immersion well batch procedure was followed using a 125 W Hg lamp and 150 ml Pyrex reactor to irradiate alkoxy-maleimide **27** (3.86 g, 15 mmol) in degassed MeCN (0.1 M). After 1.5 hrs the reaction mixture was concentrated *in vacuo* and chromatography on silica (5% Et₂O in DCM) yielded product **28** as a white solid (3.57 g, 92%)

36 W Blue COB Irradiation: The general 36 W COB reactor procedure was followed by irradiating alkoxy-maleimide **27** (2.57 g, 10 mmol) in degassed MeCN (0.1 M) with 2,2'-MeOTX (136 mg, 0.5 mmol) in a 250 ml flask for 1.5 hrs. The reaction mixture was concentrated *in vacuo* and triturated with hexane and filtered, washing with cold Et₂O to give **28** as a pale yellow solid (2.38 g, 93%): m.p. 127-129°C; δ_{H} (400 MHz, CDCl₃) 7.40 – 7.25 (5H, m, Ar.H), 4.75 (1H, d, $J = 14.1$ Hz, NCHHPh), 4.71 (1H, d, $J = 14.1$ Hz, NCHHPh), 4.45 (1H, ddd, $J = 9.3, 7.7, 1.8$ Hz, OCHH), 4.09 (1H, ddd, $J = 10.7, 9.3, 5.7$ Hz, OCHH), 3.15 – 3.08 (1H, m, CH), 3.05 (1H, ddd, $J = 10.4, 4.3, 1.1$ Hz, CH), 2.20 (1H, ddd, $J = 13.7, 8.2, 4.2$ Hz, CHH), 2.15-2.06 (1H, m, CHH), 2.12 (1H, dd, $J = 10.4, 5.7$ Hz, CHH), 1.87 (1H, ddt, $J = 12.8, 5.7, 1.7$ Hz, CHH); δ_{C} (101 MHz, CDCl₃) 176.4 (C), 175.3 (C), 135.7 (C), 128.8 (2×CH), 128.7 (2×CH), 128.1 (CH), 84.6 (C), 71.0 (CH₂), 42.6 (CH₂), 42.6 (CH), 41.9 (CH), 31.9 (CH₂), 25.0 (CH₂)

Cookson's Dione [2+2]



Scheme S22

125 W Batch Irradiation: Batch irradiation previously reported when Diels Alder adduct **29** (2.61 g, 15 mmol) was irradiated in EtOAc (0.1 M) with a 125 W Hg lamp in a 150 ml Pyrex reactor for 15 min. The product **30** was isolated as an off-white solid (2.38 g, 91%)

36 W Blue COB Irradiation: The general 36 W COB reactor procedure was followed by irradiating Diels Alder adduct **29** (2.61 g, 15 mmol) in degassed EtOAc (0.5 M) with 2,2'-MeOTX (41 mg, 0.15 mmol) in a 50 ml flask for 25 min. The reaction mixture was concentrated *in vacuo* and triturated with hexane and filtered, washing with cold Et₂O to give **30** as a pale yellow solid (2.41 g, 92%)

Comparison with non-Sensitized Reaction

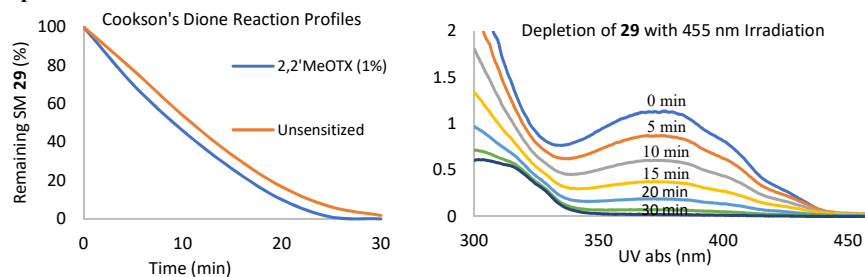


Figure S13: *left-* Depletion of **29** over time with, and without 2,2'-MeOTX (36 W blue COB); *Right-* UV absorption of **29** over time with irradiation at 455 nm showing depletion of peak at 374 nm

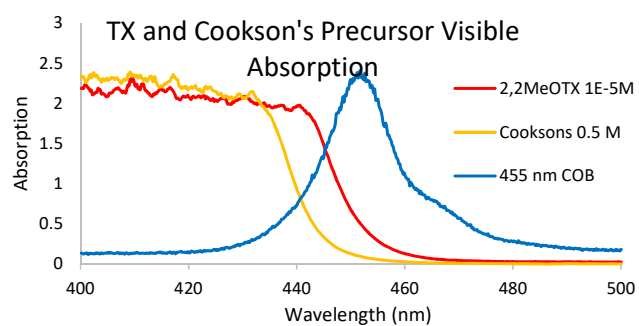


Figure S14: Comparison of vis light absorption of enedione **29** and 2,2'-MeOTX

X-Ray Data for 24 and 26

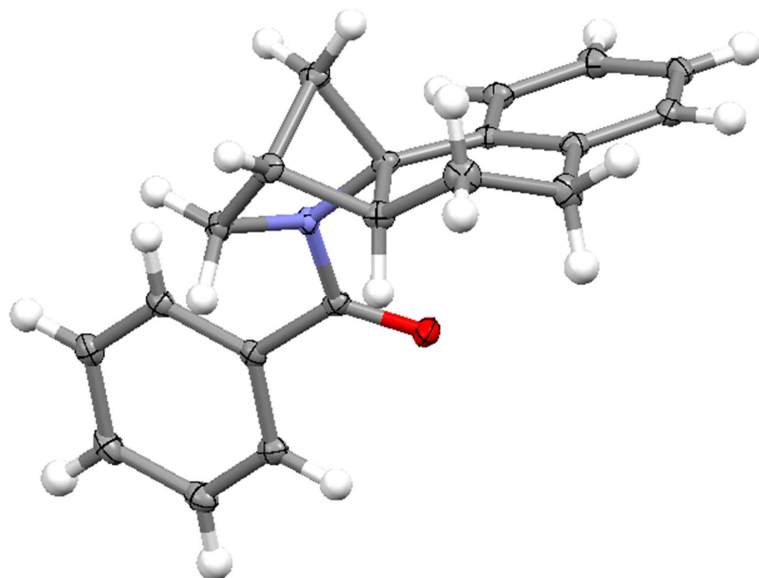


Figure S15: X-Ray structure of compound 24. Ellipsoids shown at 30% probability

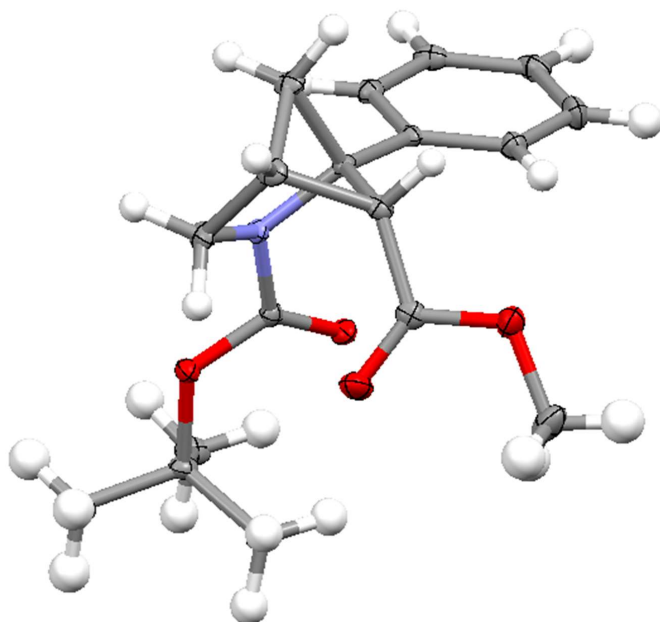


Figure S16: X-Ray structure of compound 26. Ellipsoids shown at 30% probability

Crystallography

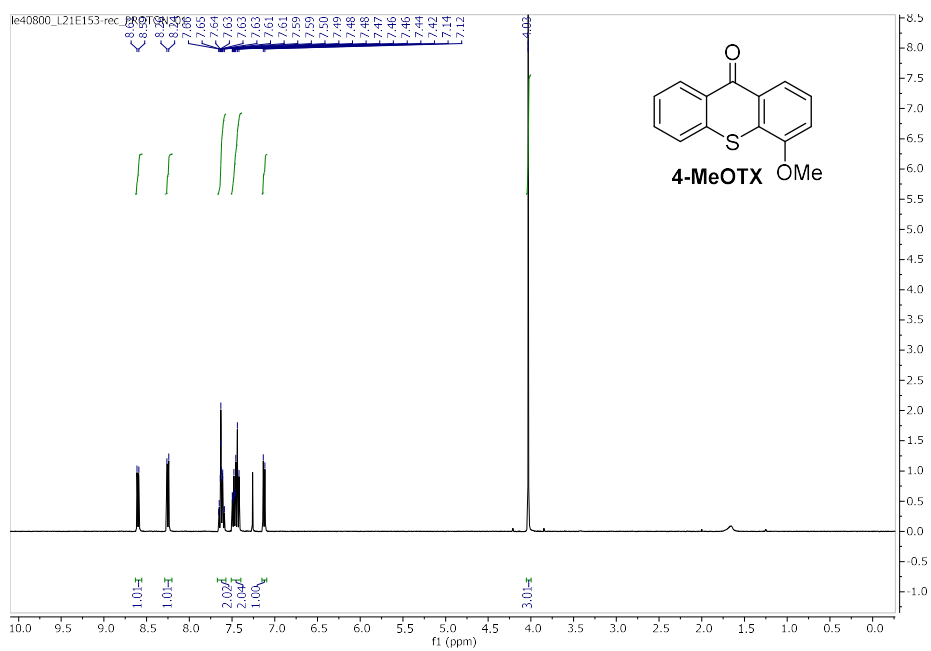
X-ray diffraction experiments on **24** and **26** were carried out at 100(2) K on a Bruker APEX II diffractometer with CCD using Mo-K α radiation ($\lambda = 0.71073$ Å). Intensities were integrated in SAINT¹² and absorption corrections based on equivalent reflections were applied using SADABS.¹³ Both structures were solved using ShelXT¹⁴ and refined by full matrix least squares against F^2 in ShelXL^{15,16} using Olex2¹⁷. All of the non-hydrogen atoms were refined anisotropically. While all of the hydrogen atoms were located geometrically and refined using a riding model. Crystal structure and refinement data are given in Table S37. Crystallographic data for compounds **24** and **26** have been deposited with the Cambridge Crystallographic Data Centre as supplementary publication CCDC 1989743-1989744. Copies of the data can be obtained free of charge on application to CCDC, 12 Union Road, Cambridge CB2 1EZ, UK [fax(+44) 1223 336033, e-mail: deposit@ccdc.cam.ac.uk].

Identification code	24	26
Empirical formula	C ₂₀ H ₁₉ NO	C ₁₈ H ₂₃ NO ₄
Formula weight	289.36	317.37
Temperature/K	100(2)	100(2)
Crystal system	monoclinic	monoclinic
Space group	<i>P2₁/c</i>	<i>P2₁/n</i>
<i>a</i> /Å	18.0122(7)	12.9756(6)
<i>b</i> /Å	7.3245(2)	7.5343(3)
<i>c</i> /Å	11.5355(4)	17.9068(8)
α /°	90	90
β /°	97.158(2)	100.916(3)
γ /°	90	90
Volume/Å ³	1510.02(9)	1718.93(13)
Z	4	4
ρ_{calc} /cm ³	1.273	1.226
μ /mm ⁻¹	0.078	0.086
F(000)	616.0	680.0
Crystal size/mm ³	0.456 × 0.198 × 0.14	0.495 × 0.405 × 0.373
Radiation	MoK α (λ = 0.71073)	MoK α (λ = 0.71073)
2 θ range for data collection/°	4.558 to 50.694	3.574 to 55.886
Index ranges	-21 ≤ <i>h</i> ≤ 21, -8 ≤ <i>k</i> ≤ 8, -13 ≤ <i>l</i> ≤ 13	-16 ≤ <i>h</i> ≤ 17, -9 ≤ <i>k</i> ≤ 9, -23 ≤ <i>l</i> ≤ 23
Reflections collected	21808	15326
R _{int} / R _{sigma}	0.0653 / 0.0358	0.0340 / 0.0327
Data/restraints/parameters	2759/0/199	4103/0/212
Goodness-of-fit on F ²	1.034	1.035
Final R indexes [<i>I</i> ≥ 2 σ (<i>I</i>)]	R ₁ = 0.0400, wR ₂ = 0.0933	R ₁ = 0.0400, wR ₂ = 0.0950
Final R indexes [all data]	R ₁ = 0.0590, wR ₂ = 0.1040	R ₁ = 0.0515, wR ₂ = 0.1018
Largest diff. peak/hole / e Å ⁻³	0.17/-0.21	0.24/-0.24

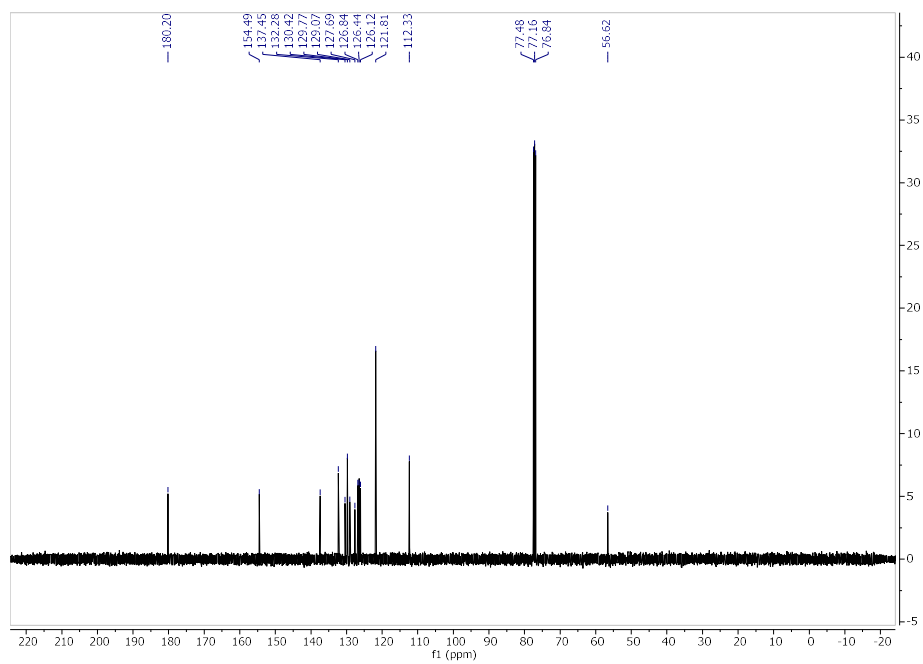
Table S37: Crystal data and structure refinement for **24** and **26**.

Copies of ^1H and ^{13}C NMR Spectra

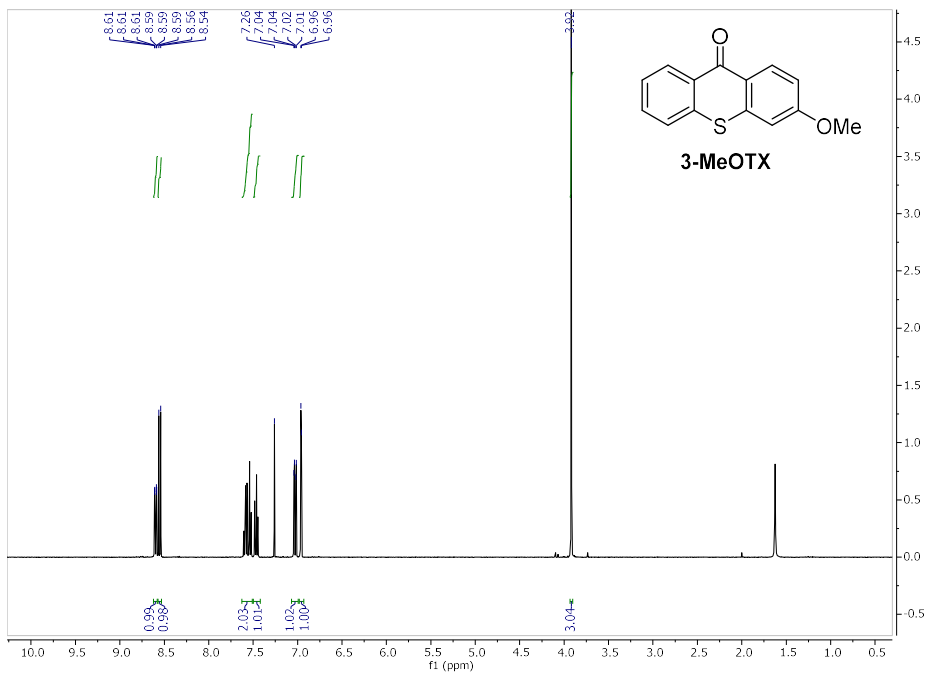
^1H -NMR (400 MHz, CDCl_3)



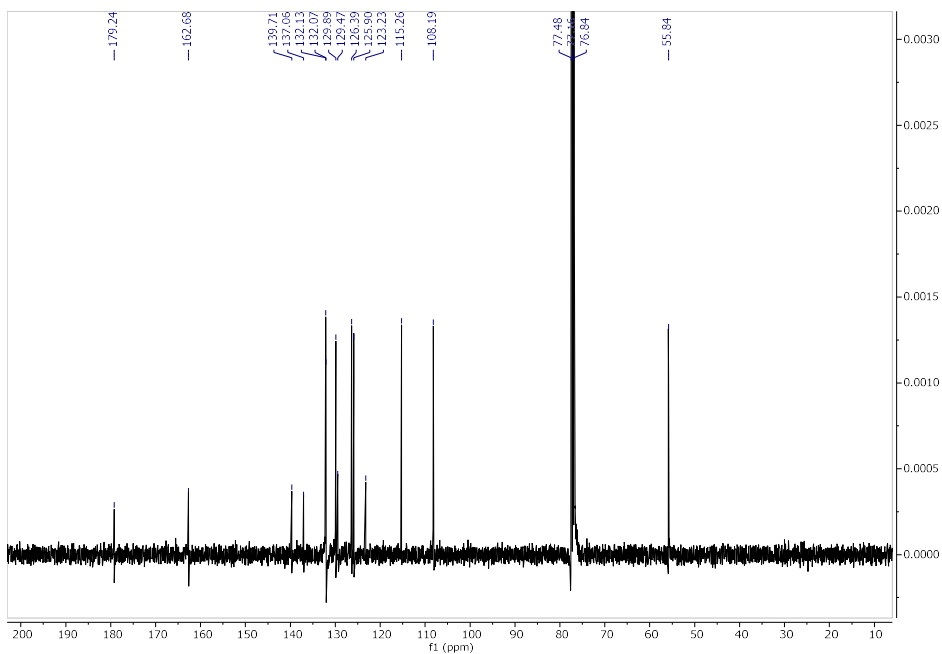
^{13}C -NMR (101 MHz, CDCl_3)



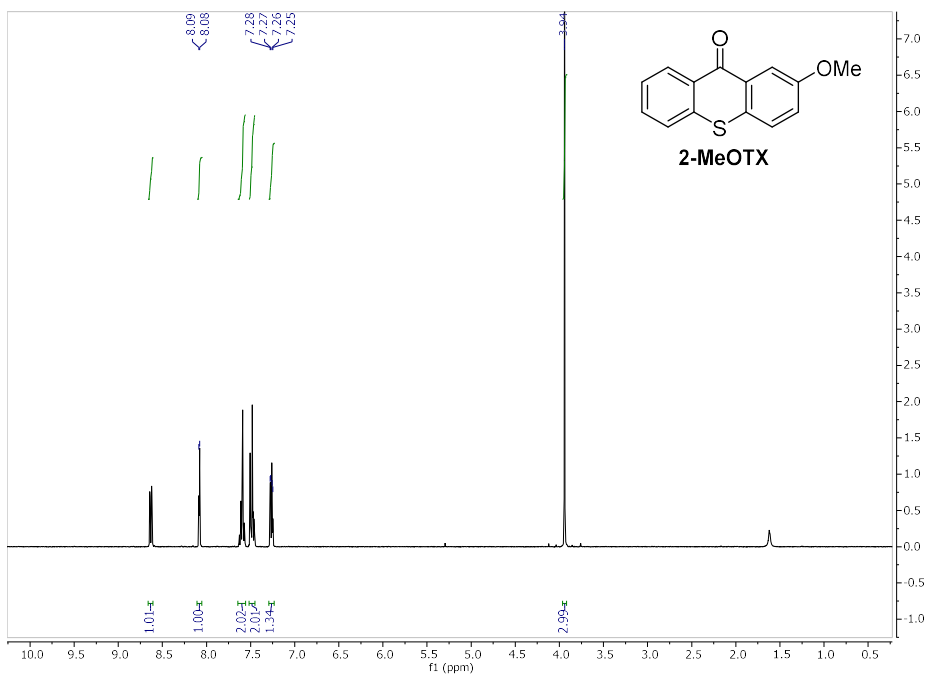
¹H-NMR (400 MHz, CDCl₃)



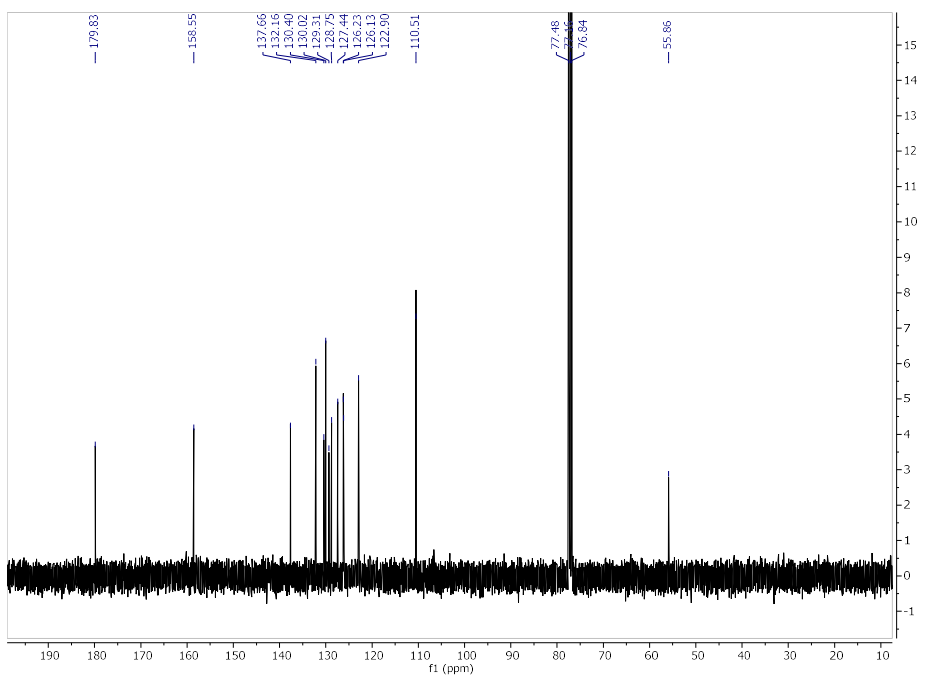
¹³C-NMR (101 MHz, CDCl₃)



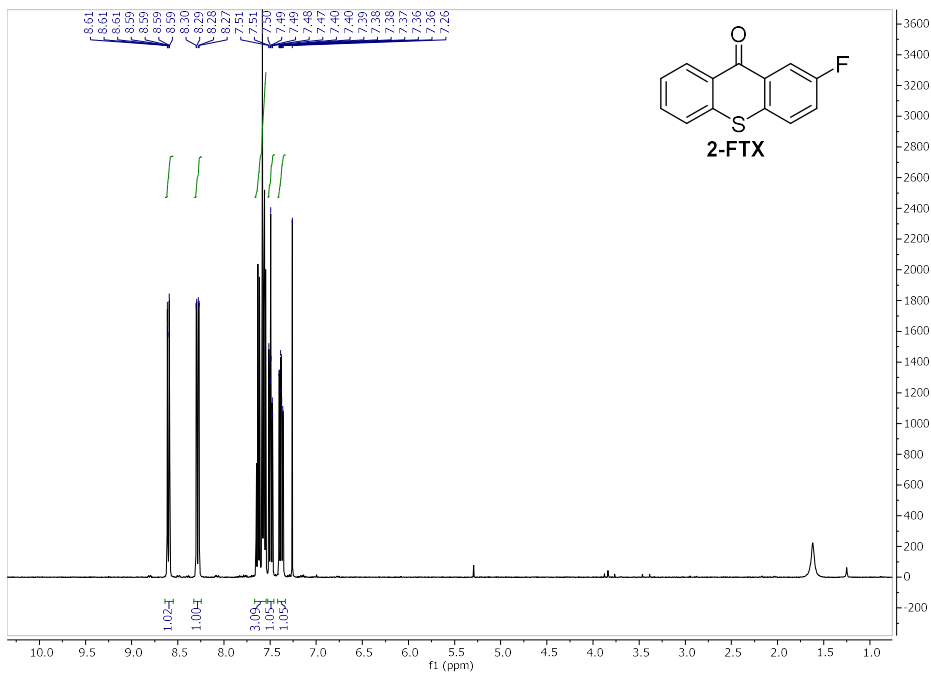
¹H-NMR (400 MHz, CDCl₃)



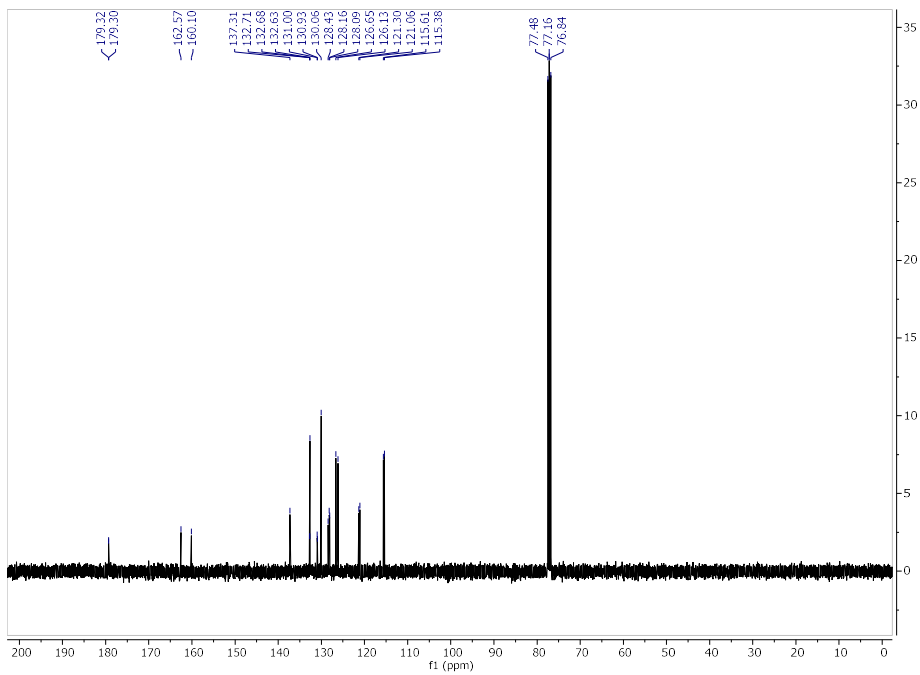
¹³C-NMR (101 MHz, CDCl₃)



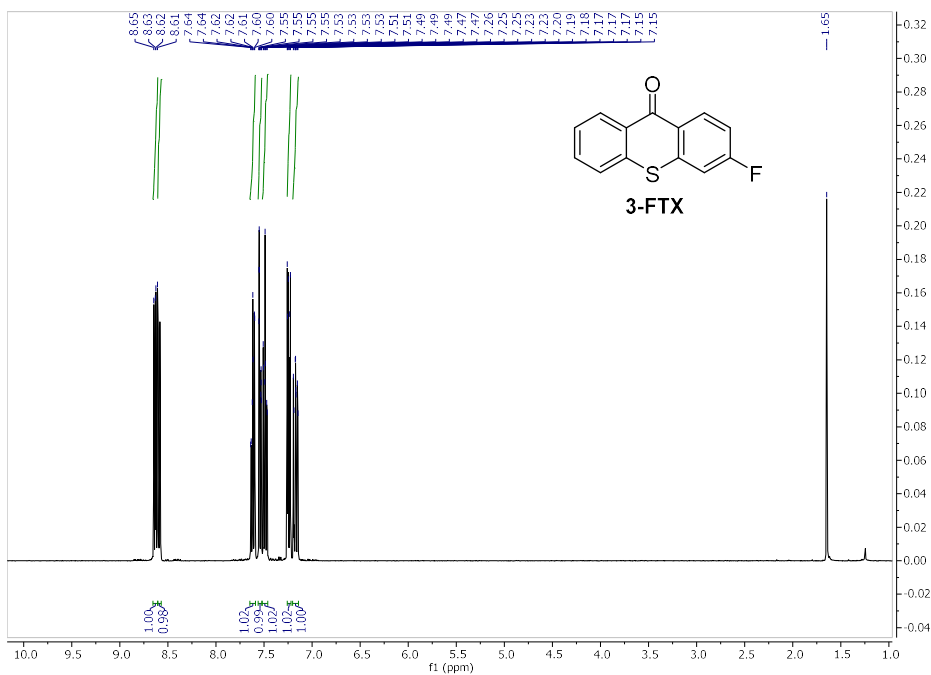
¹H-NMR (400 MHz, CDCl₃)



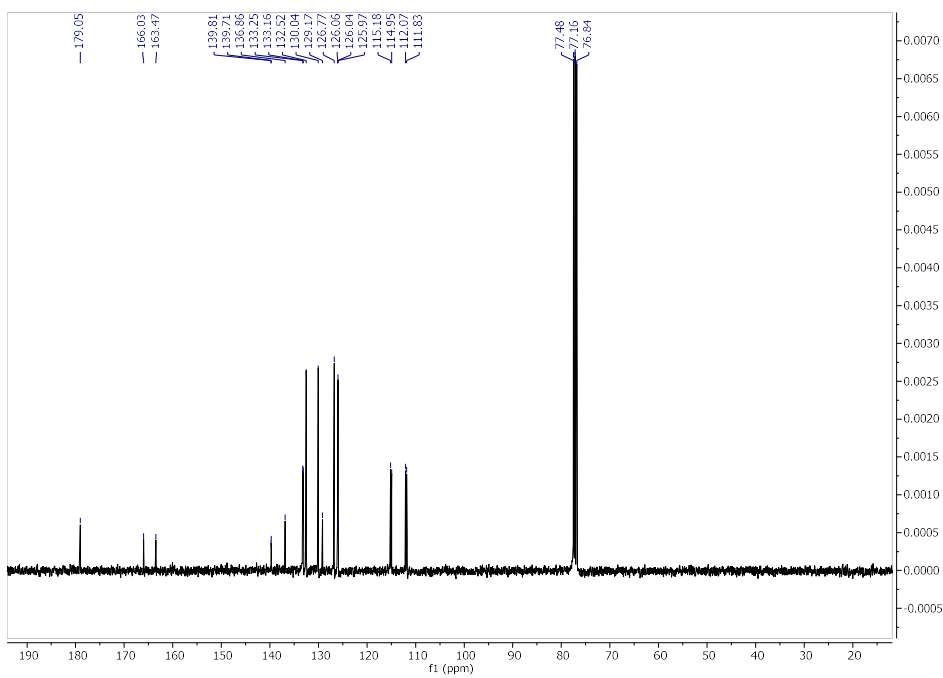
¹³C-NMR (101 MHz, CDCl₃)



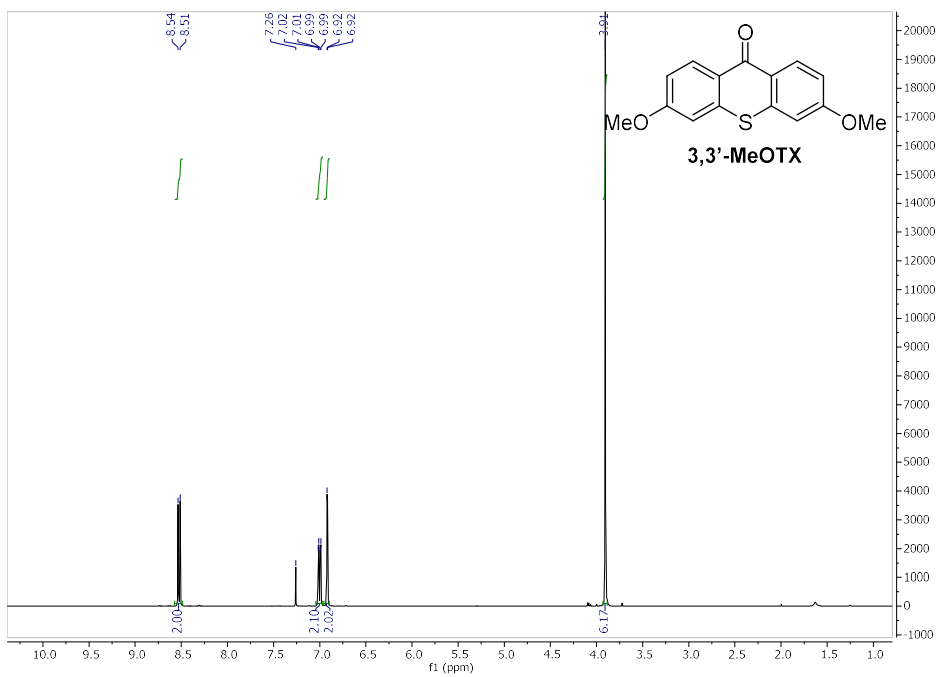
¹H-NMR (400 MHz, CDCl₃)



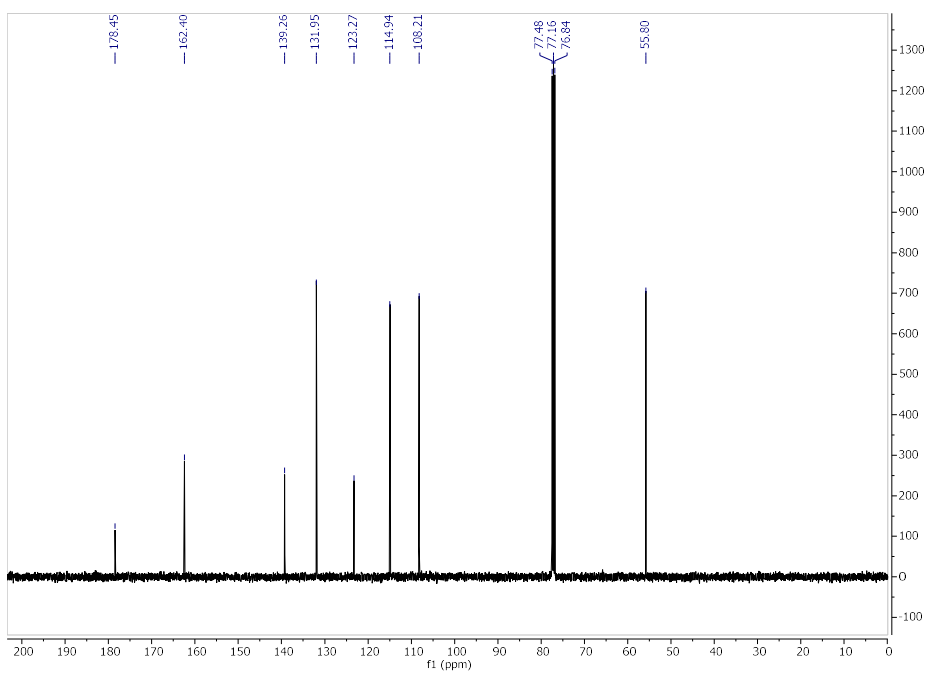
¹³C-NMR (101 MHz, CDCl₃)



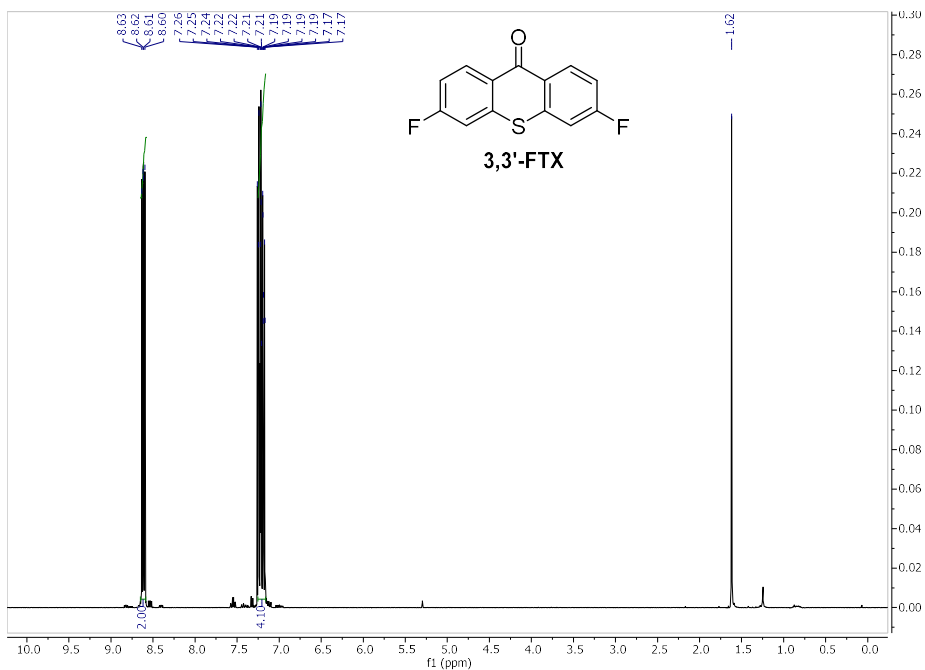
¹H-NMR (400 MHz, CDCl₃)



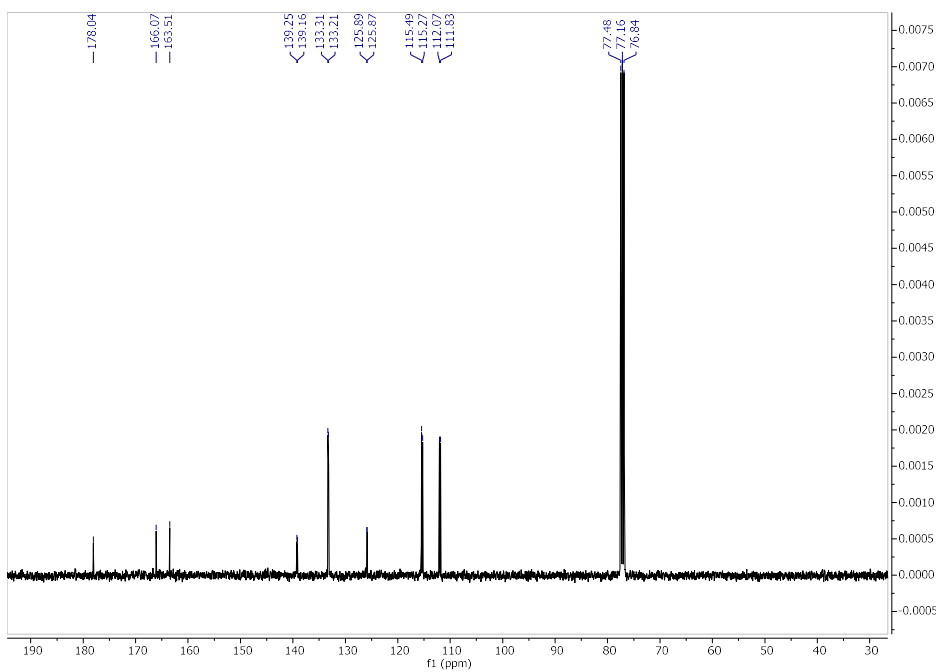
¹³C-NMR (101 MHz, CDCl₃)



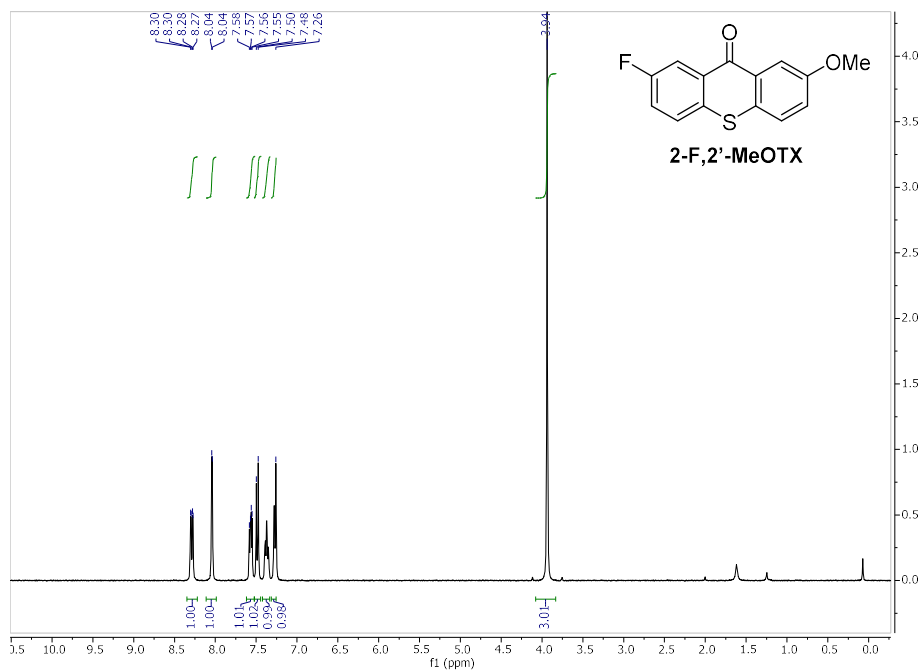
¹H-NMR (400 MHz, CDCl₃)



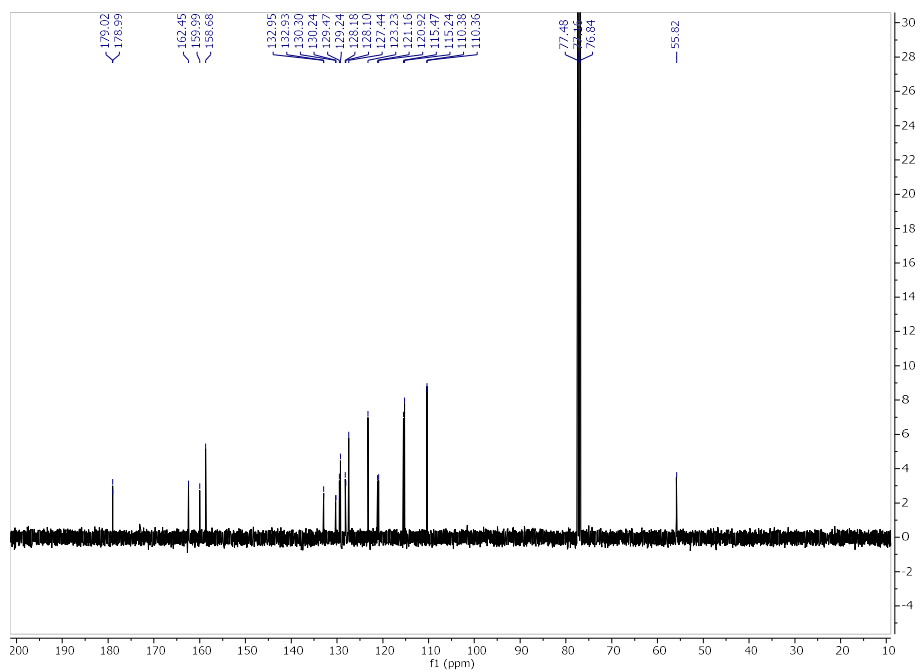
¹³C-NMR (101 MHz, CDCl₃)



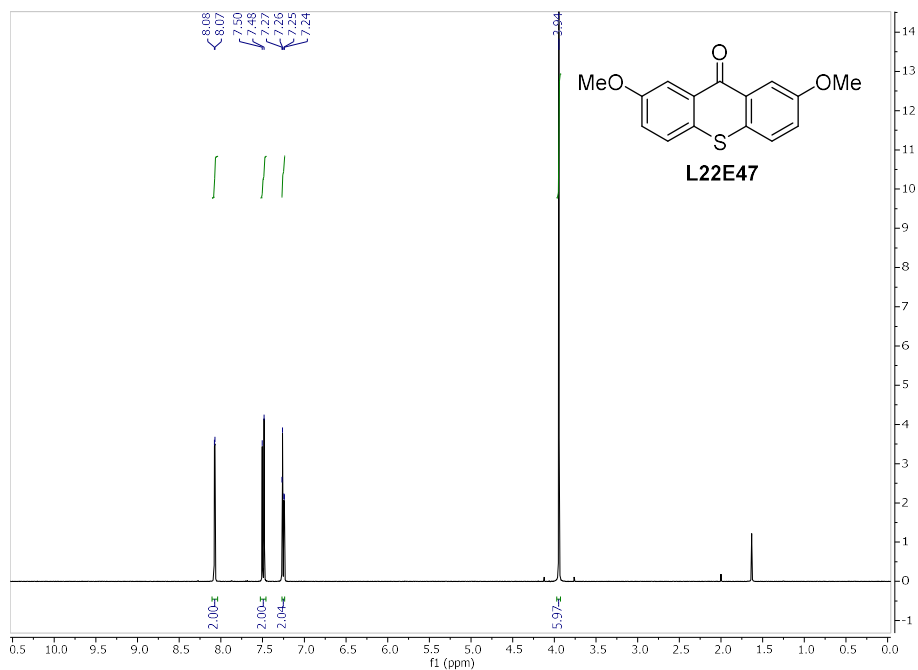
¹H-NMR (400 MHz, CDCl₃)



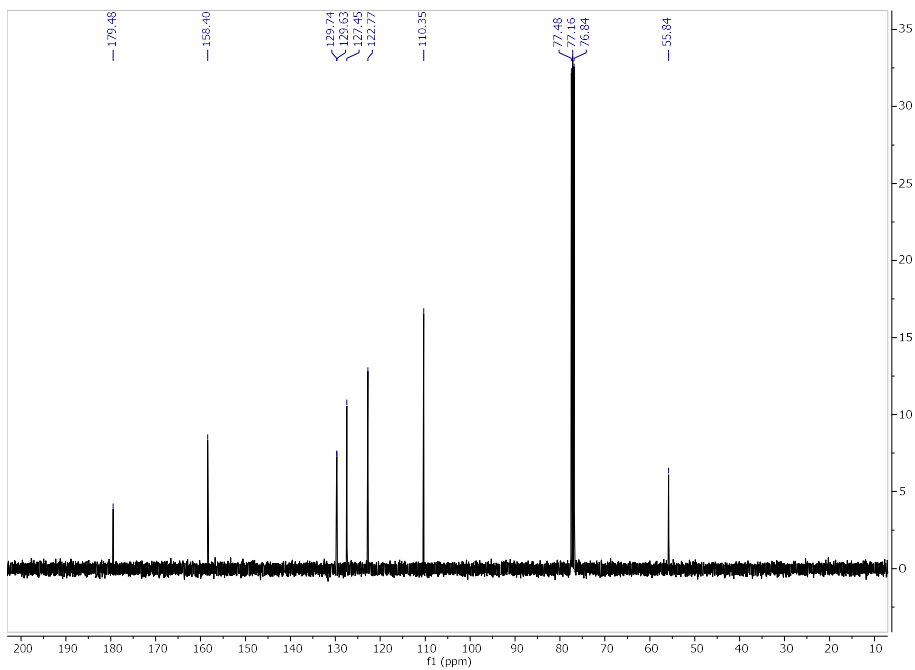
¹³C-NMR (101 MHz, CDCl₃)



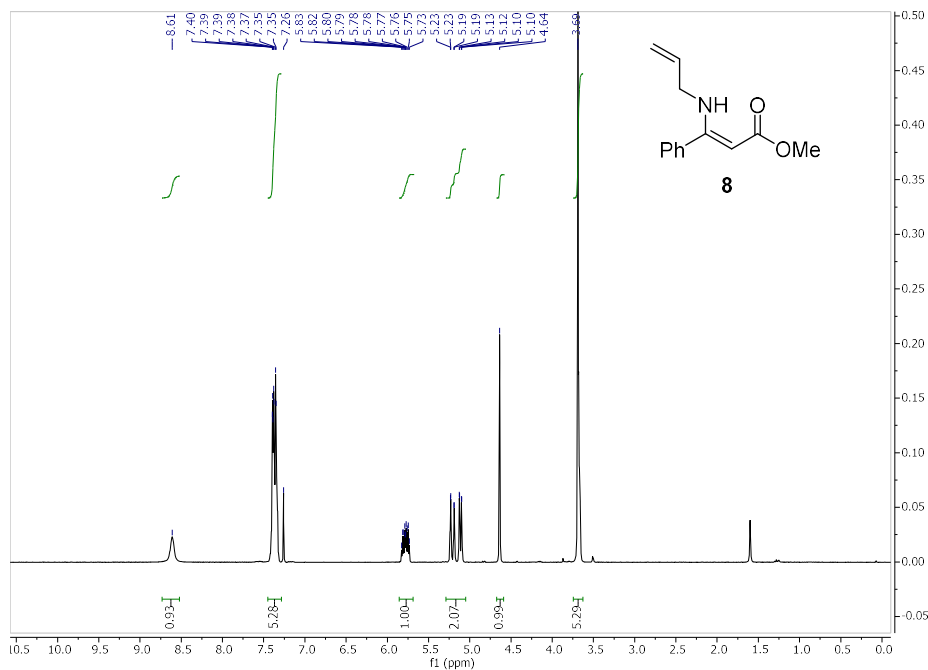
¹H-NMR (400 MHz, CDCl₃)



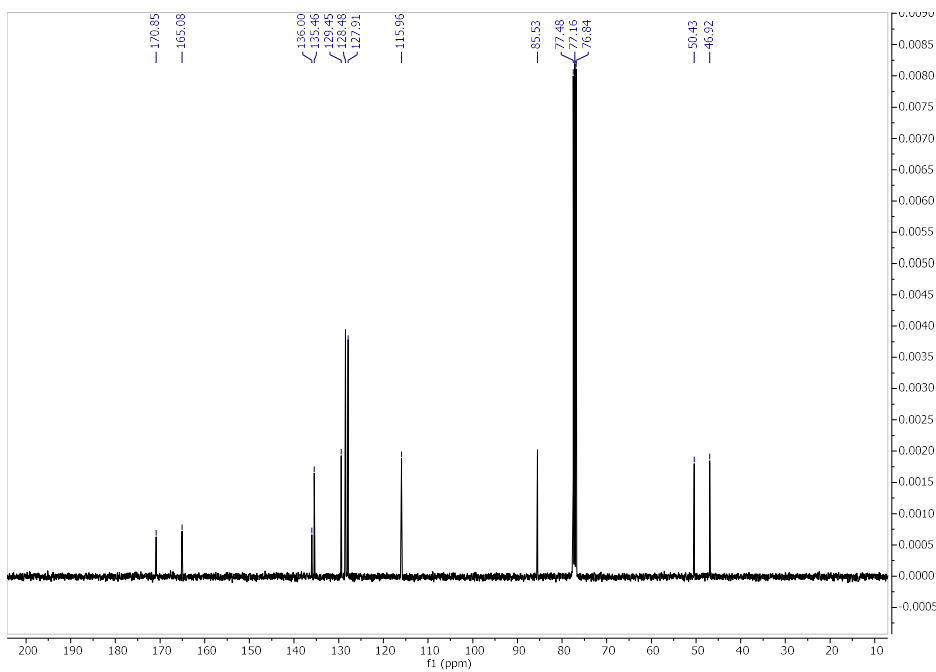
¹³C-NMR (101 MHz, CDCl₃)



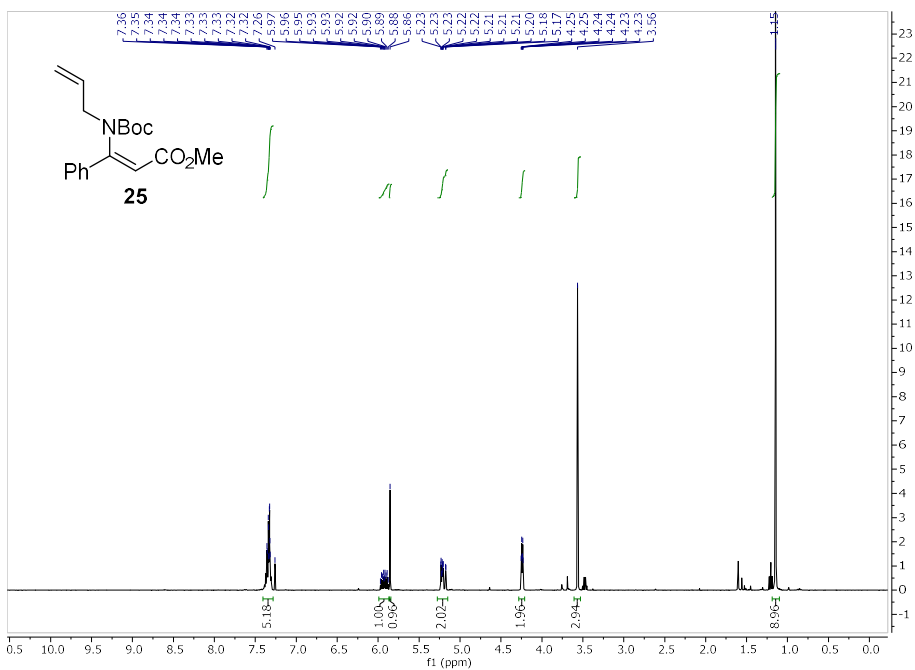
¹H-NMR (400 MHz, CDCl₃)



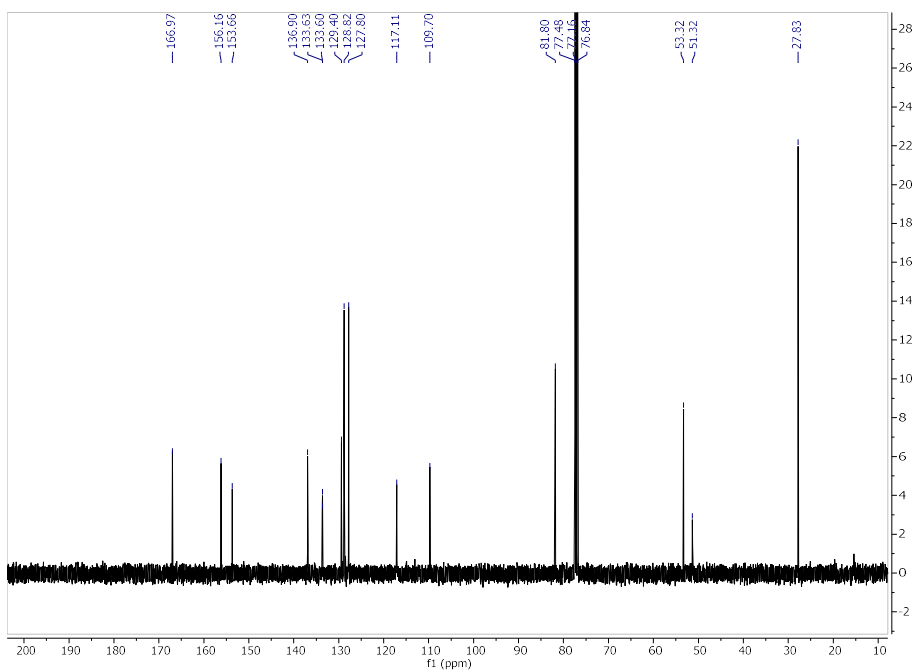
¹³C-NMR (101 MHz, CDCl₃)



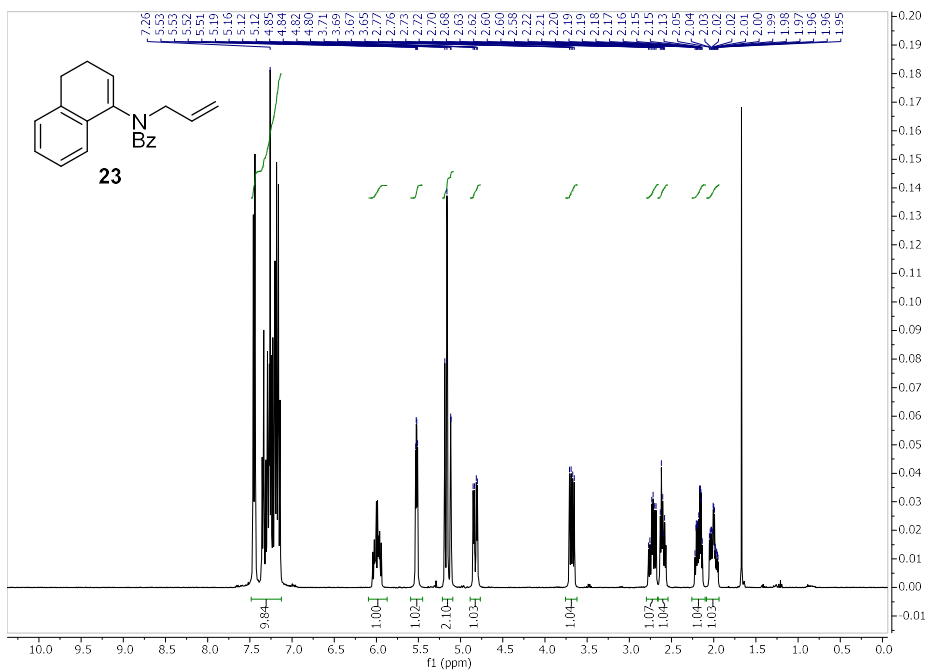
¹H-NMR (400 MHz, CDCl₃)



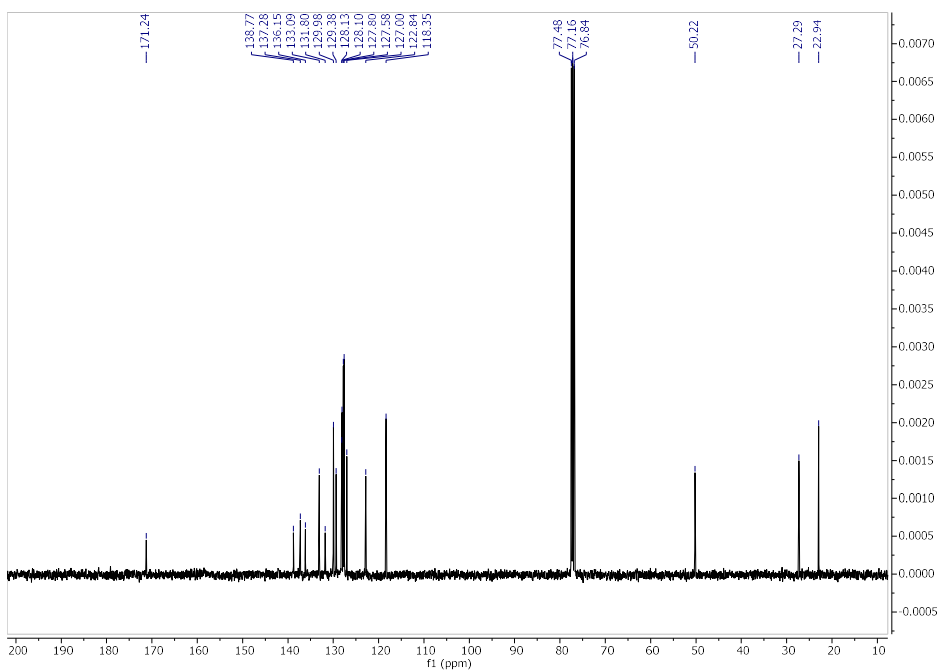
¹³C-NMR (101 MHz, CDCl₃)



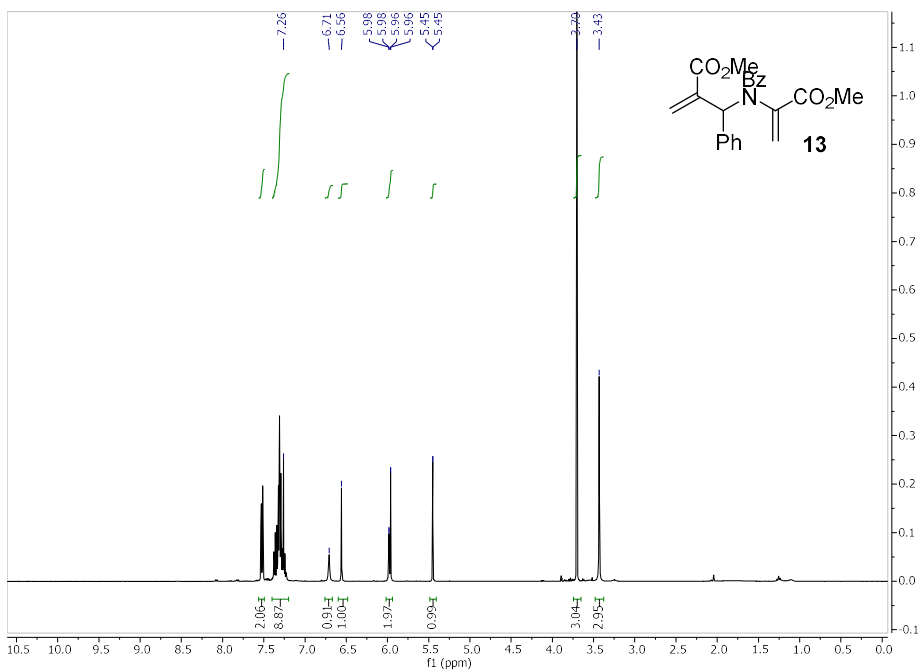
¹H-NMR (400 MHz, CDCl₃)



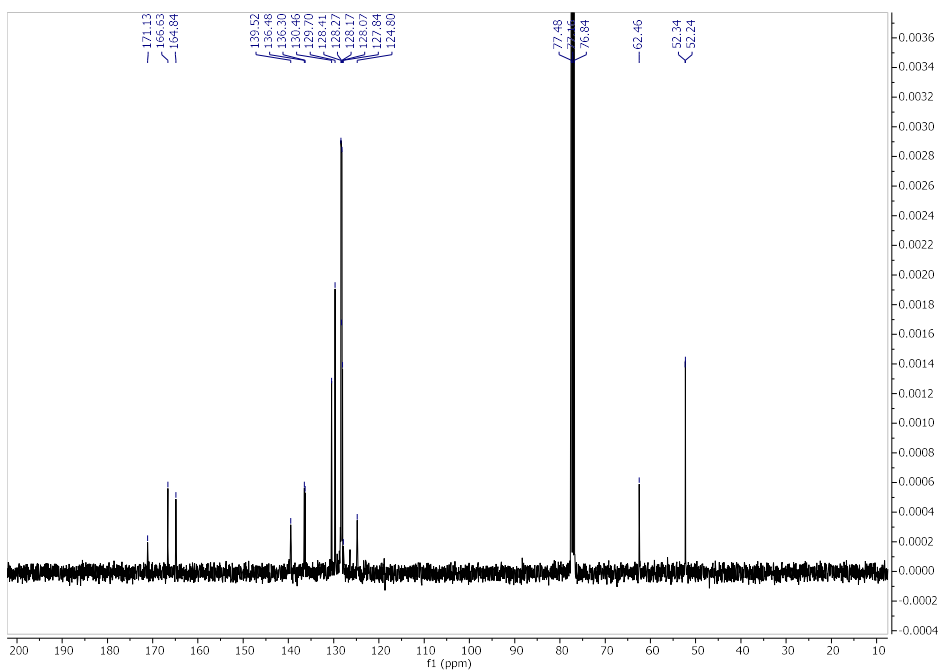
¹³C-NMR (101 MHz, CDCl₃)



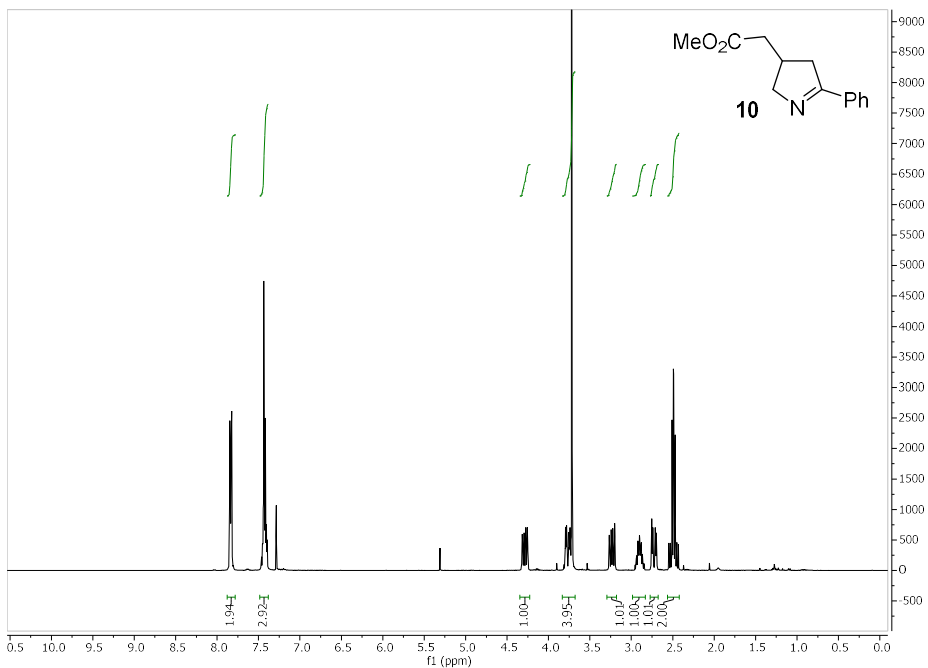
¹H-NMR (400 MHz, CDCl₃)



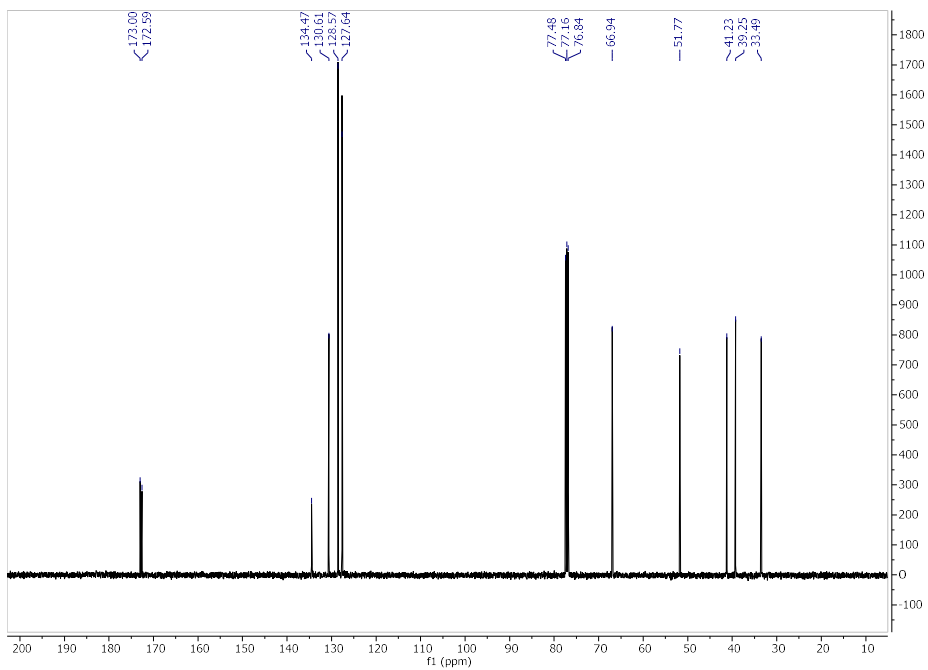
¹³C-NMR (101 MHz, CDCl₃)



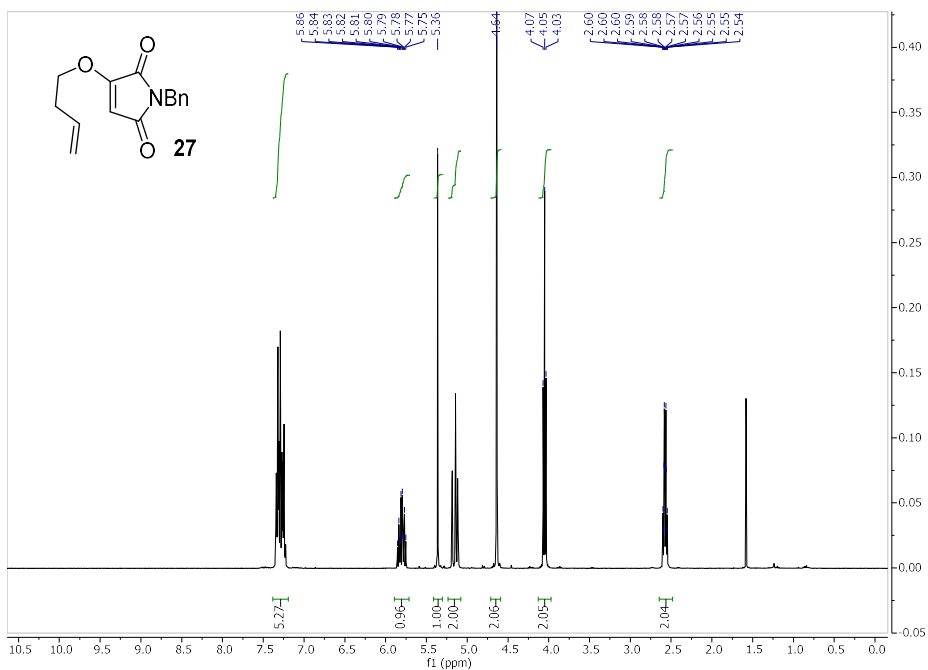
¹H-NMR (400 MHz, CDCl₃)



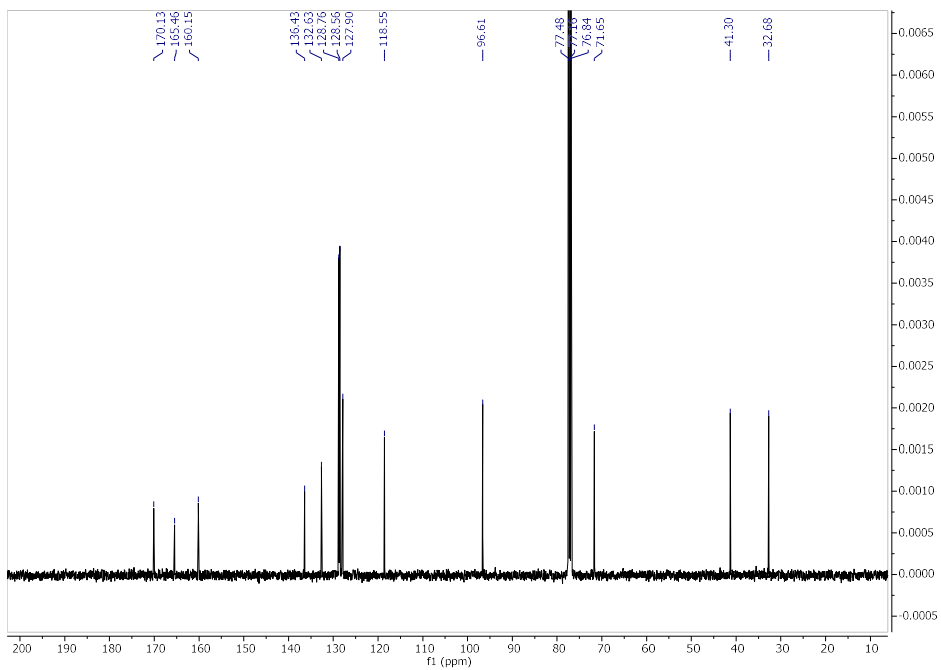
¹³C-NMR (101 MHz, CDCl₃)



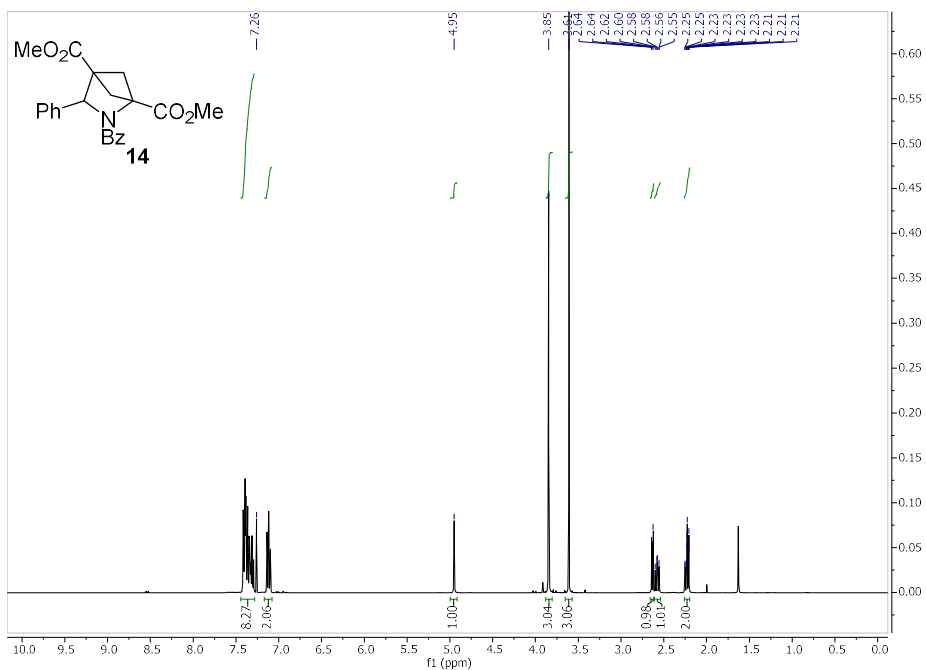
¹H-NMR (400 MHz, CDCl₃)



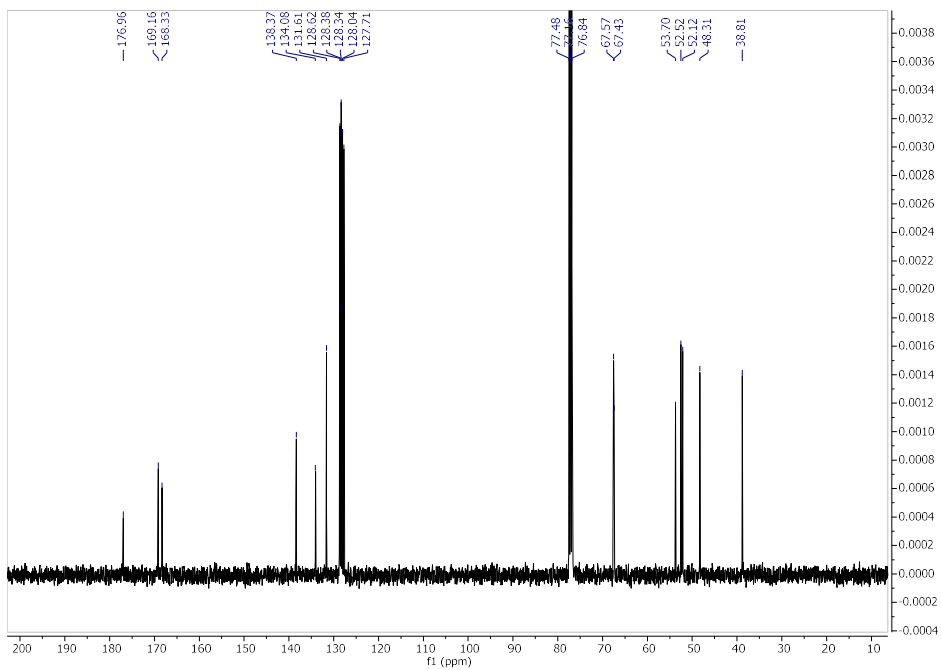
¹³C-NMR (101 MHz, CDCl₃)



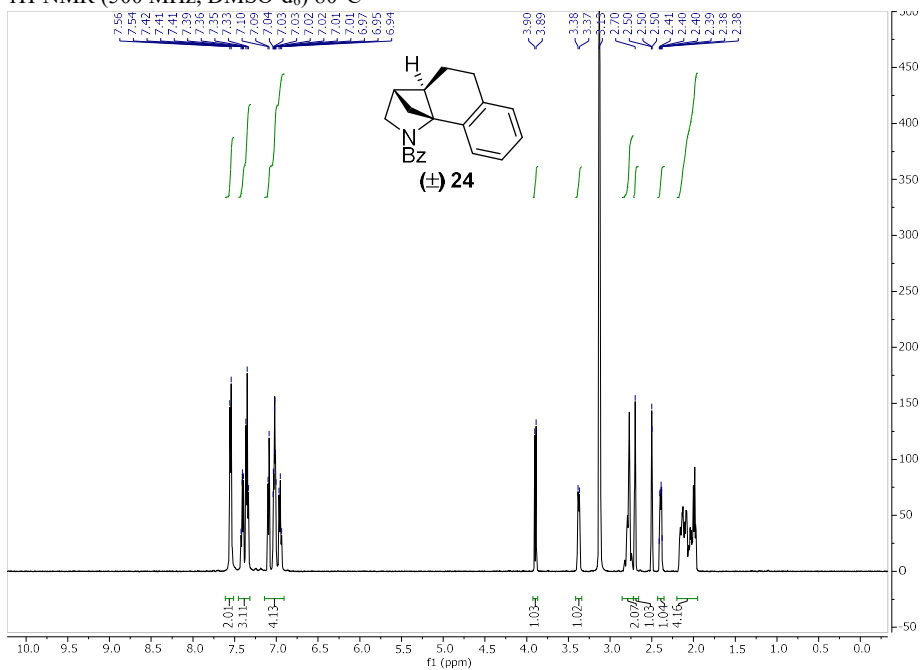
¹H-NMR (400 MHz, CDCl₃)



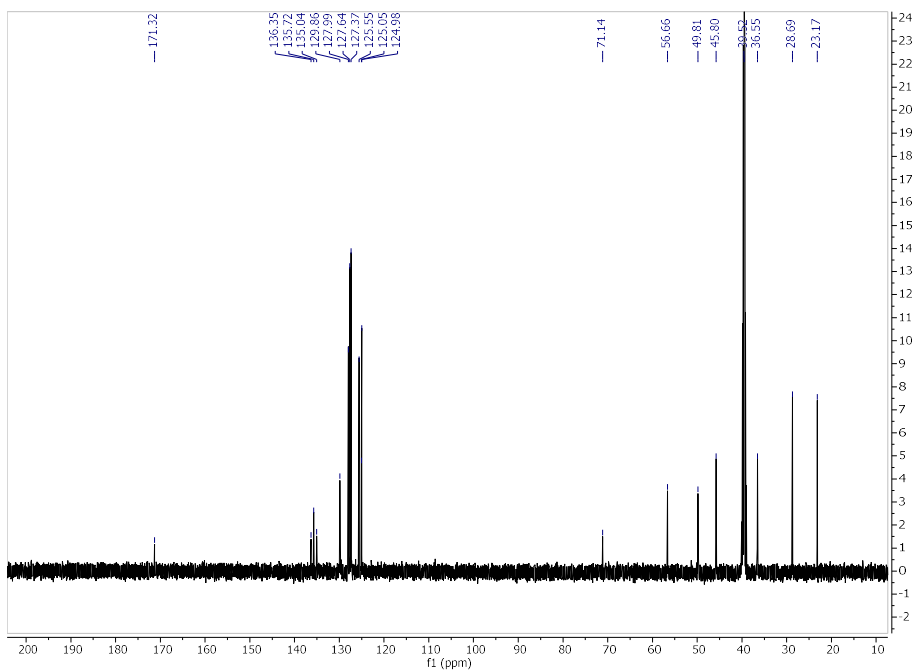
¹³C-NMR (101 MHz, CDCl₃)



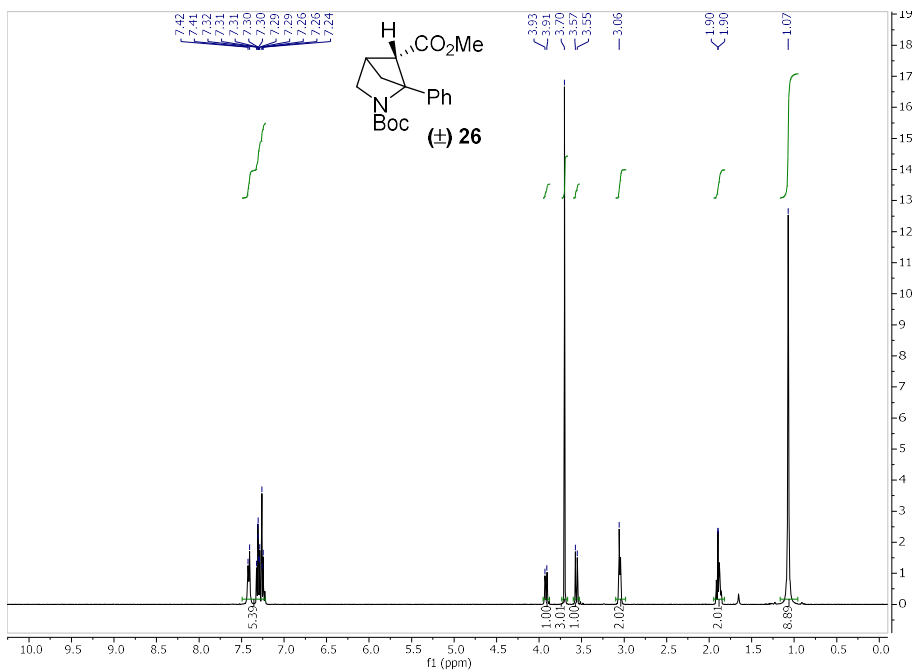
¹H-NMR (500 MHz, DMSO-d₆) 80°C



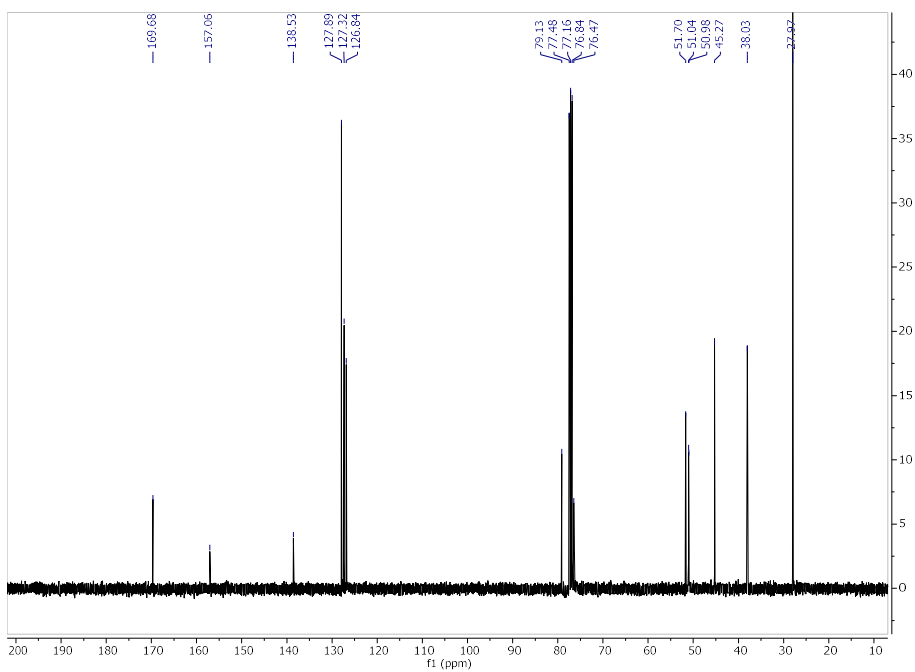
¹³C-NMR (126 MHz, DMSO-d₆) 80°C



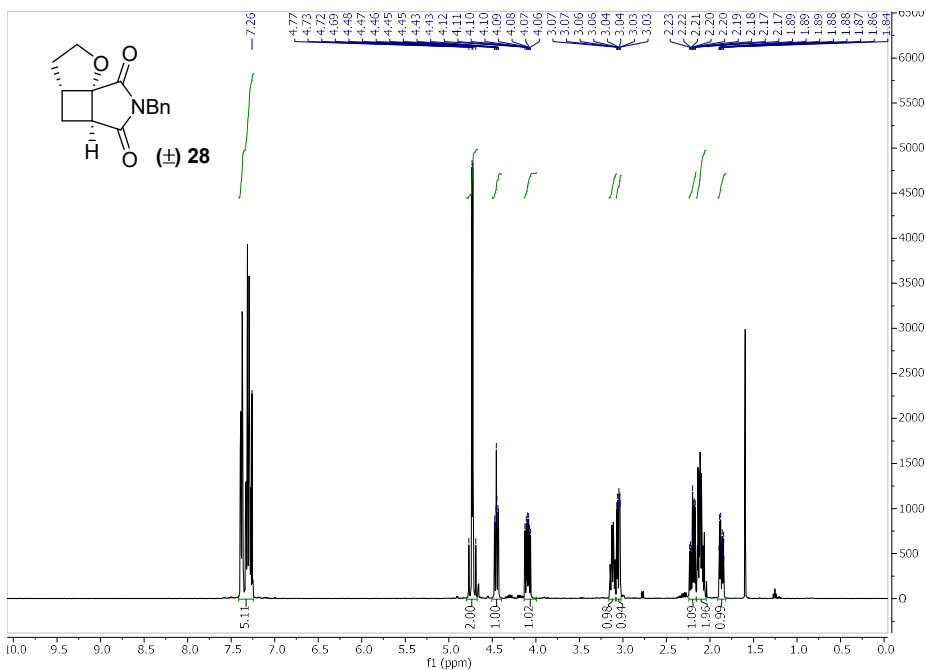
¹H-NMR (400 MHz, CDCl₃)



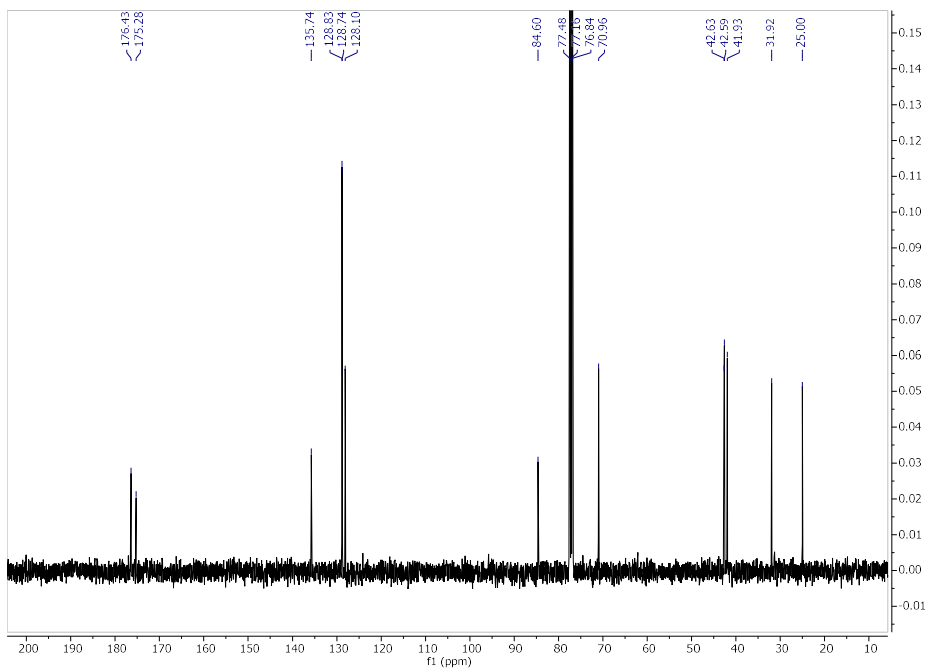
¹³C-NMR (101 MHz, CDCl₃)



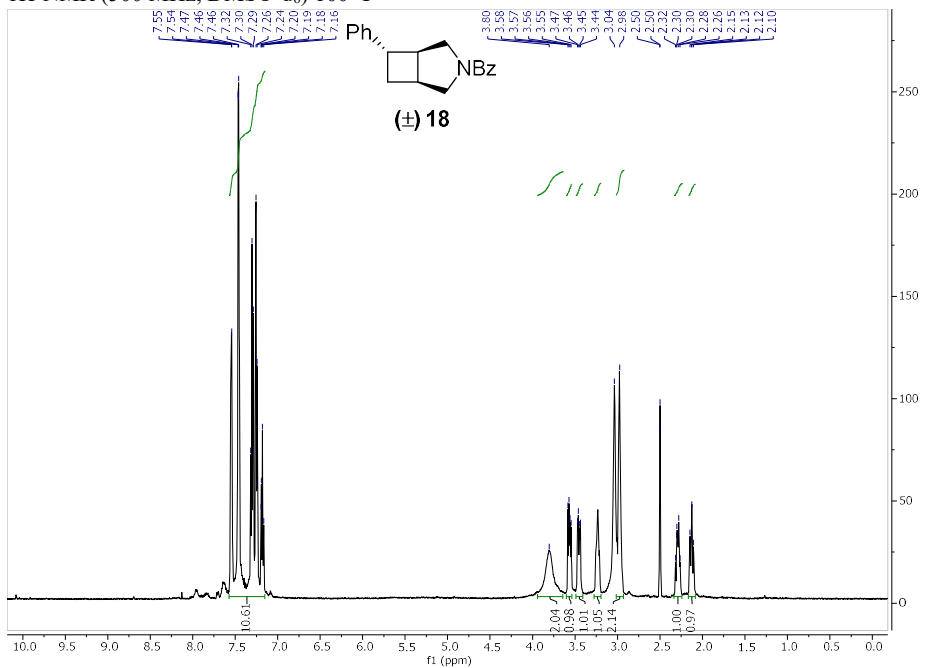
¹H-NMR (400 MHz, CDCl₃)



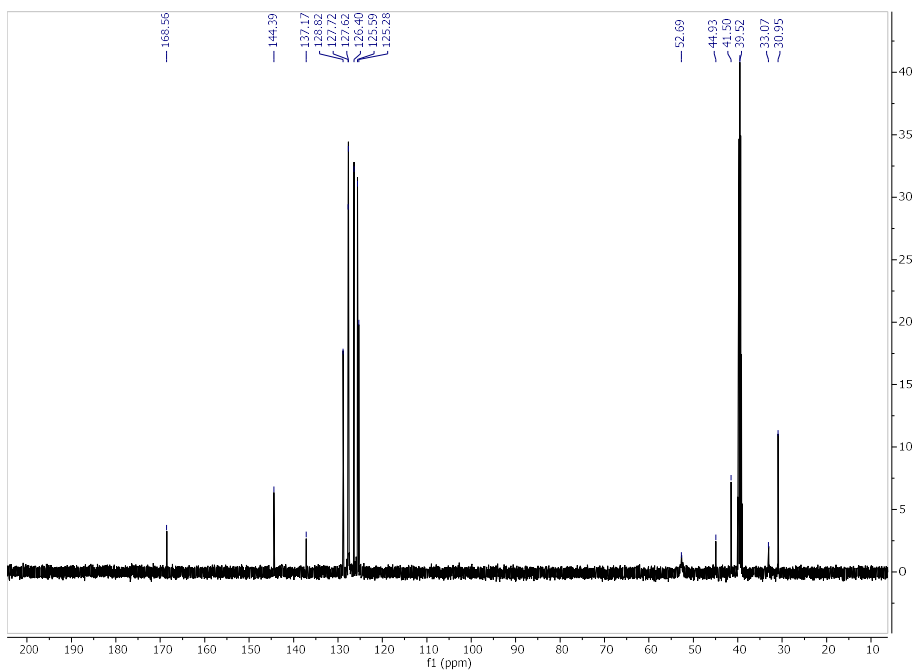
¹³C-NMR (101 MHz, CDCl₃)



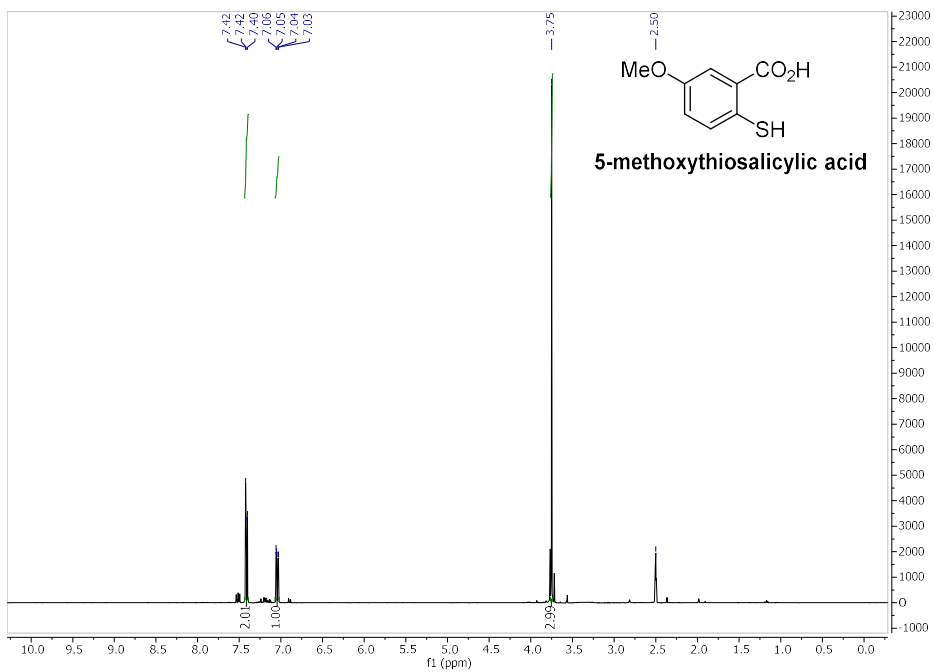
¹H-NMR (500 MHz, DMSO-d₆) 100°C



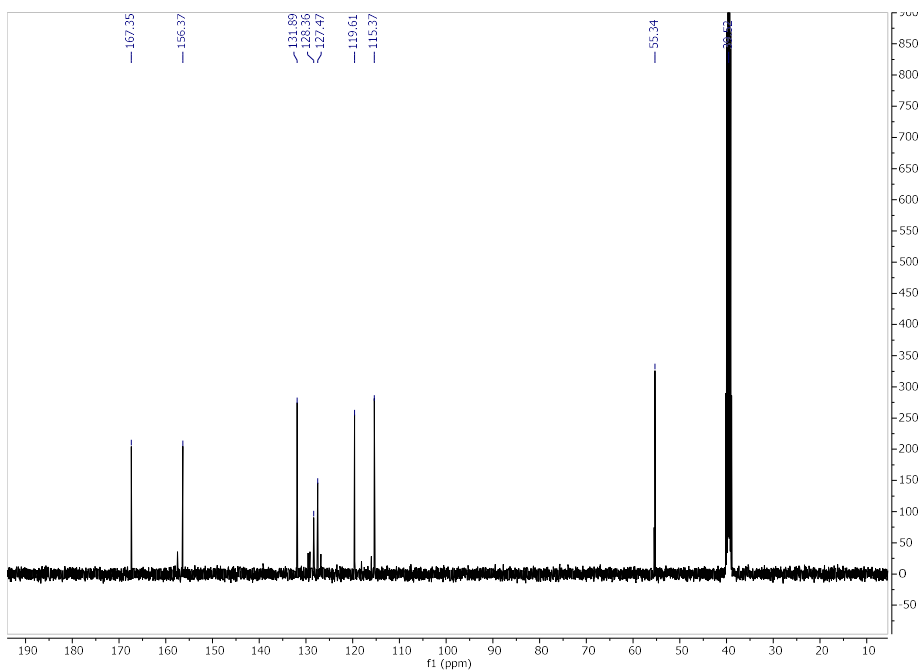
¹³C-NMR (126 MHz, DMSO-d₆) 120°C



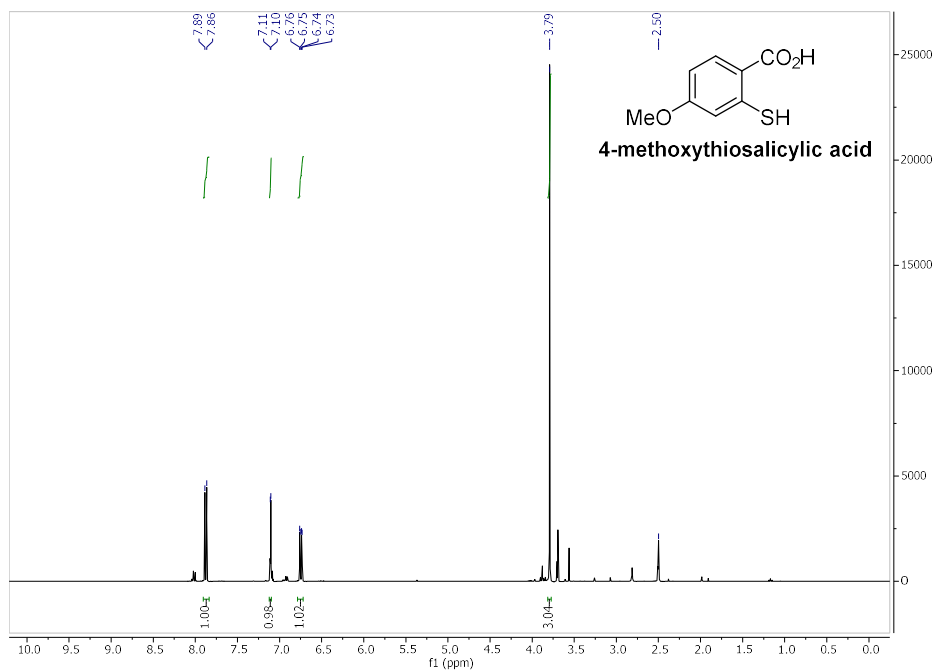
¹H-NMR (400 MHz, DMSO-d₆)



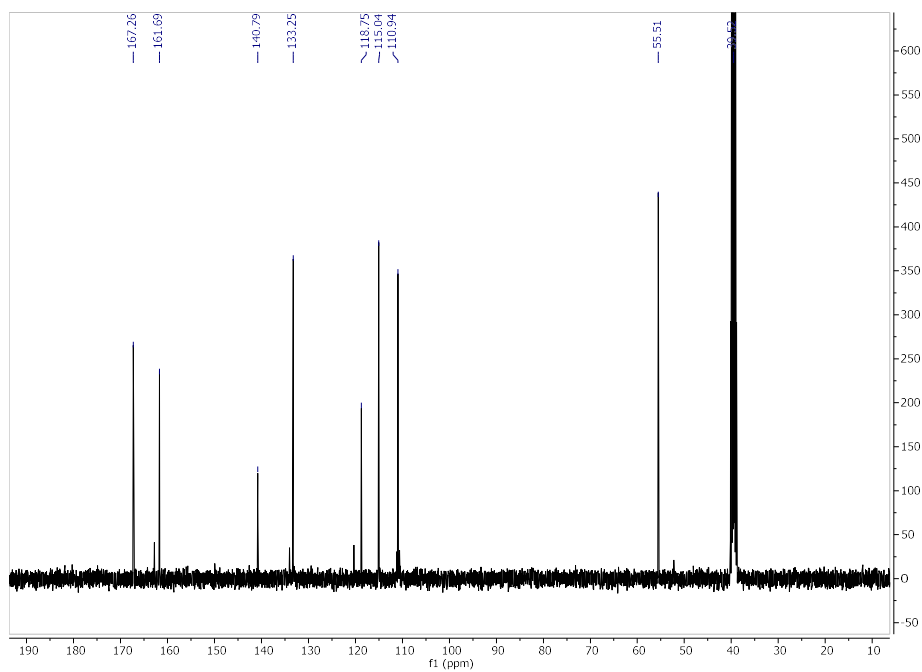
¹³C-NMR (101 MHz, DMSO-d₆)



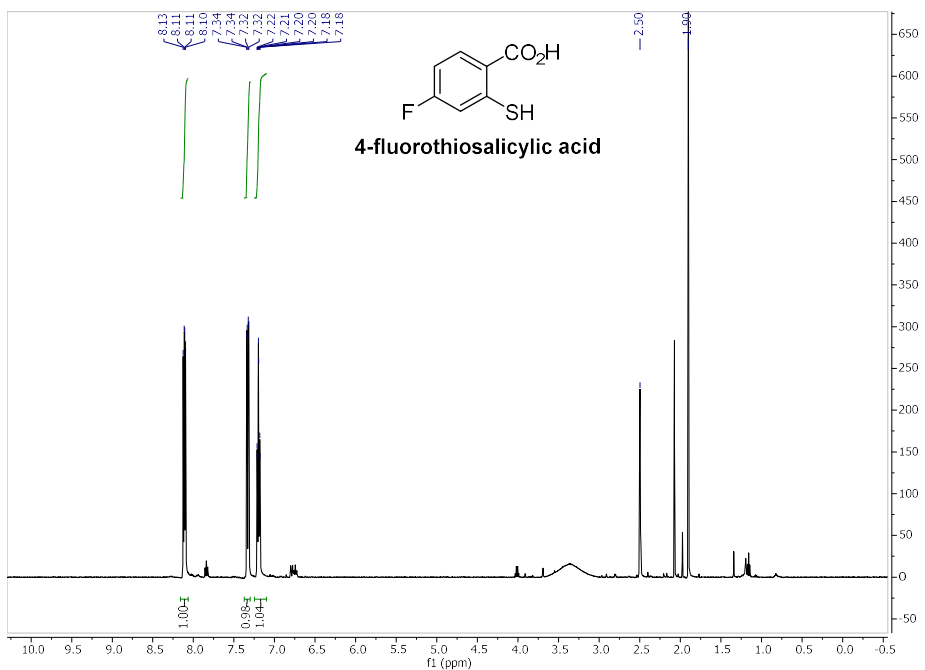
¹H-NMR (400 MHz, DMSO-d₆)



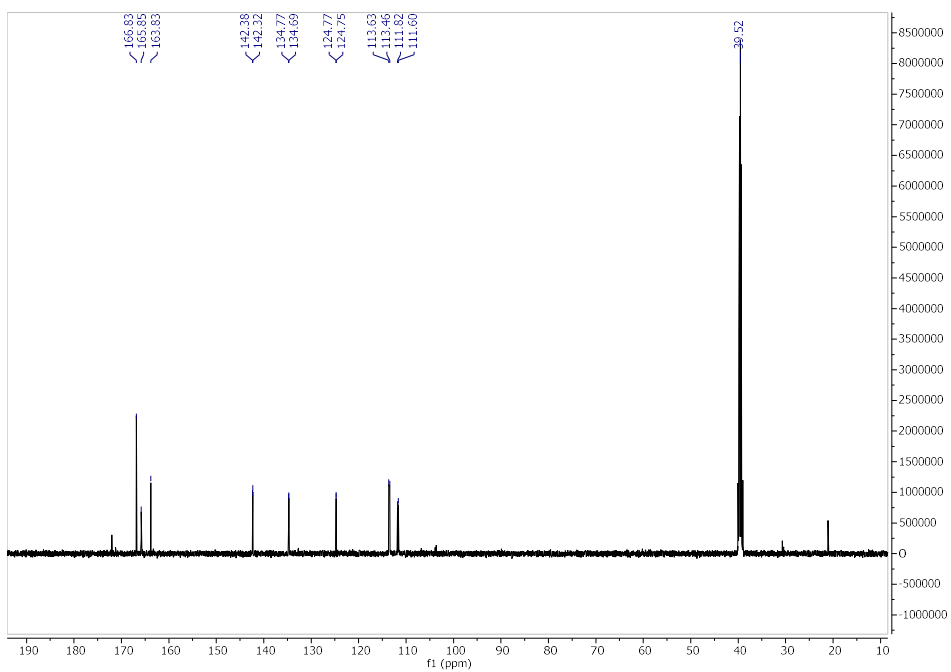
¹³C-NMR (101 MHz, DMSO-d₆)



¹H-NMR (500 MHz, DMSO-d₆)



¹³C-NMR (126 MHz, DMSO-d₆)



References

- ¹ Perkowski, A. J.; Cruz, C. L.; Nicewicz, D. A. An Ambient Temperature Newman-Kwart Rearrangement Mediated by Organic Photoredox Catalysis. *J. Am. Chem. Soc.* **2015**, *137*, 15684–15687
- ² Herbicidal sulphonamides, Patent US4632693 (A), 1986
- ³ 1,3-BENZOTHIAZINONE DERIVATIVES AND USE THEREOF, Patent EP1424336 (A1), 2004
- ⁴ 1,4-benzothiazepine derivatives, Patent US5416066 (A), 1995
- ⁵ Watanabe, M.; Date, M.; Tsukazaki, M.; Furukawa, S. *Chem. Pharm. Bull.* **1989**, *37*, 36 – 41
- ⁶ Roberts, K. C.; Smiles, S. CXIII. -Methoxy-derivatives of thioxanthone. *J. Chem. Soc.* **1929**, 863-872
- ⁷ Novel thioxanthene derivatives and salts thereof and a process for the manufacture of same. Patent GB861521 (A), 1961
- ⁸ Brennan, Peter, Michael W. George, Omar S. Jina, Conor Long, Jennifer McKenna, Mary T. Pryce, Xue-Zhong Sun, and Khuong Q. Vuong. Photoinduced Se–C Insertion Following Photolysis of $(\eta^5\text{-C}_4\text{H}_4\text{Se})\text{Cr}(\text{CO})_3$. A Picosecond and Nanosecond Time-Resolved Infrared, Matrix Isolation, and DFT Investigation. *Organometallics*, **2008**, *27*, 3671-3680
- ⁹ Gaussian 16, Revision C.01, Frisch, M. J.; Trucks, G. W.; Schlegel, H. B.; Scuseria, G. E.; Robb, M. A.; Cheeseman, J. R.; Scalmani, G.; Barone, V.; Petersson, G. A.; Nakatsuji, H.; Li, X.; Caricato, M.; Marenich, A. V.; Bloino, J.; Janesko, B. G.; Gomperts, R.; Mennucci, B.; Hratchian, H. P.; Ortiz, J. V.; Izmaylov, A. F.; Sonnenberg, J. L.; Williams-Young, D.; Ding, F.; Lipparini, F.; Egidi, F.; Goings, J.; Peng, B.; Petrone, A.; Henderson, T.; Ranasinghe, D.; Zakrzewski, V. G.; Gao, J.; Rega, N.; Zheng, G.; Liang, W.; Hada, M.; Ehara, M.; Toyota, K.; Fukuda, R.; Hasegawa, J.; Ishida, M.; Nakajima, T.; Honda, Y.; Kitao, O.; Nakai, H.; Vreven, T.; Throssell, K.; Montgomery, J. A., Jr.; Peralta, J. E.; Ogliaro, F.; Bearpark, M. J.; Heyd, J. J.; Brothers, E. N.; Kudin, K. N.; Staroverov, V. N.; Keith, T. A.; Kobayashi, R.; Normand, J.; Raghavachari, K.; Rendell, A. P.; Burant, J. C.; Iyengar, S. S.; Tomasi, J.; Cossi, M.; Millam, J. M.; Klene, M.; Adamo, C.; Cammi, R.; Ochterski, J. W.; Martin, R. L.; Morokuma, K.; Farkas, O.; Foresman, J. B.; Fox, D. J. Gaussian, Inc., Wallingford CT, 2016.
- ¹⁰ Elliott, L. D.; Berry, M.; Harji, B.; Klauber, D.; Leonard, J.; Booker-Milburn, K. I. *Org. Process Res. Dev.* **2016**, *20*, 1806-1811
- ¹¹ Elliott, L. D.; Booker-Milburn, K. I. Photochemically Produced Aminocyclobutanes as Masked Dienes in Thermal Electrocyclic Cascade Reactions. *Org. Lett.* **2019**, *21*, 1463–1466
- ¹² Bruker, *SAINT+ v8.38A Integration Engine, Data Reduction Software, Bruker Analytical X-ray Instruments Inc., Madison, WI, USA 2015.*
- ¹³ Bruker, *SADABS 2014/5, Bruker AXS area detector scaling and absorption correction, Bruker Analytical X-ray Instruments Inc., Madison, Wisconsin, USA 2014/5.*
- ¹⁴ Sheldrick, G. M., SHELXT - Integrated space-group and crystal-structure determination. *Acta Crystallographica a-Foundation and Advances* **2015**, *71*, 3-8.
- ¹⁵ Sheldrick, G. M., A short history of SHELX. *Acta Crystallographica Section A* **2008**, *64*, 112-122.
- ¹⁶ Sheldrick, G. M., Crystal structure refinement with SHELXL. *Acta Crystallographica Section C-Structural Chemistry* **2015**, *71*, 3-8.
- ¹⁷ Dolomanov, O. V.; Bourhis, L. J.; Gildea, R. J.; Howard, J. A. K.; Puschmann, H., OLEX2: a complete structure solution, refinement and analysis program. *Journal of Applied Crystallography* **2009**, *42*, 339-341.